REVIEW PAPER

Antidiabetic nanotherapeutics of bioengineered silver and gold nanomaterials: a state-of-the-art review

Hamed Barabadi[1], Hesam Noqani[1], Kamyar Jounaki[1], Ayeh Sabbagh Kashani[2], Fatemeh Ashouri[1], Ebrahim Mostafavi[3,4]**

[1]*Department of Pharmaceutical Biotechnology, School of Pharmacy, Shahid Beheshti University of Medical Sciences, Tehran, Iran*
[2]*Faculty of Pharmacy, Tehran Medical Sciences, Islamic Azad University, Tehran, Iran.*
[3]*Stanford Cardiovascular Institute, Stanford University School of Medicine, Stanford, CA, United States*
[4]*Department of Medicine, Stanford University School of Medicine, Stanford, CA, United States*

ABSTRACT

Diabetes is a global health challenge that significantly reduces quality of life and poses serious risks to human health. Despite advancements in medicine, current antidiabetic treatments often fail to effectively control the disease, particularly given the increasing prevalence of diabetes worldwide. This situation highlights the urgent need for innovative therapeutic approaches. Nanobiotechnology has emerged as a promising field for the eco-friendly production of nanosized metal-based particles with potential biomedical applications. Among these nanoparticles (NPs), biosynthesized colloidal silver and gold particles have attracted considerable interest due to their unique physicochemical properties and broad-spectrum biological activities. These nanostructures are created using biological resources such as plant extracts, algae, and microbes, resulting in particles with various sizes and shapes. Recent studies, including both in vitro and in vivo models, have explored the antidiabetic potential of these NPs. This review offers a comprehensive evaluation of the existing evidence, emphasizing their ability to inhibit key enzymes involved in diabetes (α-amylase and α-glucosidase) and to improve critical biomarkers in animal models. Notably, treatment with these NPs resulted in reductions in blood glucose and HbA1C levels, as well as increased insulin levels in diabetic animals. These findings indicate that bioengineered silver and gold nanomaterials can be considered innovative candidates for antidiabetic nanotherapeutics after future safety investigations.

Keywords: *Biosynthesis; Metal nanoparticles; Silver nanoparticles; Gold nanoparticles; Antidiabetic activity*

How to cite this article
Barabadi H, Noqani H, Jounaki K, Sabbagh Kashani A, Ashouri F, Mostafavi E. Antidiabetic nanotherapeutics of bioengineered silver and gold nanomaterials: a state-of-the-art review. Nanomed J. 2025; 12(4): 546-592. DOI: 10.22038/nmj.2025.81522.2027

INTRODUCTION

Diabetes as a global health issue: presenting problems

Typically, diabetes is a chronic illness that happens either with inadequate insulin production by the pancreas or inefficient insulin utilization by the body [1]. Insulin is a hormone that modulates blood glucose levels. When the body is unable to absorb sugar (glucose) into its cells and utilize it for energy, diabetes occurs. This leads to a buildup of extra sugar in your bloodstream [2]. Hyperglycemia is a frequent consequence of uncontrolled diabetes that, over time, can cause severe life-changing and life-threatening impairment to many body systems, particularly the nerves and blood vessels. By type of diabetes, the principal reason for diabetes varies. Regardless of what type of diabetes you have, you may have extra glucose in your blood [3]. Too much glucose in the blood can result in dangerous well-being difficulties [4]. Heart disease, kidney failure, blindness, stroke, and lower extremity amputation can all be possible consequences of diabetes [5]. Diabetes and hearing loss [6], dementia [7], and some forms of cancer [8] have also been indicated in recent research. As a result of such complications, 6.7 million deaths in 2021 - 1 every 5 seconds individuals worldwide die of diabetes each year, most of them prematurely [9]. Type 1 diabetes and type 2 diabetes are chronic diabetes states [10]. Furthermore, prediabetes and gestational diabetes are possibly reversible diabetes conditions [11, 12]. When blood glucose levels are higher, more than normal prediabetes goes on. Just the blood glucose levels aren't high enough to be named diabetes. Some steps can be taken to prevent the process in which prediabetes results in diabetes. During pregnancy, gestational diabetes occurs. When blood glucose levels are higher, more than effect normal prediabetes goes

**Corresponding author(s) Emails:*
barabadi@sbmu.ac.ir; ebimsv@stanford.edu
Note. This manuscript was submitted on July 29, 2024; approved on February 04, 2025.

on. Just the blood glucose levels are not high enough to be named diabetes. Some steps can be taken to prevent the process in which prediabetes results in diabetes. During pregnancy, gestational diabetes occurs. However, it may disappear after the baby is born. Diabetes increases the probability of early death, and diabetes-related complications can affect the quality of life [13]. Individuals, families, nations and healthcare systems are affected by the high global burden of diabetes [14].

At least USD 966 billion in healthcare spending caused by diabetes - a 316% increase over the past 15 years by 2021. As reported by the International Diabetes Federation (IDF), the ongoing global rise in diabetes prevalence highlights the significant challenge posed by this condition worldwide. Current estimates indicate that 537 million adults aged 20-79 are living with diabetes, representing approximately 1 in 10 individuals. This number is projected to increase to 643 million by 2030 and reach 783 million by 2045 [9]. More than three-quarters of adults with diabetes reside in low- and middle-income countries. Additionally, 541 million adults are affected by Impaired Glucose Tolerance (IGT), placing them at an elevated risk for developing type 2 diabetes [9]. The high prevalence rates of DM, demonstrated in many epidemiological examinations, served as a rationale for improving health services related to DM, especially in primary health care. For all cases with diabetes mellitus, the general management is lifestyle alteration, such as diet and physical activity [15]. The current management of patients with type 1 diabetes mellitus involves insulin therapy, dietary adjustments, and regular physical exercise [16]. At first, individuals with type 2 diabetes mellitus are frequently handled with diet and physical activity. Insulin, oral antihyperglycemics, injectable glucagon-like peptide-1 (GLP-1) receptor agonists, or a mixture of these medications can be ordered when these measures are insufficient to control blood glucose levels [17]. For preventing long-term complications of diabetes and decreasing the total expenditure of handling the illness, the proper glycemic control and achievement of other nonglycemic goals like body weight, blood pressure and lipids are substantial. These patients with diabetes get therapies to prevent diabetes complications such as aspirin, blockers of the renin-angiotensin-aldosterone system (angiotensin-converting enzyme (ACE) inhibitors or angiotensin II receptor blockers (ARBs)) and cholesterol-lowering drugs like statins [18]. Adequate controlling blood glucose levels is essential for managing complications of diabetes. The chance of diabetic complications relies on the grade of glycemic control in diabetic cases that currently is demonstrated [19]. To prevent or lessen the complications linked with this condition, decreasing hyperglycemia is the goal of antidiabetic therapy. Antidiabetic treatment proposes to decrease glycated hemoglobin (HbA1C) to a regular grade (<6.0%) without stimulating hypoglycemia as a criterion of glycemic control [20]. As a widespread disease, diabetes mellitus and its complications, like diabetic nephropathy, cardiomyopathy, retinopathy, diabetic foot, and peripheral neuropathy, have prompted individuals to struggle with the prevention and management of the disease. Besides physical and psychological pain in some cases, diabetes complications also impose a massive economic burden and impairment on families. Furthermore, once diabetic complications occur, they are frequently permanent and difficult to manage. Injection of Insulin and blood glucose observation can be irritating and time-consuming for patients. A wide range of medicines and their combinations from different classes, such as sulfonylureas, biguanides, glinides, thiazolidinediones, etc are currently used to combat diabetes. However, due to their side effects of these drugs and their inability to manage diabetes, the search for new drugs is ongoing. Additionally, diverse technologies like continuous glucose monitoring devices and insulin pumps have been produced to eliminate the disadvantages of injection and improve patient compliance [21, 22]. These devices are still incapable of reaching true euglycemia even though they have improved their blood glucose levels to some level because insulin is injected subcutaneously by measuring glucose levels in the interstitial fluid. Due to the implanted sensing element, there is a chance of infection and scarring. Besides, the devices must be substituted often, which is sometimes expensive. Consequently, there is an urgent necessity to create secure and cost-effective medical care.

Nanotechnology in treating diabetes

A novel and essential technology of the 21st century is nanotechnology. The properties and utilizations of substances with a structure size of 0.1 to 100 nm are examined. A new arrangement of substance is made, by positioning and mixing various particles. Materials science, life science, environmental science, medication, chemical science and other fields of study are the fields of nanotechnology with the fast improvement of nanotechnology [23, 24]. There are diverse interactions between variant nano units. The quantum effect of rising surface energy, small crystal structure, and small size, the interface effect

due to the rapid increase of the atomic ratio of the surface, and the size effect caused by the large specific surface area are nanomaterials specific effects due to this property [25, 26]. Nanotechnology is taking a new way by aggregating modern medical research and nanotechnology; furthermore, medical investigation has also achieved a new level, particularly in diagnosing and treating illnesses [27]. Nanotechnology is also used in developing drugs, which helps resolve problems in conventional care [28]. Transportation of targeted drugs and decreasing or preventing the side effects of medicines can be done by nano-drugs. Concurrently, nanodrugs can extend the length of drug action, help the storage of drugs, and improve the stability of drug action as a delayed release characteristic. Small volume and high drug-loading function are the characteristics of nanomedicine [29]. They do not induce alteration to the vascular endothelium and easily penetrate blood vessels. They can improve the effectiveness of medicines and decrease or even prevent the side effects by protecting the medicines from chemical decomposition reactions and producing a local drug concentration higher than other delivery methods [30]. Sensor technologies and small devices are provided for precise and well-timed illness identification by nanotechnology, a primary scientific method. Over the last few years, the investigation has progressively utilized nanotechnology to examine diabetic complications, particularly management and strategy [31]. In the last few years, nanotechnology has enabled several ways for non-invasive observation of blood glucose levels. Figure 1 showed a schematic overview of diabetes classifications, current medications and opportunities for nanotherapeutics. Currently, for insulin delivery in diabetes management, various forms of nanoparticles (NPs) are being examined, like a) polymeric biodegradable NPs, b) ceramic NPs, c) polymeric micelles, d) dendrimer, and e) liposomes [32, 33]. Interestingly, metallic NPs and in particular, biofabricated silver nanoparticles (AgNPs) and gold nanoparticles (AuNPs) have shown impressive potential to inhibit the activity of key enzymes of diabetes (a-amylase and a-glucosidase). More interestingly, the animal-based studies revealed a drop in the blood glucose level and HbA1C in the treated diabetic animals with these nanomaterials as well as an increase in the blood insulin level. This review study aimed to focus on the role of biosynthesized nanosized silver and gold particles to combat diabetes.

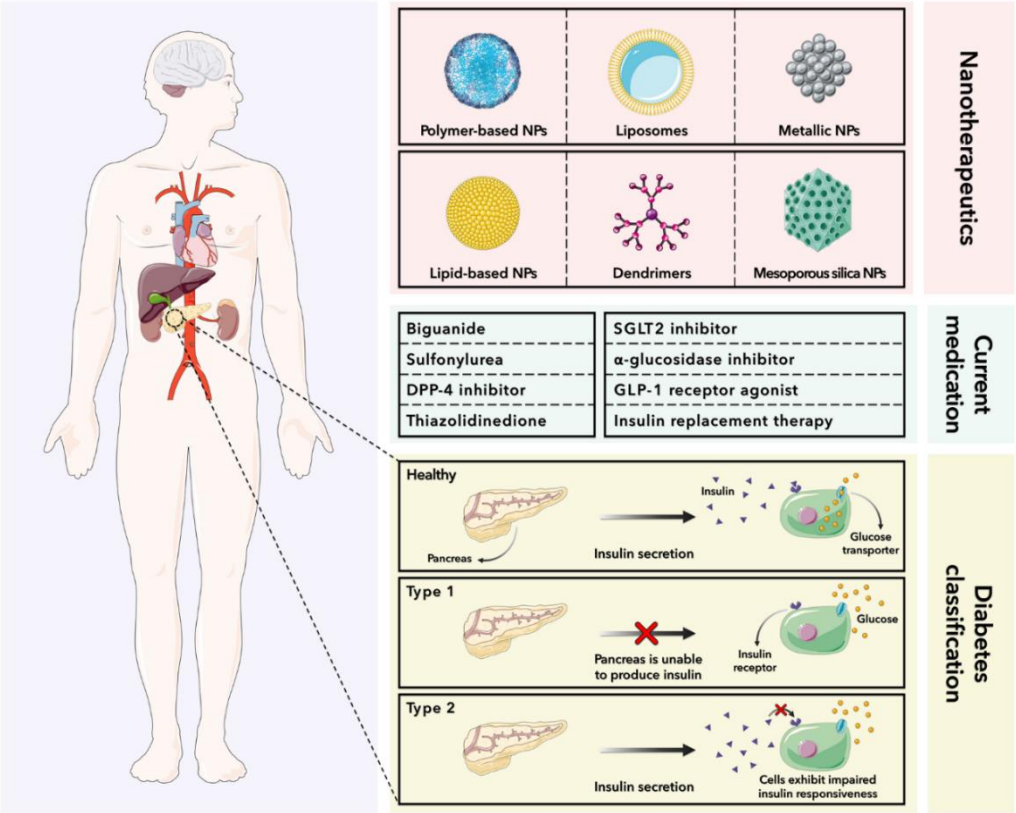

Fig. 1. A schematic representation of diabetes classifications, current medications, and opportunities for nanotherapeutics. The figure was to some extent created using Servier Medical Art, which is provided by Servier and authorized under a Creative Commons Attribution 3.0 Unported License (https://creativecommons.org/licenses/by/3.0/).

Green synthesis of silver and gold nanomaterials

Nanosized silver and gold particles can be synthesized using three primary approaches: physical, chemical, and biological methods. Physical methods involve high-energy processes such as evaporation-condensation and laser ablation, which often require expensive equipment and consume significant energy. Chemical methods rely on reducing agents to synthesize NPs, but these techniques pose risks due to the potential presence of toxic chemical residues, raising concerns about environmental and biomedical safety. In contrast, biological synthesis utilizes natural resources like plant extracts, algae, or microorganisms as reducing and stabilizing agents. This ecofriendly and cost-effective approach not only minimizes the need for hazardous chemicals but also aligns with sustainable practices, making it an attractive alternative for nanoparticle fabrication [34, 35]. Biological resources are employed for the green synthesis of the AgNPs and AuNPs. Figure 2 summarizes different procedures for bioengineering of AgNPs and AuNPs by using plant extracts, algae and microorganisms. In this section, recent advances in the green synthesis of nanosized silver and gold particles were reviewed.

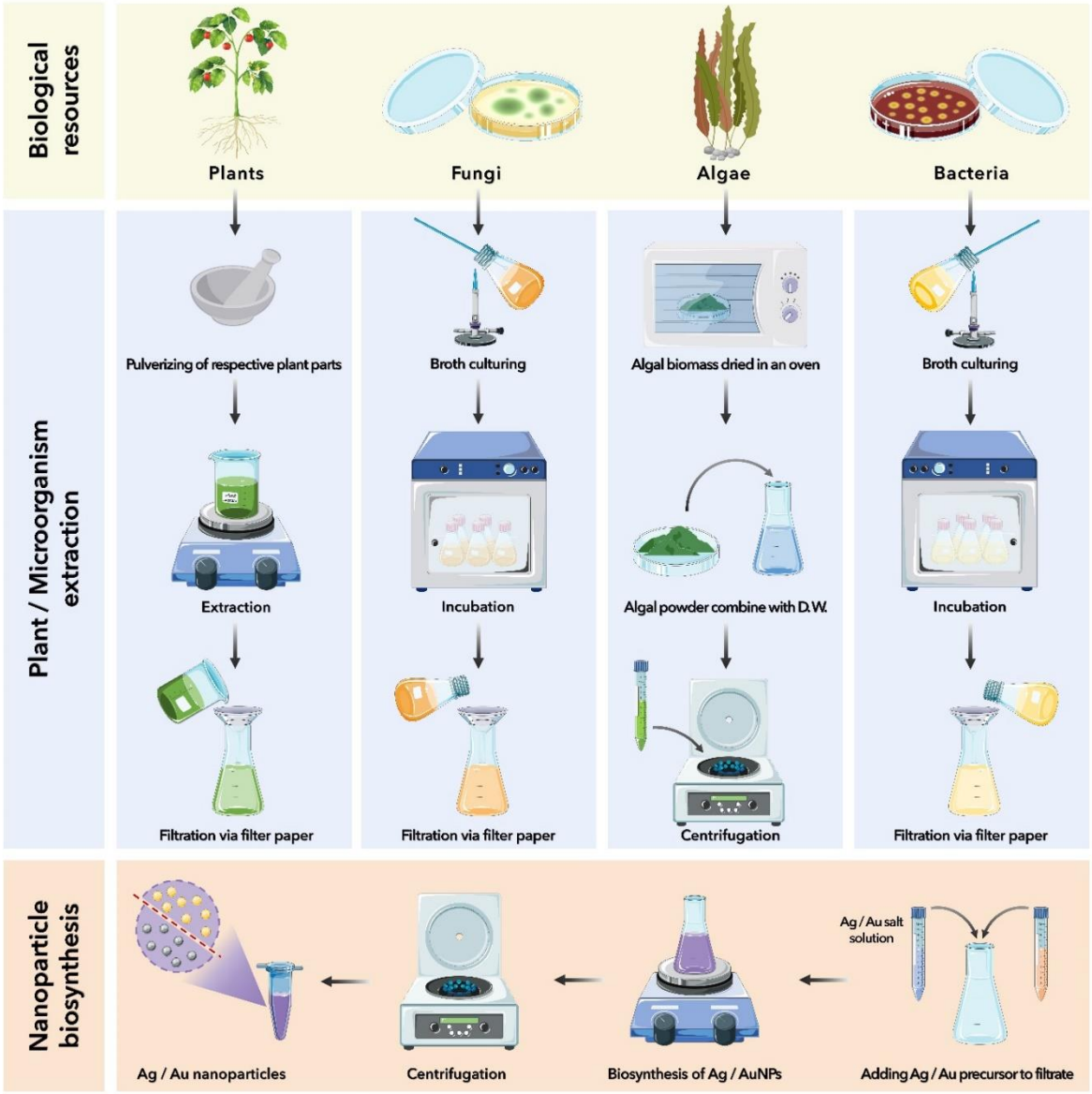

Fig. 2. A schematic representation of the green synthesis of silver and gold nanomaterials by using plant extracts, algae, and microorganisms. The figure was to some extent created using Servier Medical Art, which is provided by Servier and authorized under a Creative Commons Attribution 3.0 Unported License (https://creativecommons.org/licenses/by/3.0/).

Bacterium-mediated synthesis of silver and gold nanomaterials

Bacteria have exhibited great potential as biological resources and are known to have an intrinsic ability to reduce ions of heavy metals into NPs [36]. Extracellular and intracellular approaches are considered the main routes for bacterium-mediated fabrication of NPs. The extracellular way is more favorable as the harvest and recovery of NPs is more facile and economical owing to no special purification method required [37]. In a study, Elbahnasawy et al. reported the extracellular biosynthesis of AgNPs using *Rothia endophytica* with cubic morphology and size ranging from 47 to 72 nm. The authors suggested that the existence of metabolites consisting of carboxylic acids, alcohols, proteins, and amino acids in the cell-free extract of *R. endophytica* was responsible for forming NPs and acting as the stabilizing and capping agent [38]. Similarly, Ibrahim et al. employed the endophytic bacterium *Bacillus siamensis* strain C1 for the biogenic synthesis of spherical AgNPs with a size range of 25-50 nm [39]. In a similar study, Patil et al. used an extracellular approach for the biofabrication of AuNPs through *Paracoccus haeundaensis* BC74171. They reported the morphology and average diameter of the NPs as spherical and 20.93 ± 3.46 nm, respectively. The authors indicated that the formation of the biogenic AuNPs was probably affected by the extracellular secretion of microbial enzymes leading to the reduction of Au ions [40]. Li, S. et al. generated AgNPs utilizing *Pseudomonas aeruginosa* CI109 in extracellular and intracellular ways. Extracellularly-fabricated AgNPs were reported to be able to pass the purification and cell-crashing processes. However, characteristic analyses exhibited that the intracellularly-formed NPs were smaller (6 nm) than the AgNPs synthesized extracellular (14 nm). Further, the intracellular bio-fabrication resulted in more round particles than the extracellular process. It was hypothesized that coating particles with proteins was responsible for the bigger size and irregular dimension of extracellular AgNPs [41]. Likewise, Shunmugam and coworkers biosynthesized *vibrio alginolyticus* mediated-AuNPs in an extracellular manner. The average diameter of green AuNPs was measured as 100 to 150 nm, and their morphology was reported as sphered according to different analytical techniques. The secretion of bacterial secondary metabolites was suggested to play a role in the bioreduction of metallic ions [42]. In addition, *Thiosphaera pantotropha* was utilized as the biofactory for forming AgNPs extracellularly with a spherical shape and an average size of 14.6 nm. It is similarly suggested that different substances (secondary metabolites, soluble redox mediators, enzymes, and proteins) secreted from the bacteria affected the formation of NPs by reducing the Ag ions [43]. Also, Eid et al. looked into an extracellular approach for manufacturing bacterium-mediated AgNPs. In their study, the usage of *Streptomyces laurentii* R-1 led to the formation of sphered-shaped NPs with a diameter ranging from 7 to 28 nm. It was mainly suggested that the presence of proteins affected the bioreduction procedure as the carbonyl groups of amino acids stabilized the NPs [44]. Iqtedar et al. performed a similar experiment regarding the extracellular preparation of AgNPs. They employed an extracellular extract of *Bacillus mojavensis* BTCB15 as the reducing agent and generated AgNPs with irregular morphology in an average particle size of 105 nm. It was indicated that the presence of functional groups (amide and carboxyl) in the bacterial extract was possibly attributed to the reduction of Ag ions and their stabilization [45]. Mortazavi and coworkers also reported the biofabrication of AuNPs extracellularly using *the Salmonella enterica* subspecies of *enterica serovar* Typhi. It was mentioned that the bacterium-assisted AuNPs were detected with an average diameter of 42 nm [46]. In the research of Parikh and coworkers, another extracellular method for green synthesis of AgNPs was introduced utilizing *Morganella* sp. the characterization analyses revealed that the biofabricated AgNPs were spherical in morphology and had an average size of 20 nm. Proteins in the bacterial extract were reported to have a significant role in capping and stabilizing the NPs [47]. Moreover, Rajasekar et al. prepared metabolites secreted from zebrafish gut bacteria, viz., *Panna microdon*, *Selachimorpha* sp., and *Rastrelliger kanagurta* and employed them for bioreduction of Au ions to AuNPs. The bacterial biosynthesized AuNPs were characterized using different analytical techniques. The results demonstrated that AuNPs were almost rod-shaped and spherical morphologically and possessed a diameter ranging from 45 to 80 nm. Functional groups (alcohol, primary amine, phenol, alkyl, and aromatic C═C) present in the bacterial metabolites were detected by FTIR. The authors suggested they could contribute to the bioreduction and formation of NPs [48]. Similarly, Shivaji et al. biosynthesized AgNPs extracellularly using different bacteria, including *Bacillus cecembensis*, *Bacillus indicus*, *Pseudomonas antarctica*, *Pseudomonas meridian*, *Pseudomonas proteolytica*, *Arthrobacter gangotriensis*, and *Arthrobacter kerguelensis*. The biofabricated AgNPs appeared spherical and ranged from 6 to 13 nm [49]. In another study, Singh and coworkers investigated the process of AgNPs formation using the

extracellular content of *Pseudomonas* sp. It was stated that the biologically synthesized AgNPs were irregular morphologically, and their size was recorded as 10-40 nm. The possible role of secreted bacterial proteins and enzymes in the biofabrication process of NPs was also mentioned. Further, it was addressed that extracellular techniques were more beneficial than the intracellular way as the steps like purification in the intracellular procedure were complicated and time-consuming compared to the extracellular approach [50]. According to the studies mentioned above, the exact mechanism by which bacteria synthesize NPs is yet to be fully addressed, and the characteristics of NPs are not quite controllable [51]. Hence, other biofactories have been explored as alternatives for bacteria.

Fungus-mediated synthesis of silver and gold nanomaterials

Fungi are of high interest among microorganisms for the biosynthesis of NPs owing to the facile biomass handling, simple culturing and growth, remarkable accumulation of metals, and the low-priced procedure [36, 52, 53]. Production of NPs by fungi can be conducted in either intracellular or extracellular ways, like the bacterial synthesis method. It is thought that metabolites secreted from fungi, i.e. lovastatin, cyclosporine, mevastatin, and griseofulvin, are responsible for the formation of NPs. Moreover, fungal enzymes (peroxidases, NADPH, NADH, and ACCases) probably play an essential role in the bioreduction of ions [51]. Different scholars have investigated fungi for the green synthesis of AgNPs and AuNPs. For instance, Naimi-Shamel et al. looked into the biosynthesis of AuNPs using *Fusarium oxysporum* in an extracellular way. The NPs were spherical and hexagonal, ranging from 22 to 30 nm. It was suggested that the secretion of proteins by *F. oxysporum* cells could lead to reduced activity and formation of AuNPs from Au ions in the solution [54]. In a similar study, Potbhare and coworkers reported the extracellular biofabrication of sphered-shaped AgNPs having a particle diameter of 10-20 nm using *Rhizoctonia solani*. It was similarly indicated that the possible mechanism of NPs formation is the release of many fungal enzymes and their effect on the bioreduction process. Further, the authors pointed out that the extracellular method is highly desired due to the lack of cellular component presence [53]. Alternatively, Qu et al. reported a similar extracellular method for the green synthesis of AuNPs utilizing *Trichoderma* sp. WL-Go. The results of different analytical techniques showed that the biosynthesized AuNPs were spherical and pseudo-spherical morphologically, and their average size was 9.8 nm. The authors also hypothesized that biomoleculesisted in the cell-free extract of *Trichoderma*could possiblyle to provide nucleation sites of Au ions [55]. *Aspergillus terreus* was also used as a green machine for the biosynthesis of AgNPs by Kumari and coworkers. The size of *A. terreus*-assisted AgNPs was recorded as approximately 25 nm, and their morphology was spherical.

The metabolites released from *A. terreus*, i.e., erdin and geodin, were known to be the possible reducing agents and capping agents stabilizing the NPs [56]. Likewise, Taha et al. assessed the biosynthesis of AgNPs using an extracellular extract of *Penicillium italicum*. The eco-friendly fabricated AgNPs were found to have a spherical structure and a size of less than 50 nm. The formation of NPs was confirmed by observation of colour change in the solution, and the surface plasmon resonance of AgNPs could be the effective agent in this case [57]. *Penicillium verrucosum*-drived AgNPs were also synthesized extracellularly by Yassin and coworkers. It was reported that a cell-free extract of *P. verrucosum* could reduce Ag ions to spherical-shaped AgNPs in a diameter range of 10 to 12 nm [58]. Additionally, the mycosynthesis of AuNPs was carried out through an extracellular process using an aqueous extract of *Trichoderma hamatum* SU136. The biologically fabricated AuNPs were found to be hexagonal, pentagonal, and spherical and in a size range of 5-30 nm. Secretion of biocompounds such as tyrosine and tryptophan and the significant role of their amide groups was reported to be the probable reason why the formation of AgNPs occurred by the fungal extract in this study [59]. Unlike the studies mentioned above, Samanta et al. reported a fungi-assisted production of AuNPs in an intracellular manner. *Laccaria fraterna* EM-1083 mycelia was used as the reducing and stabilizing agent for forming approximately 32 nm-sized AuNPs. The biogenic AuNPs have appeared to have various shapes, including triangles, hexagons, pentagons, and spherical. The authors suggested that the negative charge of functional groups present on the mycelial surface was responsible for the attachment of $AuCl_4$ and the bioformation of AuNPs [60]. In addition, Murillo-Rábago et al. reported *Trichoderma harzianum* and *Ganoderma sessile* as effective reducing agents for extracellular and intracellular fabrication of AgNPs. According to the characterization results, the NPs manufactured by both fungi were quasi-spherical morphologically. Employment of the supernatant of *T. harzianum and G. sessile* led to the formation of 9.6 and 5.4 nm-sized AgNPs. Notably, AgNPs manufactured by the intracellular extract of the fungi were more significant in diameter (19.1 nm for *T. harzianum* and 8.9 nm for *G. sessile*), indicating that the extracellular

approach is more advantageous than the intracellular way [61]. As it is evident, the extracellular method of fungal synthesis has been looked into with more interest in different published papers compared to the intracellular method, given the facile and economical procedure of NPs purification.

Plant-mediated synthesis of silver and gold nanomaterials

Herb-assisted method of synthesis is more preferred than using microorganisms as bioresources for the fabrication of NPs since plants are known to be less toxic, easy to access, and consist of various metabolites, namely reductase, alkaloids, terpenes, polyphenolic ascorbic acid, citric acid, phenols, and flavonoids aiding the oxidation reaction [62, 63]. It is worth mentioning that there is no requirement for additional reducing, capping, and stabilizing agents since these bioactive compounds play the same role naturally in the mixture [64]. Furthermore, different parts of plants, such as stems, seeds, fruits, leaves, and roots, can be utilized as biofactories, of which leaves are more common. Accordingly, the constitution of metabolites in each part varies, providing a chance to control the biosynthesis process and characteristics of NPs. Above all, using plants instead of other biological resources increases the cost-effectiveness given the lack of requirement for cell culture growth and high pressure or temperature in the synthesis procedures [65]. The reaction time is also concise with high efficacy, confirming the plant-based fabrication as the best green method of NPs production [62, 65]. Different researchers have looked into the herbal synthesis of AgNPs and AuNPs, mostly in extracellular ways, and reported promising results. Balachandar et al. explored a phytofabrication process in which AgNPs were formed via *Phyllanthus pinnatus* stem extract. The morphological structure of the green synthesized AgNPs was found to be mostly cubical, and their particle diameter was recorded as 100> nm. The authors believed that the phytochemical (e.g., proteins, terpenes, phenols, alcohols, saponins, and alkaloids) present in the stem extracted not only reduced the Ag ions but also capped and stabilized the NPs. This method was highly rapid, cost-effective, facile, and energy efficient [66]. Alomar and coworkers also managed to prepare AgNPs in an environment-friendly way using the aqueous leaf extract of *peganum harmala* with a mean size of 184 nm and spherical shape [67]. In other green approaches, Baruah et al. reported the biological production of spherical AgNPs utilizing the fruit extract of *Alpinia nigra*. According to analytical methods, the biosynthesized AgNPs were fairly small, with a mean dimension of 6 nm. It was suggested that hydroxyl groups in the phenols and flavonoids in the herbal extract were responsible for the reduction of Ag+ to Ag0 and the stability and prevention of agglomeration. The probable mechanism lay under the NP's formation is the transformation of enol form to keto form in the polyphenolic compounds, which releases reactive hydroxyl atoms that reduce the metallic ions [68]. Likewise, Gopinath et al. performed an extracellular synthetic procedure to prepare *Mimosa pudica*-mediated AgNPs. The phytofabricated AgNPs appeared to be uniformly sphere-shaped with an average size of 100 nm. The authors indicated that the leaf extract of *M. pudica* was a rich source of different phytochemicals, e.g., coumarins, quinines, terpenoids, saponins, flavonoids, tannins, alkaloids, and phenols, possibly playing a role in the uniformity of the green synthesized AgNPs and the bioreduction process [69]. In the case of AuNPs, Hosny and coworkers reported the biosynthesis of AuNPs using two halophytic plants, i.e., *Chenopodium amperosidies* and *Atriplex halimus*. The *C. amperosidies*-mediated and *A. halimus*-mediated AuNPs had an average diameter of 6 and 40 nm, respectively and were found to be mostly spherical morphologically. The mechanism by which AuNPs were formed was probably the activity of lutein available in both extracts as the stabilizing agent and reductant by donating hydrogen atoms or electrons to Au ions. In addition, other herbal compounds were suggested to have a synergistic effect and aid the bioreduction process [70]. Similarly, Ameen and coworkers conducted other green approaches for the biologically extracellular synthesis of AgNPs. In this study, the flower extract of *Mangifera indica* actively reduced Ag ions to AgNPs with a spherical structure and a particle diameter recorded as 10-20 nm according to results obtained from analytical techniques. The chemical compounds, including proteins, amino acids, flavonoids and alkaloids, probably exhibited a reductive effect and capped the NPs [71]. Alternatively, AuNPs were biofabricated by Kureshi et al. using the extracts of *Garcinia indica* and *Garcinia cambogia* fruit-pericarps. It was similarly suggested that phytoconstituents present in the extracts like flavonoids, organic acids, amino acids, vitamins, xanthones, PIBs, and phenols effectively reduced the Au ions to spherical-triangular AuNPs with a size range of 2-10 nm [72]. In a similar paper, Islam and coworkers reported a one-spot fabrication of eco-friendly AuNPs with a dimensions ranging from 20 to 200 nm. *Pistacia integerrima* gall extract assisted the formation of AuNPs by acting as both a reducing and capping agent. The reducing activity was possibly attributed to the carbonyl and other groups present in the extract. Further, it was suggested that carboxylate ions also had a shielding effect [73]. Although plants have drawn much attention as the most convenient

bioresources for the synthesis of NPs, the exact mechanism by which plant-mediated NPs are formed is not fully explained yet, and the determination of the phytochemical responsible for the bioreduction among the diverse compounds in the herbal extracts is difficult [65]. Plant-assisted NPs can also be synthesized intracellularly when grown in a metal-rich hydroponic solution, soil, or organic media [64]. However, the data is limited and metallic ions were found to destroy the physiology of living herbal cells and their natural growth and metabolism undesirably [74].

Alga-mediated synthesis of silver and gold nanomaterials

Algae are another biological agent gaining attention for the fabrication of NPs among different biofactories and are categorized into two groups, i.e., microalgae and macroalgae. Algae are known to propagate fast and be able to accumulate and form NPs by reducing metallic ions. These bioresources are locally available and can be vastly found on the Earth's crust in marine water, freshwater, rocks, and moist soil surfaces [75, 76]. Further, the pigment and cell wall structure of algae, their stages of development, and their immobility have made algae more advantageous compared to high plants. Chemical groups like amino, carboxyl, and hydroxyl available in the algal metabolites are probably responsible for reducing metallic elements into their ions [77]. Algal synthesis of NPs can be conducted through two primary manners, i.e., extracellular and intracellular.

In an extracellular way, the extract can be prepared by incubation of algal biomass for 6 to 12 h, sonication of biomass with distilled water, or drying the biomass under shadow for a while, followed by treating it with distilled water and filtering it out. On the other hand, in the intracellular process, the biomass is in direct contact with the elemental solution. However, centrifugation and sonication are required at the end for harvesting the formed NPs [75]. In various studies, the role of algae as reducing agents in the AgNPs and AuNPs synthetic processes have been discussed either intra or extracellularly, some of which are as follows. El-Sheekh et al. reported an extracellular approach for the biosynthesis of AuNPs using *Spirulina platensis*. The characterization results revealed that the alga-mediated AuNPs had a size ranging from 15.49 to 55.08 nm and pentagonal, triangular, and slightly spherical morphologies [76]. Likewise, Dağlıoğlu and coworkers investigated a green method for intracellularly producing alga-assisted AgNPs. A green alga *Desmodesmus* sp. was employed for the bioreduction, and this resulted in spherical NPs forming a maximum diameter of 15–30 nm. The biosynthesized AgNPs were detected inside the algal cells in which chlorophylls probably acted as the effective reductants and turned Ag^{+} to Ag^{0}. It was emphasized that the process was fast and cost-effective compared to other biofabrication techniques of NPs [77]. Additionally, Priyadharshini et al. biosynthesized AgNPs utilizing the extracellular extract of macro-alga *Gracilaria edulis*. The biogenic AgNPs were detected in a spherical shape and 55-99 nm dimension [78].

In vitro enzyme inhibitory activity of biosynthesized silver and gold nanomaterials

Laboratory investigations have demonstrated the remarkable potential of biogenically synthesized AgNPs and AuNPs in inhibiting key enzymes associated with diabetes, namely α-amylase and α-glucosidase (Table 1). A study revealed that *Elsholtzia communis* leaf extract can be used for the biosynthesis of spherical AgNPs with an average size of 11.38 nm. These NPs exhibited significant inhibition of α-amylase and α-glucosidase, with IC_{50} values of 40.6 ± 1.77 $\mu g.mL^{-1}$ and 26.87 ± 1.74 $\mu g.mL^{-1}$, respectively. In comparison, the standard inhibitor acarbose showed IC_{50} values of 65.7 ± 0.40 $\mu g.mL^{-1}$ and 51.46 ± 2.38 $\mu g.mL^{-1}$ for the same enzymes [79]. A study demonstrated that *Persea americana* peel extract can synthesize spherical AgNPs (average size: 24 nm) with notable α-amylase inhibition. The results indicated that the AgNPs had an IC_{50} of 66.04 $\mu g.mL^{-1}$, exhibiting stronger enzyme inhibition than acarbose, which had an IC_{50} of 86.5 $\mu g.mL^{-1}$ [80]. Alternatively, a study demonstrated the phytofabrication of spherical AgNPs using *Salvia blepharophylla* and *Salvia greggii* extracts, resulting in nanoparticles with average sizes of 52.4 nm and 62.5 nm, respectively. The antidiabetic potential was assessed by α-amylase inhibition at concentrations of 20 to 100 μg.mL-1. The IC_{50} for AgNPs from *S. blepharophylla* ranged from 40 to 60 $\mu g.mL^{-1}$, compared to acarbose, which had an IC_{50} of 20 to 40 $\mu g.mL^{-1}$. AgNPs from *S. greggii* exhibited an IC_{50} of approximately 50 $\mu g.mL^{-1}$ [81]. A study demonstrated that *Physalis minima* extract was used to synthesize spherical AuNPs with an average size of 15 nm. The NPs were tested for α-amylase inhibition at concentrations ranging from 100 to 500 $\mu g.mL^{-1}$. The results showed that at the highest concentration, the AuNPs inhibited the enzyme by 93% [82].*(See Table 1 after references)*

Besides, Balu et al. reported the green synthesis of spherical AgNPs with spherical morphology and an average size of 18, 12, and 770 nm, employing Rosa indica (L.) extract by ethanol, acetone, and water as solvents. In this work, the inhibition of α-amylase and α-glucosidase enzymes was examined. According to the technique outlined in Table 1, they utilized various amounts of AgNPs and acarbose as a positive control.

In the *α-amylase inhibition* assay, RE-Ac-Ag (AgNPs biosynthesized using acetone as solvent), Re-Et-Ag (AgNPs biosynthesized using ethanol as solvent), RE-Aq-Ag (AgNPs biosynthesized using water as solvent), and acarbose had respective half maximal inhibitory concentration (IC_{50}) values of 50, 50, 75, and between 25 and 50 $\mu g.mL^{-1}$ and *α*-glucosidase have an approximate IC_{50} of 50, 50, 75 and 50 $\mu g.mL^{-1}$, respectively (Figure 3A) [83]. Moreover, a study explored the plant-mediated synthesis of spherical AgNPs ranging in size from 15.71 to 84.97 nm using *Ixora brachiata* leaf extract. The antidiabetic activity of these nanoparticles was assessed through α-amylase and α-glucosidase inhibition assays. AgNP concentrations of 25, 50, 100, 150, and 200 $\mu g.mL^{-1}$ were tested, and the highest concentration led to approximately 20% inhibition of α-amylase and 50% inhibition of α-glucosidase (Figure 3B) [84]. In addition, a study focused on the green synthesis of spherical AgNPs (5 to 15 nm) using *Embelia robusta* seed extract. The *in-vitro* antidiabetic activity of these biosynthesized AgNPs was assessed through α-amylase and α-glucosidase inhibition assays. AgNPs and acarbose were tested at concentrations of 20, 40, 60, 80, and 100 $\mu g.mL^{-1}$, with IC_{50} values reported. While the IC_{50} for acarbose was below 20 $\mu g.mL^{-1}$ in all tests, the IC_{50} values for AgNPs were 32.3 $\mu g.mL^{-1}$ for α-amylase and 30.1 $\mu g.mL^{-1}$ for α-glucosidase (Figure 3C) [85].

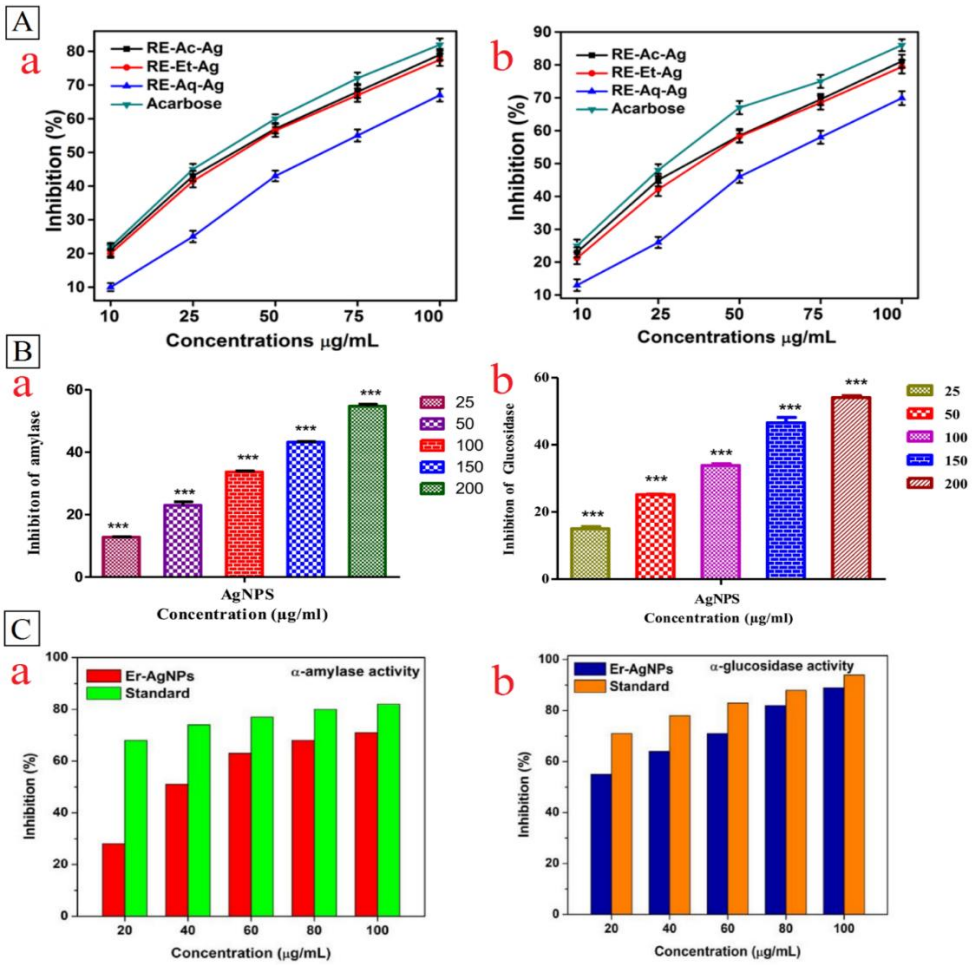

Fig. 3. A) Investigating the inhibition activity of *α*-amylase and *α*-glucosidase enzymes, with different biosynthesized AgNPs and acarbose in different concentrations: (a) *α*-amylase inhibition, (b) *α*-glucosidase, (RE-Ac-Ag) AgNPs biosynthesized using acetone as a solvent, (Re-Et-Ag) AgNPs biosynthesized using ethanol as solvent, and (RE-Aq-Ag) AgNPs biosynthesized using water as a solvent [83] [Copyright © 2022 by the authors, Licensee MDPI, Basel, Switzerland. Open access article distributed under the terms and conditions of the Creative Commons Attribution (CC BY4.0) license]; B) The dose-dependent inhibition of α-amylase (a) and *α*-glucosidase (b) by biosynthesized AgNPs from *Ixora brachiate.* [84]. Copyright © 2021 Published by Elsevier B.V. Open access article distributed under the terms and conditions of Attribution-NonCommercial-NoDerivatives 4.0 International (CC BY-NC-ND 4.0)]; C) α-amylase and *α*-glucosidase inhibition activity at different doses of AgNPs and acarbose: (a) α-amylase inhibition and (b) *α*-glucosidase [85]. Copyright © 2022 Vietnam National University, Hanoi. Published by Elsevier B.V. Open access article distributed under the terms and conditions of Attribution-NonCommercial-NoDerivatives 4.0 International (CC BY-NC-ND 4.0)].

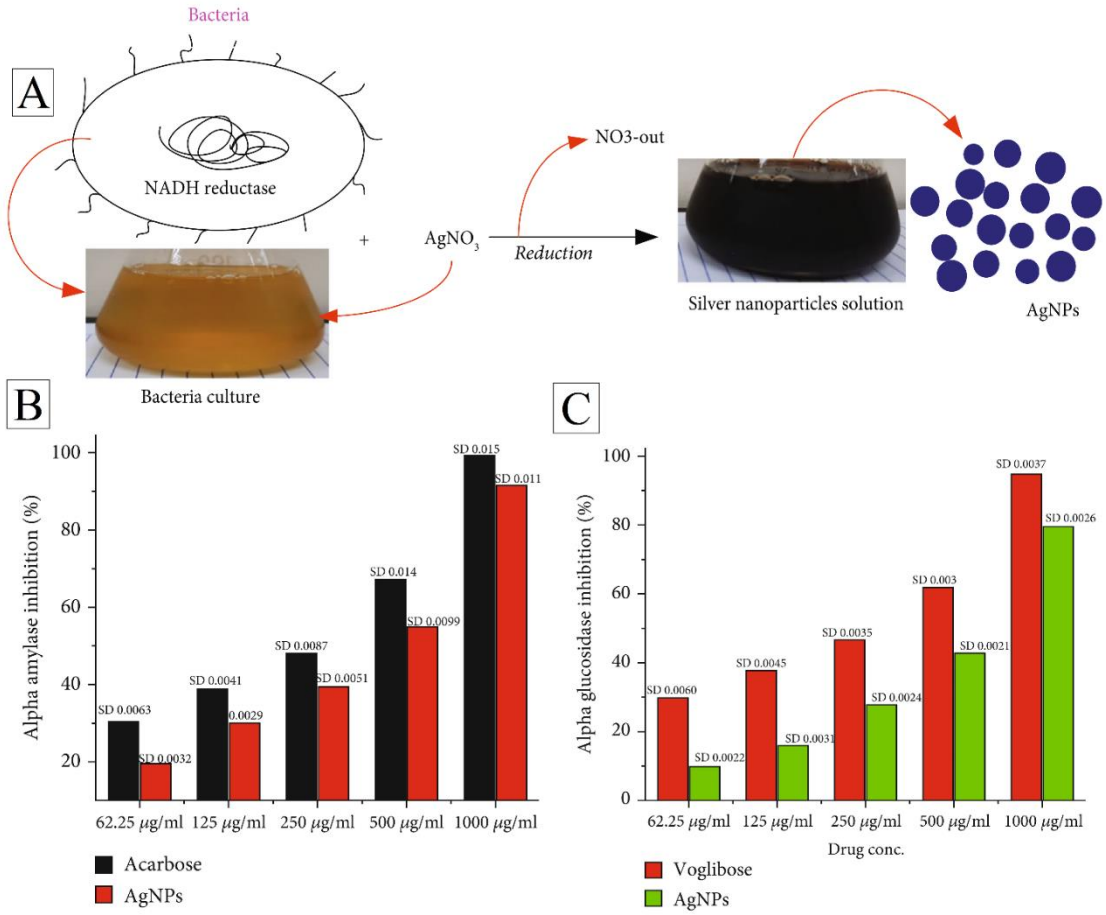

Fig. 4. An overview of bacterial-mediated fabrication of AgNPs (A), α-amylase inhibition activity of different concentrations of AgNPs compared to acarbose (positive control) (B), and α-glucosidase inhibition activity of different concentrations of AgNPs and voglibose (positive control) (C) [87] [Copyright © 2022 Shahnaz Majeed et al., Hindawi Limited. Open access article distributed under the terms and conditions of the Creative Commons Attribution (CC BY4.0) license].

A study investigated the biofabrication of nearly spherical AgNPs using an aqueous extract of *Brassica oleracea*. The antidiabetic activity of the biosynthesized AgNPs was evaluated by testing their ability to inhibit the α-glucosidase enzyme at concentrations of 1, 2.5, and 5 μg.mL^{-1}, following standard procedures. The outcome demonstrated that the IC_{50} for these NPs is 2.29 μg.mL^{-1} [86]. Furthermore, a study reported the bacterium-mediated synthesis of spherical AgNPs (7.18 to 13.24 nm) using *Salmonella enterica* supernatant. The nanoparticles inhibited α-amylase and α-glucosidase, with IC_{50} values of 428.60 μg.mL^{-1} and 562.02 μg.mL^{-1}, respectively, compared to acarbose (295.42 μg.mL^{-1}) and voglibose (313.62 μg.mL^{-1}) as controls (Figure 4) [87].

A study reported the synthesis of 33 nm AgNPs using *Zephyranthes candida* flower extract. In an α-amylase inhibition assay, AgNPs inhibited enzyme activity by 78%, comparable to 80% inhibition by acarbose at the highest concentration (Figure 5A) [88]. Moreover, a study reported the herbal-mediated synthesis of spherical AgNPs using Equisetum arvense extract. At a concentration of 2.5 μg.mL^{-1}, the AgNPs inhibited 95.77% of α-amylase activity. Figure 5B illustrates the phytosynthesis process and enzyme inhibition at various AgNP concentrations [89].

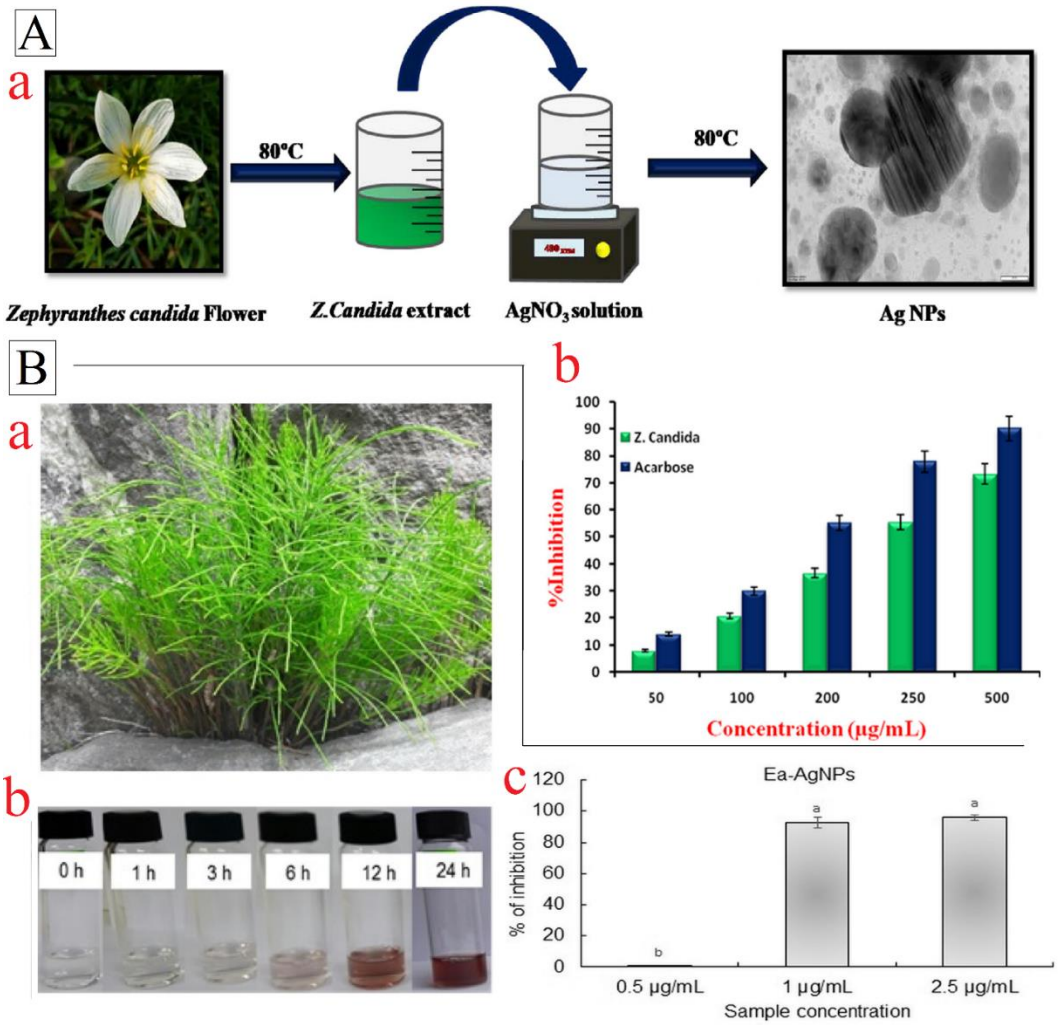

Fig. 5. A) Schematic illustration of phytofabrication of AgNPs by using *Zephyranthes candida* flower (a) and their *in vitro* antidiabetic activity (b)[88]. Copyright © 2021 The Society of Powder Technology Japan. Published by Elsevier B.V. and The Society of Powder Technology Japan. All rights reserved]; B) An overview of phytosynthesis of AgNPs by using *E. arvense* (a), gradual color change to brown representing the biofabrication of colloidal AgNPs during the biosynthesis process over 24 h (b) and the percentage of their a-amylase enzyme inhibition at different concentrations of AgNPs (c) [89]. Copyright © 2020 Published by Elsevier B.V. All rights reserved].

Besides, a study reported the plant-mediated synthesis of mostly spherical AgNPs (72.656 nm) using Arctium lappa root extract. The α-glucosidase inhibition was evaluated by using AgNPs at concentrations of 0.12, 0.25, and 0.50 µg.mL^{-1}, with an IC_{50} value of 0.653 µg.mL^{-1}. At 5 µg.mL^{-1}, the AgNPs achieved 95.41% inhibition of α-glucosidase activity [90]. Furthermore, a study reported the green synthesis of spherical AuNPs (25.31 nm) using Hylocereus polyrhizus fruit extract. The antidiabetic activity was evaluated through α-amylase inhibition, with AuNPs and acarbose tested at concentrations of 50, 100, and 200 µg.mL^{-1}. At 200 µg.mL^{-1}, AuNPs inhibited enzyme activity by 40.07 ± 0.65%, while acarbose inhibited it by 50.10 ± 0.13% [91]. Similarly, a study reported the phytofabrication of spherical AgNPs (35 to 55 nm) from Aeonium haworthii leaf extract. The antidiabetic activity was evaluated through α-amylase inhibition, with AgNPs and acarbose tested at concentrations of 10 to 120 µg.mL^{-1}. The IC_{50} values for the AgNPs and acarbose were 62.84 µg.mL^{-1} and 100.73 µg.mL^{-1}, respectively [92].

In addition, a study described the plant-mediated synthesis of spherical AuNPs (15.6 nm) using *Carduus edelbergii* extract. The antidiabetic potential was assessed via α-amylase inhibition, with AuNPs tested at concentrations ranging from 250 to 1000 µg.mL^{-1}. At the highest dose, enzyme inhibition reached 63.7 ± 5.1% [93]. Similarly, a study reported the green synthesis of AgNPs (25–125 nm) using Brachychiton populneus leaf extract. Their antidiabetic potential was evaluated through α-amylase inhibition, with AgNPs and acarbose tested at concentrations of 25–125 µg.mL^{-1}. The IC_{50} values were 67 µg.mL^{-1} for AgNPs and 110

μg.mL^{-1} for acarbose [94]. Furthermore, AgNPs (42 nm) were biosynthesized using *Eysenhardtia polystachya* extract and evaluated for antidiabetic activity via an α-amylase inhibition assay. Tested at concentrations of 10–100 μg.mL^{-1}, the IC_{50} values were 10 μg.mL^{-1} for AgNPs and 7.5 μg.mL^{-1} for acarbose [95]. Alternatively, AgNPs (50–100 nm) synthesized using *Myristica fragrans* extract were assessed for antidiabetic activity through α-amylase and α-glucosidase inhibition assays. At 1000 μg.mL^{-1}, AgNPs inhibited α-amylase by 52.48% and α-glucosidase by 56%, while acarbose showed 59.15% and 71% inhibition, respectively [96]. Besides, AgNPs (30–60 nm) synthesized using *Pueraria lobata* extract were evaluated for α-amylase inhibition to determine their antidiabetic potential. At the highest concentration (1000 μL), these NPs inhibited the enzyme by 36.33% [97]. Moreover, spherical AgNPs (15–20 nm) synthesized from Vitis vinifera fruit waste tannin extract were assessed for antidiabetic activity via α-amylase and α-glucosidase inhibition assays. The IC_{50} values for AgNPs were 43.94 μg.mL^{-1} and 48.5 μg.mL^{-1}, respectively, while acarbose exhibited IC_{50} values of 40.2 μg.mL^{-1} and 40 μg.mL^{-1} (Figure 6A) [98]. Likewise, AgNPs synthesized from Ananas comosus peel extract exhibited complete (100%) α-glucosidase inhibition at 0.063 μg.mL^{-1} (Figure 6B) [99].

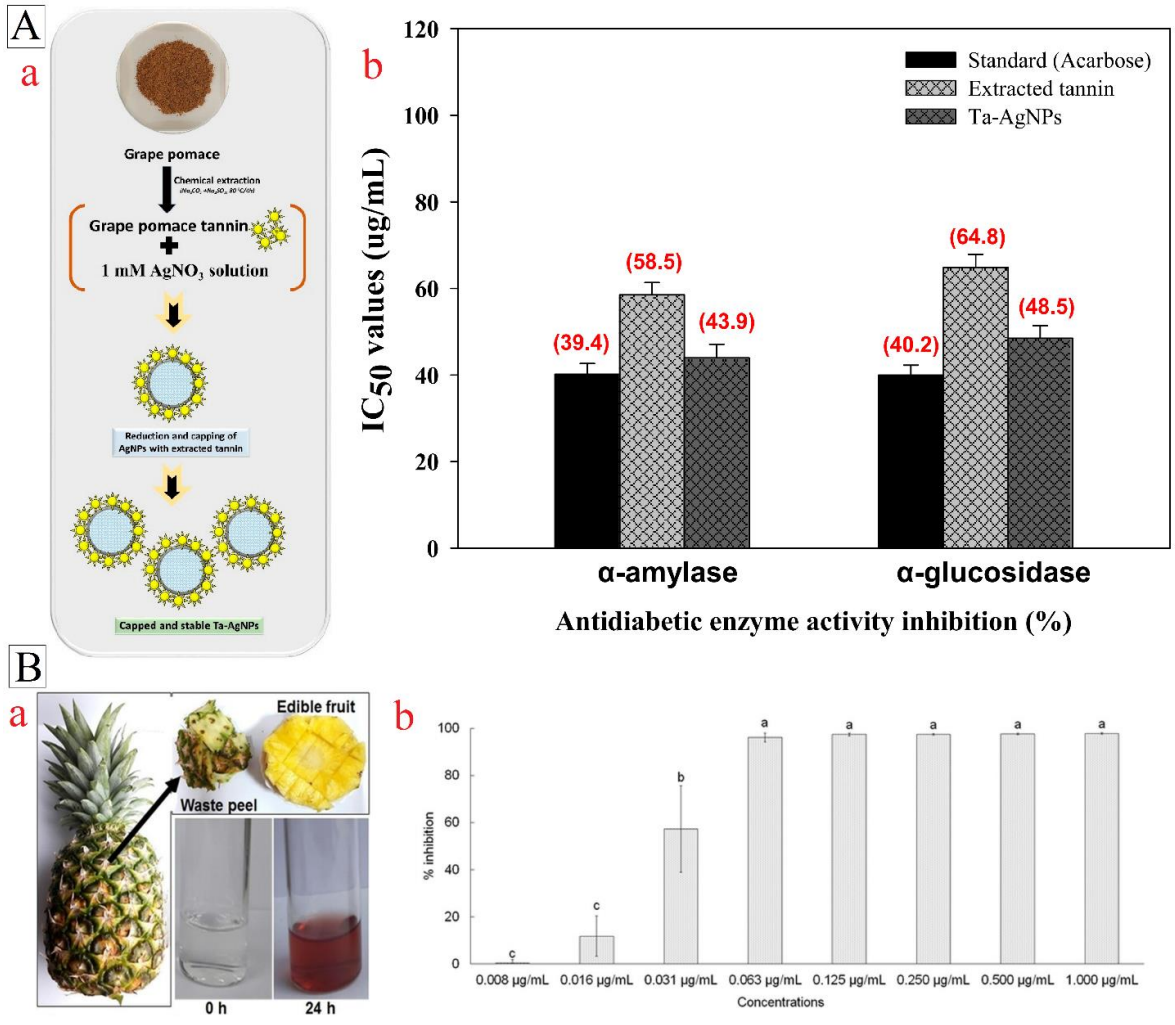

Fig. 6. A) *Vitis vinifera* fruit waste tannin as a natural source for the biosynthesis of AgNPs (a), and α-amylase/glucosidase inhibitory effect of biogenic AgNPs (b) [98] [Copyright © 2022 by the authors, Licensee MDPI, Basel, Switzerland. Open access article distributed under the terms and conditions of the Creative Commons Attribution (CC BY4.0) license]; B) Phytofabrication of AgNPs using outer peel extract of the fruit *Ananas comosus* led to a brown color colloidal AgNPs after 24 h incubation (a) and their α-glucosidase enzyme inhibition at different concentrations (b). Groups labeled with different letters (a, b, c) indicate statistically significant differences at $P<0.05$ [99] [Copyright © 2019, Das et al. Open access article distributed under the terms and conditions of the Creative Commons Attribution (CC BY4.0) license].

Likewise, spherical AgNPs were synthesized using *Hemigraphis repanda* peel extract, and the α-glucosidase inhibition assay revealed an IC_{50} of 1.98 $\mu g.mL^{-1}$ [100]. Additionally, spherical AgNPs (60–118 nm) synthesized from *Cissampelos pareira* leaf extract were tested for antidiabetic activity via α-glucosidase inhibition assay. At the highest concentration (100 $\mu g.mL^{-1}$), AgNPs exhibited 93% enzyme inhibition [101]. In a study, spherical AgNPs (500–5000 nm) synthesized from *Ajuga bracteosa* root and aerial component extracts were assessed for antidiabetic activity via α-glucosidase inhibition assay. At a concentration of 50 $\mu g.mL^{-1}$, AgNPs and acarbose inhibited the enzyme by 85.14% and 90.1%, respectively [102]. Likewise, spherical AgNPs (15.96 nm) synthesized from *Solanum khasianum* leaf extract were evaluated for α-amylase inhibition at concentrations of 200–1000 $\mu g.mL^{-1}$. The highest doses of AgNPs and acarbose inhibited α-amylase activity by 79.56% and 86.43%, respectively [103]. Furthermore, spherical AgNPs (40 nm) synthesized from *Hippeastrum hybridum* extract were tested for α-amylase inhibition at concentrations of 25–100 $\mu g.mL^{-1}$. The highest dose of AgNPs inhibited enzyme activity by 75.5% [104]. Alternatively, spherical AgNPs (10–30 nm) synthesized from *Azadirachta indica* seed extract were evaluated for α-amylase inhibition at concentrations of 50–100 $\mu g.mL^{-1}$. The IC_{50} for AgNPs was 76.80 $\mu g.mL^{-1}$, while acarbose exhibited an IC_{50} of 49.85 $\mu g.mL^{-1}$ [105]. Similarly, spherical AgNPs (21.4 nm) synthesized from *Flammulina velutipe* were evaluated for anti-diabetic activity through α-amylase and α-glucosidase inhibition assays at concentrations of 25–400 $\mu g.mL^{-1}$. The IC_{50} for acarbose was between 50 and 100 $\mu g.mL^{-1}$, while for AgNPs, the IC_{50} for α-amylase was 312 ± 0.67 $\mu g.mL^{-1}$ and for α-glucosidase, it was 357 ± 0.82 $\mu g.mL^{-1}$ [106].

In a study, spherical AgNPs (70–100 nm) synthesized from aqueous and alcoholic *Gymnema sylvestre* leaf extracts were evaluated for antidiabetic activity using the α-amylase assay at concentrations of 10–100 $\mu g.mL^{-1}$. At the maximum concentration, AgNPs synthesized from the aqueous and alcoholic extracts inhibited 42% and 46% of the enzyme activity, respectively, while acarbose inhibited 58% [107]. Besides, alga-mediated synthesis of spherical AuNPs (5.81–117.59 nm) from *Gelidiella acerosa* exhibited α-amylase and α-glucosidase inhibitory activities with IC_{50} values of 2.1 ± 0.01 $\mu g.mL^{-1}$ and 2.8 ± 0.02 $\mu g.mL^{-1}$, respectively [108]. Moreover, phytofabricated spherical AgNPs (5–15 nm) from *Bauhinia variegata* flower extract demonstrated α-amylase inhibitory potential with an IC_{50} value of 38 $\mu g.mL^{-1}$ [109].

Despite the notable enzyme inhibitory effects of biosynthesized nanosized silver and gold particles reported in the studies, the IC_{50} values for α-amylase and α-glucosidase inhibition differed among the various AuNPs and AgNPs. This could be attributed to the different particle sizes, shapes, surface charges and surface chemistries as well as the capping agents of biofabricated NPs. The above studies confirmed that every biological resources had their specific potential to fabricate Ag/Au nanostructures with unique physicochemical properties resulting in a unique biological performance. Overall, the in vitro studies ascertained the antidiabetic performance of these NPs which makes them interesting for their in vivo studies.

Antidiabetic activity of biosynthesized silver and gold nanomaterials: Animal-based evidence

Animal-based studies represented the considerable antidiabetic properties of biogenic AgNPs and AuNPs (Table 2). *(See Table 2 after references)* Figure 7 represents the interface of nanobiotechnology, animal studies, and clinical trials for the diabetes treatment. Here, we summarized the studies that evaluated the antidiabetic performance of the biogenic Ag/Au nanostructures in animal models. For instance, spherical AgNPs (1–100 nm) synthesized from *Ziziphora clinopodioides* extract were tested for antidiabetic activity using streptozotocin-induced diabetic Wistar rats. AgNPs were administered at concentrations of 50, 100, 200, and 400 $mg.kg^{-1}$. After 10 to 20 days of treatment, significant reductions in blood glucose levels were observed in the AgNP-treated groups compared to the untreated control group ($P<0.05$) [110]. Besides, quasi-spherical AgNPs (40 ± 5 nm) synthesized from *Salvia sclarea* extract were tested for antidiabetic activity in streptozotocin-induced diabetic Wistar rats. AgNPs were administered intraperitoneally at 10 $mg.kg^{-1}$. After treatment, significant reductions in fasting blood glucose (FBG) and HbA1c levels were observed, while insulin levels were significantly elevated in the AgNP-treated group compared to the control ($P<0.001$) [111]. Likewise, spherical AgNPs (30 ± 5 nm) synthesized from *Origanum majorana* extract were evaluated for antidiabetic activity in streptozotocin-induced diabetic rats. AgNPs were administered orally at 20 $mg.kg^{-1}$. Significant reductions in blood glucose levels were observed in the treated groups compared to the control group [112]. Alternatively, spherical AgNPs (35–40 nm) synthesized from

Ferula assafoetida extract were evaluated for antidiabetic activity in streptozotocin-induced diabetic rats. AgNPs were administered orally at 100 mg.kg^{-1} for 28 days. The treated group showed a significant reduction in blood glucose levels compared to the untreated group (P<0.05) [113]. Moreover, spherical AgNPs (42.47 nm) synthesized from *Kickxia elatine* extract were evaluated for antidiabetic activity in alloxan-induced diabetic Sprague-Dawley rats. AgNPs were administered orally at concentrations of 150, 300, and 450 mg.kg^{-1} for 7, 14, and 21 days. The treated groups showed a significant decrease in FBG levels compared to the control group (P<0.01) [114].

In a study, spherical AgNPs (40–100 nm) synthesized from Cassia *auriculata* flower extract were assessed for antidiabetic activity in streptozotocin-induced diabetic Wistar rats. AgNPs were administered at doses of 50 and 200 mg.kg^{-1}, with glibenclamide as the positive control. After 10 days of treatment, the groups receiving AgNPs showed significant reductions in FBG levels compared to the control group (P<0.01) [115]. Alternatively, spherical AgNPs (14.9 nm) synthesized from *Lawsonia inermis* extract were administered orally (200 mg.kg^{-1}) to streptozotocin-induced diabetic Wistar rats. After 14 days, significant reductions in FBG and increases in insulin levels were observed (P<0.001) [116]. Similarly, spherical AgNPs (22.5 nm) synthesized from *Momordica charantia* fruit extract were administered to streptozotocin-induced diabetic Wistar rats at 100 and 200 mg.kg^{-1}. After 14 days, both doses significantly reduced blood sugar levels (P<0.001), with an initial drop observed in an oral glucose tolerance test (OGTT) [117].

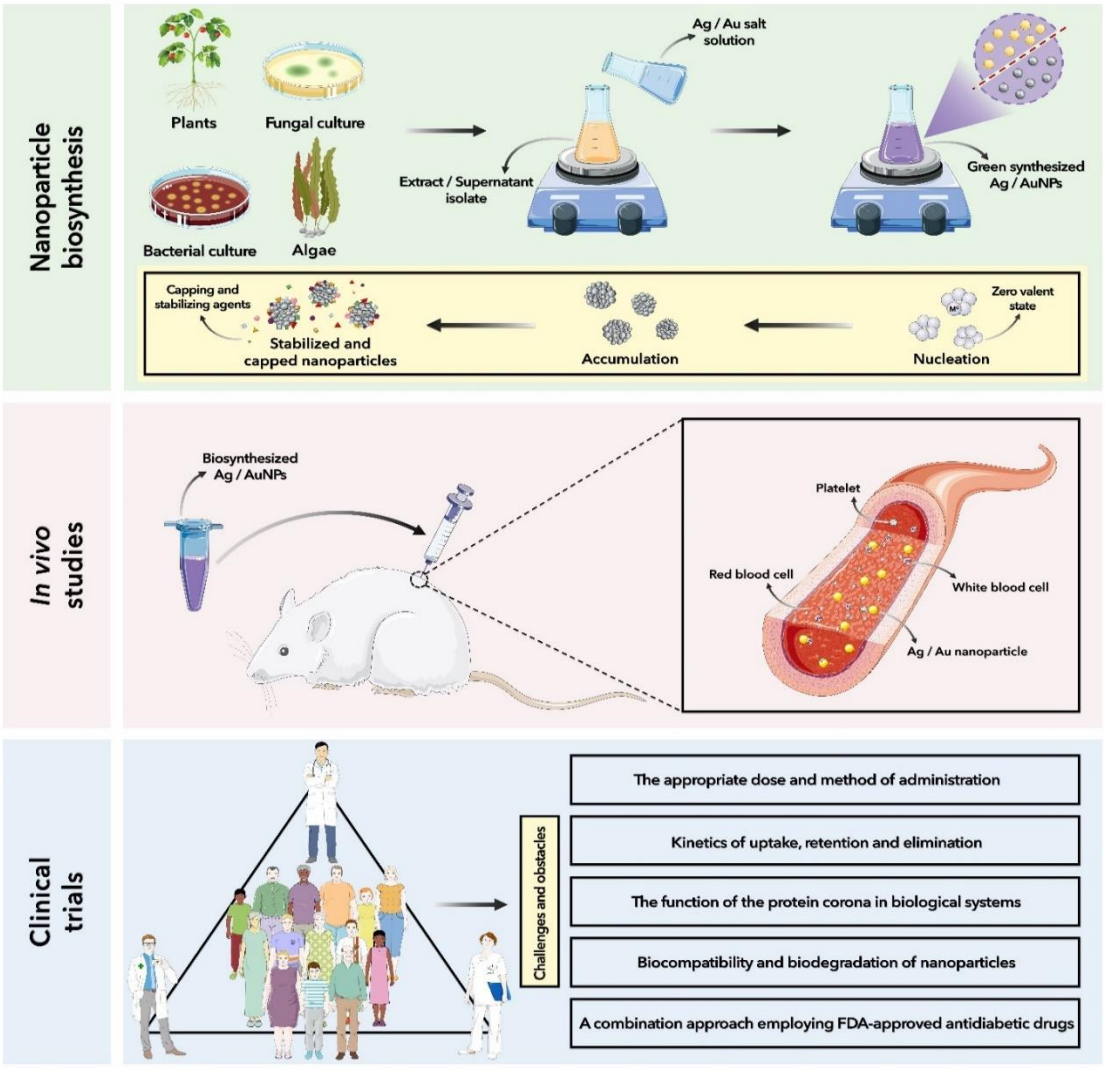

Fig. 7. A schematic representation of the relationship between nanoparticle biosynthesis, in vivo studies, and clinical trials for antidiabetic therapeutics. The figure was to some extent created using Servier Medical Art, which is provided by Servier and authorized under a Creative Commons Attribution 3.0 Unported License (https://creativecommons.org/licenses/by/3.0/).

Likewise, spherical AgNPs (10–50 nm) synthesized from *Ventilago maderaspatana* leaf extract were administered to streptozotocin-induced diabetic albino rats at doses of 20 $mg.kg^{-1}$ (AgNPs) and 5 $mg.kg^{-1}$ (glibenclamide), with a negative control group receiving only streptozotocin. After 15 days, a significant decrease in HbA_1C and blood sugar levels, along with an increase in insulin levels, was observed [118]. Besides, spherical AgNPs (5–47 nm) synthesized from *Emblica Phyllanthus* leaf extract were administered orally to alloxan-induced diabetic albino mice at doses of 150 and 300 $mg.kg^{-1}$. Blood sugar levels were significantly reduced after both short-term (3 and 5 hours) and long-term (4, 7, 10, and 15 days) evaluations (P<0.05) [119]. Moreover, spherical AgNPs (21.5 nm) synthesized from *Gymnema sylvestre* extract were orally administered to streptozotocin-induced diabetic Wistar rats at doses of 100 and 200 $mg.kg^{-1}$. After 14 days, blood sugar levels were significantly reduced, and insulin levels increased in the treated groups (P<0.05) [120]. Additionally, spherical AgNPs (45 nm) synthesized from *Catharanthus roseus* extract were administered with the plant extract at 500 $mg.kg^{-1}$ to streptozotocin-induced diabetic rats. Glimepiride (2 mg) was used as a positive control. After 60 and 120 min in the OGTT, the group receiving AgNPs plus extract showed superior results compared to glimepiride, with significant improvements (P<0.05) [121]. In a study, spherical AgNPs (15–31.44 nm) synthesized from *Taverniera couneifolia* extract were administered at 10 $mg.kg^{-1}$ to alloxan-induced diabetic Wistar rats. Glibenclamide (0.5 $mg.kg^{-1}$) and the extract (10 $mg.kg^{-1}$) were used in separate groups, with one control group receiving only alloxan. After 21 days, FBG levels significantly decreased (P<0.05) after 14 and 21 days. In the OGTT, blood sugar dropped at 60, 90, and 120 min after glucose administration (2 grams) (Figure 8A) [122]. Similarly, spherical AgNPs (12–28 nm) synthesized from *Phagnalon niveum* extract were administered orally at 10 $mg.kg^{-1}$ to alloxan-induced diabetic Wistar rats. The groups included extract alone (200 $mg.kg^{-1}$), glibenclamide (0.5 $mg.kg^{-1}$), and a control with no treatment. FBG levels significantly decreased in the AgNP-treated group after 15 and 21 days (P<0.05) (Figure 8B). The OGTT showed that rats treated with AgNPs exhibited high glucose tolerance (Figure 8C) [123]. Alternatively, spherical AgNPs (42 nm) synthesized from *Thymus serpyllum* extract were administered to streptozotocin-induced diabetic Balb/c mice at doses of 5 and 10 $mg.kg^{-1}$. Mice were divided into groups: one group received no treatment, another received metformin (100 $mg.kg^{-1}$), and the remaining groups received AgNPs. The intraperitoneal glucose tolerance test (IPGTT) showed significant reductions in blood sugar after glucose administration on day 29, and insulin tolerance tests (ITT) on day 31 also indicated improved blood sugar control (Figures 8D, 8E, and 8F) [95].

In a study, spherical AgNPs (45 nm) synthesized from *Eryngium thyrsoideum* Bioss extract was injected at 2.5 $mg.kg^{-1}$ into alloxan-induced diabetic rats (150 $mg.kg^{-1}$). FBG levels decreased significantly after 7 and 15 days, while HbA_1C declined after 15 days (P≤0.05). Chemically synthesized AgNPs exhibited similar effects [124]. Besides, spherical AuNPs (9 nm) synthesized from *Eryngium thyrsoideum* Boiss extract were injected at 1, 2.5, and 5 $mg.kg^{-1}$ into nicotinamide (110 $mg.kg^{-1}$) and streptozotocin (55 $mg.kg^{-1}$)-induced diabetic Wistar rats. FBG levels exceeded 250 $mg.dL^{-1}$ after three days. Significant reductions in FBG were observed in all AuNP-treated groups after 7, 14, and 21 days (P≤0.05) [125]. In addition, spherical AgNPs (500–5000 nm, tube-like) synthesized from *Ajuga bracteosa* root and aerial part extract were orally administered at 200 and 400 $mg.kg^{-1}$ to alloxan-induced diabetic Balb/c mice. Additional groups received the extract alone or glibenclamide. After 14 days, significant reductions in blood sugar and increases in insulin levels were observed (P<0.05) [126]. Likewise, spherical AgNPs (20–40 nm) synthesized from *Moringa oleifera* leaf extract were administered orally (0.2 $mg.kg^{-1}$) to streptozotocin-induced diabetic Wistar rats (n=6). Additional groups received glibenclamide (0.5 $mg.kg^{-1}$) or streptozotocin alone. After 28 days, blood insulin levels increased, and blood sugar levels significantly decreased (P<0.001) [127]. Similarly, spherical AgNPs (132.6 nm) synthesized from *Pterocarpus marsupium* bark extract were administered orally (200 $mg.kg^{-1}$) to streptozotocin-nicotinamide-induced diabetic Wistar rats. Additional groups received glibenclamide (2.5 $mg.kg^{-1}$), plant extract (200 $mg.kg^{-1}$), or no treatment. Blood glucose levels significantly decreased in the AgNP-treated group (P<0.001) [128]. Moreover, spherical AgNPs (123.8 nm) synthesized from *Zingiber officinale* rhizome extract were administered orally (200 $mg.kg^{-1}$) to streptozotocin-induced diabetic Wistar rats. Additional groups received metformin (10 $mg.kg^{-1}$) or no treatment. FBG levels significantly decreased after 3, 5, and 7 days [129].

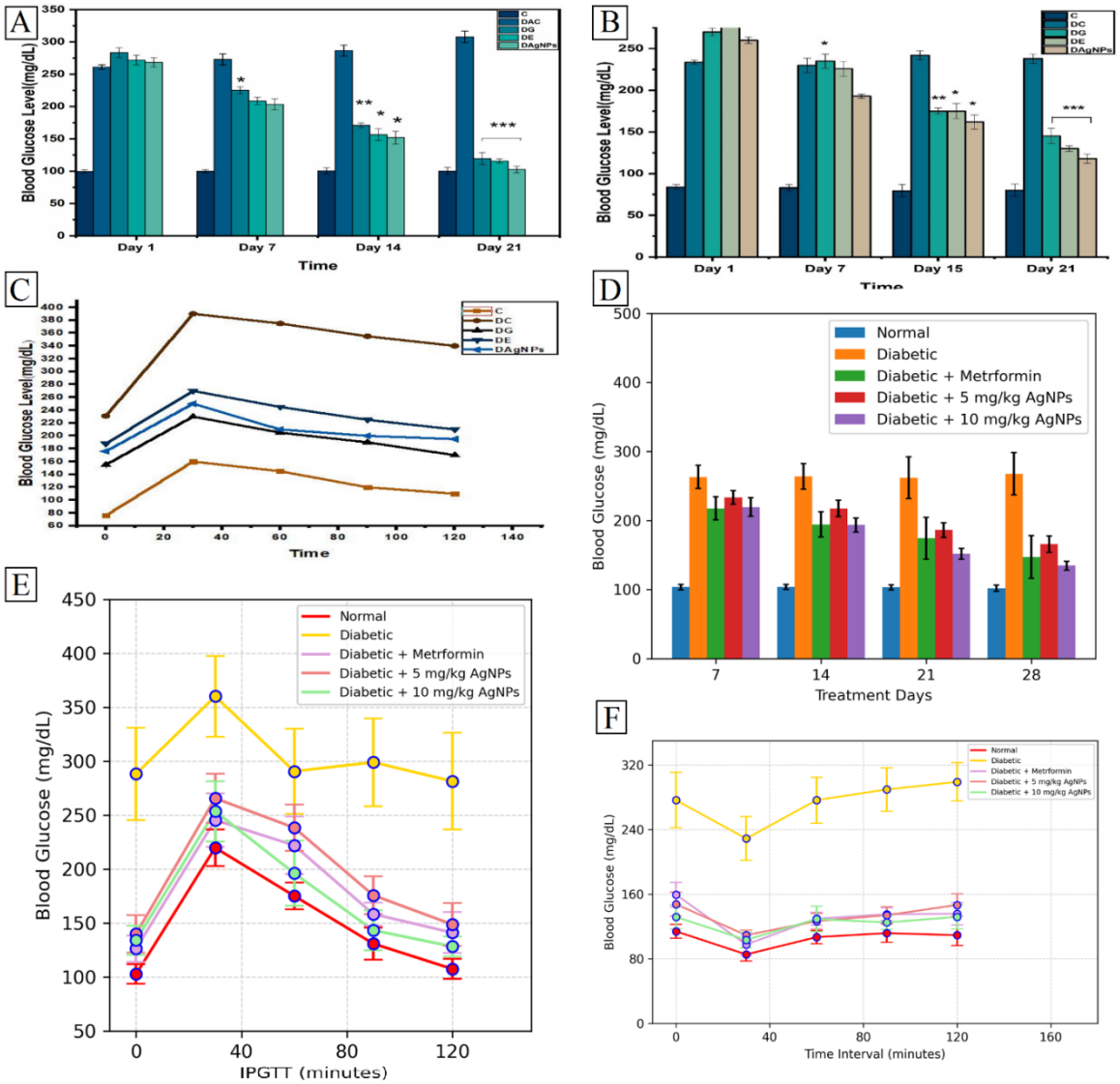

Fig. 8. A) The blood glucose levels of various Wistar rat groups were monitored over 1, 7, 14, and 21 days: (C) Non-diabetic (healthy) rats, (DAC) Diabetic Wistar rats without treatment, (DG) Diabetic Wistar rats receiving glibenclamide, (DE) Diabetic Wistar rats administered with plant extract, and (DAgNPs) Diabetic Wistar rats treated with AgNPs [122] [Copyright © 2022 by the authors, Licensee MDPI, Basel, Switzerland. Open access article distributed under the terms and conditions of the Creative Commons Attribution (CC BY4.0) license]; B) The levels of FBG found in the Wistar rats belonging to the various groups after 1, 7, 15, and 21 days: (C) Healthy rats, (DC) Diabetic rats that received no additional substances, (DG) Diabetic rats that received glibenclamide, (DE) Diabetic rats that received an extract of *Phagnalon niveum*, and (DAgNPs) Diabetic rats that received AgNPs [123] [Copyright © 2022 by the authors, Licensee MDPI, Basel, Switzerland. Open access article distributed under the terms and conditions of the Creative Commons Attribution (CC BY4.0) license]; C) The levels of OGTT found in the Wistar rats belonging to the various groups after 30, 60, 90, and 120 min: (C) Healthy rats, (DC) Diabetic rats that received no additional substances, (DG) Diabetic rats that received glibenclamide, (DE) Diabetic rats that received an extract of *Phagnalon niveum*, and (DAgNPs) Diabetic rats that received AgNPs [123] [Copyright © 2022 by the authors, Licensee MDPI, Basel, Switzerland. Open access article distributed under the terms and conditions of the Creative Commons Attribution (CC BY4.0) license]; **D)** The blood glucose level of a different group of Balb/c mice after 7, 14, 21, and 28 days [95] [Copyright © 2022 by the authors, Licensee MDPI, Basel, Switzerland. Open access article distributed under the terms and conditions of the Creative Commons Attribution (CC BY4.0) license]; **E)** IPGTT level of a different group of Balb/c mice after 30, 60, 90, and 120 mins [95] [Copyright © 2022 by the authors, Licensee MDPI, Basel, Switzerland. Open access article distributed under the terms and conditions of the Creative Commons Attribution (CC BY4.0) license]; **F)** ITT level of a different group of Balb/c mice after 30, 60, 90, and 120 mins [95] [Copyright © 2022 by the authors, Licensee MDPI, Basel, Switzerland. Open access article distributed under the terms and conditions of the Creative Commons Attribution (CC BY4.0) license].

In a study, spherical AgNPs (51.12–65.02 nm) synthesized from *Psidium guajava* extracts were administered orally (100 $mg.kg^{-1}$) to streptozotocin-induced diabetic Wistar rats. Additional groups received *Psidium guajava* extract (100 and 200 $mg.kg^{-1}$) or metformin (100 $mg.kg^{-1}$). Blood sugar levels significantly decreased ($P<0.001$) [130]. Besides, spherical AgNPs (77.7 nm) synthesized from *Nigella sativa* seed extract were administered to alloxan-induced diabetic albino mice. Blood

glucose levels were measured on days 0, 14, and 28, revealing a significant reduction in the AgNP-treated group [131]. Moreover, spherical AgNPs synthesized from *Momordica charantia* extract (10 $mg.kg^{-1}$) were administered orally to streptozotocin-induced diabetic rats. After 21 days, the AgNP-treated group showed a significant reduction in blood sugar levels ($P<0.05$) compared to the control groups [132]. Similarly, spherical AgNPs synthesized from *Musa paradisiaca* stem extract (50 $\mu g.kg^{-1}$) were administered to streptozotocin and nicotinamide-induced diabetic Sprague-Dawley rats. After 8 weeks, blood sugar and insulin levels in the AgNP group significantly decreased and increased, respectively ($P<0.05$), compared to the control groups [133]. Additionally, Spherical AgNPs (10–12 nm) synthesized from *Eysenhardtia polystachya* bark extract were administered to glucose-induced diabetic Zebrafish at doses of 5 and 10 $\mu g.mL^{-1}$. After 14 days, blood sugar levels decreased and insulin levels increased significantly in the AgNP-treated groups compared to the control group ($P<0.05$) [134]. Moreover, spherical AgNPs (4–25 nm) synthesized from *Solanum nigrum* extract were orally administered at 10 mg/kg to alloxan-induced diabetic Wistar rats at a dose of 10 $mg.kg^{-1}$. After 21 days, blood sugar levels were significantly reduced in the AgNP-treated group, with the OGTT showing lower blood glucose levels at 60, 90, and 120 min ($P<0.05$) [135]. In a study, spherical AuNPs (75.1–156.5 nm) synthesized from *Datura stramonium* seed extract were administered to alloxan-induced diabetic albino rats at doses of 500, 750, and 1000 $\mu g.mL^{-1}$ for 21 days. The FBG levels significantly decreased in all groups receiving AuNPs, with the glibenclamide-treated group serving as a positive control [136]. Alternatively, spherical AuNPs (7–27 nm) synthesized from *Ziziphus jujube fruit extract were administered* to streptozotocin-induced diabetic Sprague-Dawley rats at doses of 0.5 and 1 $mg.kg^{-1}$ for 21 days. After 21 days, the group receiving 1 $mg.kg^{-1}$ AuNPs showed significant reductions in FBG and Homeostatic Model Assessment of Insulin Resistance (HOMA-IR) levels and increased insulin levels ($P<0.03$). In the 0.5 $mg.kg^{-1}$ AuNPs group, HOMA-IR significantly decreased ($P<0.05$), FBG decreased, and insulin increased, but the differences were not statistically significant [137]. Besides, spherical AuNPs (15 nm) synthesized using *Bauhinia variegata* extract were administered to streptozotocin-induced diabetic Wistar rats at a dose of 2.58 $mL.kg^{-1}$ for 28 days. After 28 days, significant reductions in FBG levels were observed ($P<0.000$). The study also included groups treated with *Bauhinia variegata* extract at a dose of 1.83 $mL.kg^{-1}$ and a control group with no additional treatment [138]. Likewise, rectangular and triangular AuNPs (55.2–98.2 nm) synthesized using *Cassia fistula* stem bark extract were administered to streptozotocin-induced diabetic Wistar rats at a dose of 60 $mg.kg^{-1}$ for 30 days. After 15 and 30 days, FBG levels significantly decreased, and HbA_1C levels were dramatically reduced at the 30-day mark ($P<0.05$). In contrast, the extract and AuNPs did not affect FBG and HbA_1C levels in healthy rats. The study also included groups receiving insulin (3 $IU.kg^{-1}$) as the positive control and no treatment as the negative control [139]. In addition, spherical AuNPs (20–50 nm) synthesized using *Dittrichia viscosa* leaf extract were administered to streptozotocin-induced diabetic Sprague-Dawley rats at a dose of 2.5 $mg.kg^{-1}$. Significant reductions in blood sugar levels were observed in the AuNPs-treated group compared to the control group ($P<0.02$) [140]. Moreover, spherical AuNPs (50 nm) synthesized using *Gymnema sylvestre* leaf extract were administered to alloxan-induced diabetic Wistar rats at a dose of 0.5 $mg.kg^{-1}$ for 28 days. Significant reductions in FBG and HbA_1C levels, along with increased insulin levels, were observed ($P<0.001$). The study also included a positive control group treated with glibenclamide and a negative control group with no treatment. No significant differences were observed in healthy rats treated with AuNPs [141]. Notably, despite the heterogeneity across the above studies, such as differences in animal models, biological resources for NP fabrication, administration routes, treatment durations, administered NP doses, diabetes induction methods, particle morphology, and size distribution, most studies reported significant reductions in blood glucose levels and HbA_1C, along with a notable increase in blood insulin levels in diabetic animals treated with these nanomaterials.

Challenges of bioengineered nanosized silver and gold particles for future antidiabetic nanomedicine

The utilization of biofabricated AgNPs and AuNPs in antidiabetic therapies holds significant promise due to their unique physicochemical properties and biological activities. However, translating these advancements from the laboratory to clinical applications presents numerous challenges. These challenges must be addressed to ensure the safe and effective integration of these nanomaterials into therapeutic practices [142]. One of the foremost concerns in employing nanosized particles for therapeutic applications is their potential toxicity and

biocompatibility. Although many in vitro studies demonstrate low cytotoxicity, in vivo applications reveal potential risks such as accumulation in vital organs, including the kidneys, liver, and spleen. This accumulation can trigger oxidative stress, inflammation, and even organ damage [143]. Moreover, long-term exposure raises concerns about the prolonged retention of NPs in the body and the possibility of unforeseen chronic side effects. The dose-dependent effects of NPs further complicate their therapeutic use, as identifying an optimal dose that is both effective and non-toxic remains challenging. These issues are compounded by individual variations in metabolism and disease progression, necessitating more comprehensive studies [144]. On the other hand, while preclinical studies provide encouraging results, several obstacles hinder the clinical translation of bioengineered NPs. A significant challenge is the lack of standardization in synthesis methods, leading to variations in nanoparticle size, shape, and surface properties. These variations influence biological activity and pose difficulties in ensuring reproducibility across different batches [145]. Additionally, while green synthesis methods offer cost-effective and environmentally friendly solutions, scaling these processes for industrial production remains technically challenging. Maintaining consistent quality at such a scale is critical yet difficult to achieve. It is noted that regulatory and approval challenges further complicate the clinical translation of these nanomaterials. As a relatively new class of therapeutic agents, NPs are subject to evolving regulatory frameworks. Generating the extensive safety and efficacy data required for regulatory approval is resource-intensive and time-consuming. Moreover, the limited number of clinical trials investigating the use of metallic NPs for diabetes management delays their acceptance into mainstream medicine. Furthermore, although green synthesis addresses some environmental concerns, large-scale production of nanoparticles still raises questions. While green synthesis is more cost-effective than conventional chemical methods, scaling these processes to meet global demand can involve high initial investments, posing economic challenges. Addressing these challenges requires interdisciplinary collaboration and innovative approaches. Advanced toxicological studies, including long-term animal studies and well-designed clinical trials, are essential for understanding the biocompatibility and safety profiles of AgNPs and AuNPs. Additionally, government-industry collaborations are needed to establish regulatory policies that support the safe and ethical development of nanoparticle-based therapies. By fostering such collaborations and addressing the outlined challenges, the field can progress toward developing safer, more effective antidiabetic nanomedicines that harness the full potential of biofabricated nanosized silver and gold particles.

CONCLUSION

In this review, the current antidiabetic therapeutics were reviewed, their advantages and disadvantages were mentioned and the need to explore innovative approaches for antidiabetic therapy was discussed. Afterward, the green synthesis of nanosized silver and gold particles by using plants, algae, and microorganisms was reviewed. This study showed that a wide range of biological resources can be employed for the biosynthesis of silver and gold nanomaterials with specific particle shapes and size distribution. Interestingly, the influencingbioengineered silver and gold nanosized particles represented the enzyme inhibitory activity against two key enzymes of diabetes. More interestingly, the diabetic animal models confirmed the antidiabetic properties of the green-fabricated AgNPs and AuNPs, showing decreases in blood glucose levels and HbA_1C, along with increased blood insulin levels in the treated samples. While strong evidence supports the significant antidiabetic potential of biogenic AgNPs and AuNPs as nanotherapeutics, future research is necessary to assess the pharmacokinetics, pharmacodynamics,elucidate their pharmacokinetic and pharmacodynamic profiles and assess acute and chronic toxicities of these nanostructures.

ACKNOWLEDGMENT

Not applicable.

AUTHOR CONTRIBUTIONS

Hamed Barabadi: project administration, conceptualization, supervision, Investigation, methodology, writing – original draft, writing – review and editing; Hesam Noqani: Investigation, methodology, writing – original draft, writing – review and editing; Kamyar Jounaki: Investigation, methodology, writing – original draft, writing – review and editing; Ayeh Sabbagh Kashani: Investigation, methodology, writing – original draft, writing – review and editing; Fatemeh Ashouri: Investigation, methodology, writing – original draft, writing – review and editing; Ebrahim Mostafavi: project administration, conceptualization, supervision, Investigation, methodology, writing – original draft, writing – review and editing

FUNDING

This work was supported by a grant from Shahid Beheshti University of Medical Sciences, Tehran, Iran (Grant Number 43005657).

DATA AVAILABILITY

Not applicable.

CONFLICT OF INTEREST

The authors declare no competing interests.

HUMAN AND ANIMAL RIGHTS AND INFORMED CONSENT

This article contains no studies with human or animal subjects performed by the authors.

REFERENCES

1. Sneha N, Gangil T. Analysis of diabetes mellitus for early prediction using optimal features selection. J Big Data. 2019;6:1–19.
2. Kocher T, König J, Borgnakke WS, Pink C, Meisel P. Periodontal complications of hyperglycemia/diabetes mellitus: epidemiologic complexity and clinical challenge. Periodontol 2000. 2018;78:59–97.
3. Unnikrishnan R, Misra A. Infections and diabetes: risks and mitigation with reference to India. Diabetes Metab Syndr Clin Res Rev. 2020;14:1889–1894.
4. Van Enter BJ, Von Hauff E. Challenges and perspectives in continuous glucose monitoring. Chem Commun. 2018;54:5032–5045.
5. Wukich DK, Raspovic KM, Jupiter DC, Heineman N, Ahn J, Johnson MJ, et al. Amputation and infection are the greatest fears in patients with diabetes foot complications. J Diabetes Complications. 2022;36:108222.
6. Gupta S, Eavey RD, Wang M, Curhan SG, Curhan GC. Type 2 diabetes and the risk of incident hearing loss. Diabetologia. 2019;62:281–285.
7. Ninomiya T. Epidemiological evidence of the relationship between diabetes and dementia. Diabetes Mellitus. 2019;1:13–25.
8. Zaki N, Alashwal H, Ibrahim S. Association of hypertension, diabetes, stroke, cancer, kidney disease, and high-cholesterol with COVID-19 disease severity and fatality: a systematic review. Diabetes Metab Syndr Clin Res Rev. 2020;14:1133–1142.
9. Sun H, Saeedi P, Karuranga S, Pinkepank M, Ogurtsova K, Duncan BB, et al. IDF Diabetes Atlas: global, regional and country-level diabetes prevalence estimates for 2021 and projections for 2045. Diabetes Res Clin Pract. 2022;183:109119.
10. Barron E, Bakhai C, Kar P, Weaver A, Bradley D, Ismail H, et al. Associations of type 1 and type 2 diabetes with COVID-19-related mortality in England: a whole-population study. Lancet Diabetes Endocrinol. 2020;8:813–822.
11. Ang GY. Age of onset of diabetes and all-cause mortality. World J Diabetes. 2020;11(5):95.
12. McIntyre HD, Catalano P, Zhang C, Desoye G, Mathiesen ER, Damm P. Gestational diabetes mellitus. Nat Rev Dis Primers. 2019;5:1–19.
13. Dal Canto E, Ceriello A, Rydén L, Ferrini M, Hansen TB, Schnell O, et al. Diabetes as a cardiovascular risk factor: an overview of global trends of macro and micro vascular complications. Eur J Prev Cardiol. 2019;26(2_suppl):25–32.
14. Manne-Goehler J, Geldsetzer P, Agoudavi K, Andall-Brereton G, Aryal KK, Bicaba BW, et al. Health system performance for people with diabetes in 28 low- and middle-income countries: a cross-sectional study of nationally representative surveys. PLoS Med. 2019;16:e1002751.
15. Kabadi UM. Non-insulin therapeutic option in management of diabetes: life style modification; diet and exercise. J Diabetes Mellitus. 2021;11:288–304.
16. Perkins BA, Sherr JL, Mathieu C. Type 1 diabetes glycemic management: insulin therapy, glucose monitoring, and automation. Science. 2021;373:522–527.
17. Kahn SE, Cooper ME, Del Prato S. Pathophysiology and treatment of type 2 diabetes: perspectives on the past, present, and future. Lancet. 2014;383:1068–1083.
18. Pongwecharak J, Maila-ead C, Sakulthap J, Sripanitkulchai N. Evaluation of the uses of aspirin, statins and ACEIs/ARBs in a diabetes outpatient population in southern Thailand. J Eval Clin Pract. 2007;13:221–226.
19. Adu MD, Malabu UH, Malau-Aduli AE, Malau-Aduli BS. Enablers and barriers to effective diabetes self-management: a multi-national investigation. PLoS One. 2019;14:e0217771.
20. Ma S, Wang L, Chen J, Zhao Y, Jiang T. The effect of laparoscopic sleeve gastrectomy on type 2 diabetes remission outcomes in patients with body mass index between 25 kg/m2 and 32.5 kg/m2. Asian J Surg. 2022;45:315–319.
21. Nimase PK, Vidyasagar G, Suryawanshi D, Bathe R. Nanotechnology and diabetes. Int J Adv Pharm. 2013;2:40–44.
22. Sharma G, Sharma AR, Nam JS, Doss GPC, Lee SS, Chakraborty C. Nanoparticle based insulin delivery system: the next generation efficient therapy for type 1 diabetes. J Nanobiotechnology. 2015;13:1–13.
23. Gong R, Chen G. Preparation and application of functionalized nano drug carriers. Saudi Pharm J. 2016;24:254–257.
24. Levin E, Bud'ko S, Mao J, Huang Y, Schmidt-Rohr K. Effect of magnetic particles on NMR spectra of Murchison meteorite organic matter and a polymer-based model system. Solid State Nucl Magn Reson. 2007;31:63–71.
25. Chen W, Guo M, Wang S. Anti prostate cancer using PEGylated bombesin containing, cabazitaxel loading nano-sized drug delivery system. Drug Dev Ind Pharm. 2016;42:1968–1976.
26. Fricain JC, Schlaubitz S, Le Visage C, Arnault I, Derkaoui SM, Siadous R, et al. A nano-hydroxyapatite–pullulan/dextran polysaccharide

composite macroporous material for bone tissue engineering. Biomaterials. 2013;34:2947–2959.
27. Seelig J, Leslie K, Renn A, Kühn S, Jacobsen V, van de Corput M, et al. Nanoparticle-induced fluorescence lifetime modification as nanoscopic ruler: demonstration at the single molecule level. Nano Lett. 2007;7:685–689.
28. Surendiran A, Sandhiya S, Pradhan S, Adithan C. Novel applications of nanotechnology in medicine. Indian J Med Res. 2009;130:689–701.
29. Tewabe A, Abate A, Tamrie M, Seyfu A, Siraj EA. Targeted drug delivery—from magic bullet to nanomedicine: principles, challenges, and future perspectives. J Multidiscip Healthc. 2021;14:1711–1724.
30. Yang S, Chen C, Qiu Y, Xu C, Yao J. Paying attention to tumor blood vessels: cancer phototherapy assisted with nano delivery strategies. Biomaterials. 2021;268:120562.
31. He Y, Al-Mureish A, Wu N. Nanotechnology in the treatment of diabetic complications: a comprehensive narrative review. J Diabetes Res. 2021;2021:1–13.
32. Rashid R, Naqash A, Bader GN, Sheikh FA. Nanotechnology and diabetes management: recent advances and future perspectives. Appl Nanotechnol Biomed Sci. 2020;1(1):99–117.
33. Singh AP, Biswas A, Shukla A, Maiti P. Targeted therapy in chronic diseases using nanomaterial-based drug delivery vehicles. Signal Transduct Target Ther. 2019;4:1–21.
34. Barabadi H. Nanobiotechnology: a promising scope of gold biotechnology. Cell Mol Biol Biophys. 2017;63:3–4.
35. Burlec AF, Corciova A, Boev M, Batir-Marin D, Mircea C, Cioanca O, et al. Current overview of metal nanoparticles' synthesis, characterization, and biomedical applications, with a focus on silver and gold nanoparticles. Pharmaceuticals. 2023;16:1–25.
36. Arif R, Uddin R. A review on recent developments in the biosynthesis of silver nanoparticles and its biomedical applications. Med Devices Sens. 2021;4:e10158.
37. Garg D, Sarkar A, Chand P, Bansal P, Gola D, Sharma S, et al. Synthesis of silver nanoparticles utilizing various biological systems: mechanisms and applications—a review. Prog Biomater. 2020;9:81–95.
38. Elbahnasawy MA, Shehabeldine AM, Khattab AM, Amin BH, Hashem AH. Green biosynthesis of silver nanoparticles using novel endophytic Rothia endophytica: characterization and anticandidal activity. J Drug Deliv Sci Technol. 2021;62:102401.
39. Ibrahim E, Fouad H, Zhang M, Zhang Y, Qiu W, Yan C, et al. Biosynthesis of silver nanoparticles using endophytic bacteria and their role in inhibition of rice pathogenic bacteria and plant growth promotion. RSC Adv. 2019;9:29293–29299.
40. Patil MP, Kang MJ, Niyonizigiye I, Singh A, Kim JO, Seo YB, et al. Extracellular synthesis of gold nanoparticles using the marine bacterium Paracoccus haeundaensis BC74171T and evaluation of their antioxidant activity and antiproliferative effect on normal and cancer cell lines. Colloids Surf B Biointerfaces. 2019;183:110455.
41. Li S, Duan Y, Li R, Wang X. Intracellular and extracellular biosynthesis of antibacterial silver nanoparticles by using Pseudomonas aeruginosa. J Nanosci Nanotechnol. 2017;17:9186–9191.
42. Shunmugam R, Balusamy SR, Kumar V, Menon S, Lakshmi T, Perumalsamy H. Biosynthesis of gold nanoparticles using marine microbe (Vibrio alginolyticus) and its anticancer and antioxidant analysis. J King Saud Univ Sci. 2021;33:101260.
43. Bharti S, Mukherji S, Mukherji S. Extracellular synthesis of silver nanoparticles by Thiosphaera pantotropha and evaluation of their antibacterial and cytotoxic effects. 3 Biotech. 2020;10:237.
44. Eid AM, Fouda A, Niedbała G, Hassan SE, Salem SS, Abdo AM, et al. Endophytic Streptomyces laurentii mediated green synthesis of Ag-NPs with antibacterial and anticancer properties for developing functional textile fabric properties. Antibiotics. 2020;9:641.
45. Iqtedar M, Aslam M, Akhyar M, Shehzaad A, Abdullah R, Kaleem A. Extracellular biosynthesis, characterization, optimization of silver nanoparticles (AgNPs) using Bacillus mojavensis BTCB15 and its antimicrobial activity against multidrug resistant pathogens. Prep Biochem Biotechnol. 2019;49:136–142.
46. Mortazavi SM, Khatami M, Sharifi I, Heli H, Kaykavousi K, Sobhani Poor MH, et al. Bacterial biosynthesis of gold nanoparticles using Salmonella enterica subsp. enterica serovar Typhi isolated from blood and stool specimens of patients. J Clust Sci. 2017;28:2997–3007.
47. Parikh RY, Singh S, Prasad B, Patole MS, Sastry M, Shouche YS. Extracellular synthesis of crystalline silver nanoparticles and molecular evidence of silver resistance from Morganella sp.: towards understanding biochemical synthesis mechanism. ChemBioChem. 2008;9:1415–1422.
48. Rajasekar T, Karthika K, Muralitharan G, Maryshamya A, Sabarika S, Anbarasu S, et al. Green synthesis of gold nanoparticles using extracellular metabolites of fish gut microbes and their antimicrobial properties. Braz J Microbiol. 2020;51:957–967.
49. Shivaji S, Madhu S, Singh S. Extracellular synthesis of antibacterial silver nanoparticles using psychrophilic bacteria. Process Biochem. 2011;46:1800–1807.
50. Singh H, Du J, Singh P, Yi TH. Extracellular synthesis of silver nanoparticles by Pseudomonas sp. THG-LS1.4 and their antimicrobial application. J Pharm Anal. 2018;8:258–264.
51. Qamar SUR, Ahmad JN. Nanoparticles: mechanism of biosynthesis using plant extracts, bacteria, fungi, and their applications. J Mol Liq. 2021;334:116040.
52. Ahmad S, Munir S, Zeb N, Ullah A, Khan B, Ali J, et al. Green nanotechnology: a review on green synthesis of silver nanoparticles—an ecofriendly approach. Int J Nanomedicine. 2019;14:5087–5107.
53. Potbhare AK, Chouke PB, Mondal A, Thakare RU, Mondal S, Chaudhary RG, et al. Rhizoctonia solani

assisted biosynthesis of silver nanoparticles for antibacterial assay. Mater Today Proc. 2020;29:939–945.
54. Naimi-Shamel N, Pourali P, Dolatabadi S. Green synthesis of gold nanoparticles using Fusarium oxysporum and antibacterial activity of its tetracycline conjugant. J Mycol Med. 2019;29:7–13.
55. Qu Y, Li X, Lian S, Dai C, Jv Z, Zhao B, et al. Biosynthesis of gold nanoparticles using fungus Trichoderma sp. WL-Go and their catalysis in degradation of aromatic pollutants. IET Nanobiotechnol. 2019;13:12–17.
56. Kumari RM, Kumar V, Kumar M, Pareek N, Nimesh S. Assessment of antibacterial and anticancer capability of silver nanoparticles extracellularly biosynthesized using Aspergillus terreus. Nano Express. 2020;1:030011.
57. Taha ZK, Hawar SN, Sulaiman GM. Extracellular biosynthesis of silver nanoparticles from Penicillium italicum and its antioxidant, antimicrobial and cytotoxicity activities. Biotechnol Lett. 2019;41:899–914.
58. Yassin MA, Elgorban AM, El-Samawaty AERM, Almunqedhi BMA. Biosynthesis of silver nanoparticles using Penicillium verrucosum and analysis of their antifungal activity. Saudi J Biol Sci. 2021;28:2123–2127.
59. Abdel-Kareem MM, Zohri AA. Extracellular mycosynthesis of gold nanoparticles using Trichoderma hamatum: optimization, characterization and antimicrobial activity. Lett Appl Microbiol. 2018;67:465–475.
60. Samanta S, Singh BR, Adholeya A. Intracellular synthesis of gold nanoparticles using an ectomycorrhizal strain EM-1083 of Laccaria fraterna and its nanoanti-quorum sensing potential against Pseudomonas aeruginosa. Indian J Microbiol. 2017;57:448–460.
61. Murillo-Rábago EI, Vilchis-Nestor AR, Juarez-Moreno K, Garcia-Marin LE, Quester K, Castro-Longoria E. Optimized synthesis of small and stable silver nanoparticles using intracellular and extracellular components of fungi: an alternative for bacterial inhibition. Antibiotics. 2022;11:800.
62. Beyene HD, Werkneh AA, Bezabh HK, Ambaye TG. Synthesis paradigm and applications of silver nanoparticles (AgNPs), a review. Sustain Mater Technol. 2017;13:18–23.
63. Tarannum N, Gautam YK. Facile green synthesis and applications of silver nanoparticles: a state-of-the-art review. RSC Adv. 2019;9:34926–34948.
64. Santhoshkumar J, Rajeshkumar S, Venkat Kumar S. Phyto-assisted synthesis, characterization and applications of gold nanoparticles–a review. Biochem Biophys Rep. 2017;11:46–57.
65. Lee KX, Shameli K, Yew YP, Teow SY, Jahangirian H, Rafiee-Moghaddam R, et al. Recent developments in the facile bio-synthesis of gold nanoparticles (AuNPs) and their biomedical applications. Int J Nanomedicine. 2020;15:275–300.
66. Balachandar R, Gurumoorthy P, Karmegam N, Barabadi H, Subbaiya R, Anand K, et al. Plant-mediated synthesis, characterization and bactericidal potential of emerging silver nanoparticles using stem extract of Phyllanthus pinnatus: a recent advance in phytonanotechnology. J Clust Sci. 2019;30:1481–1488.
67. Alomar TS, AlMasoud N, Awad MA, El-Tohamy MF, Soliman DA. An eco-friendly plant-mediated synthesis of silver nanoparticles: characterization, pharmaceutical and biomedical applications. Mater Chem Phys. 2020;249:123007.
68. Baruah D, Yadav RNS, Yadav A, Das AM. Alpinia nigra fruits mediated synthesis of silver nanoparticles and their antimicrobial and photocatalytic activities. J Photochem Photobiol B. 2019;201:111649.
69. Gopinath M, Bharathiraja B, Iyyappan J, Gnanasekaran R, Yuvaraj D, Dhithya V. Extracellular green synthesis of silver nanoparticles using extract of Mimosa pudica leaves and assessment of antibacterial and antifungal activity. Proc Natl Acad Sci India B Biol Sci. 2020;90:1025–1033.
70. Hosny M, Fawzy M, Abdelfatah AM, Fawzy EE, Eltaweil AS. Comparative study on the potentialities of two halophytic species in the green synthesis of gold nanoparticles and their anticancer, antioxidant and catalytic efficiencies. Adv Powder Technol. 2021;32:3220–3233.
71. Ameen F, Srinivasan P, Selvankumar T, Kamala-Kannan S, Al Nadhari S, Almansob A, et al. Phytosynthesis of silver nanoparticles using Mangifera indica flower extract as bioreductant and their broad-spectrum antibacterial activity. Bioorg Chem. 2019;88:102970.
72. Kureshi AA, Vaghela HM, Kumar S, Singh R, Kumari P. Green synthesis of gold nanoparticles mediated by Garcinia fruits and their biological applications. Pharm Sci. 2021;27:238–250.
73. Islam NU, Jalil K, Shahid M, Muhammad N, Rauf A. Pistacia integerrima gall extract mediated green synthesis of gold nanoparticles and their biological activities. Arab J Chem. 2019;12:2310–2319.
74. Saim AK, Kumah FN, Oppong MN. Extracellular and intracellular synthesis of gold and silver nanoparticles by living plants: a review. Nanotechnol Environ Eng. 2021;6:1–11.
75. Uzair B, Liaqat A, Iqbal H, Menaa B, Razzaq A, Thiripuranathar G, et al. Green and cost-effective synthesis of metallic nanoparticles by algae: safe methods for translational medicine. Bioengineering. 2020;7:129.
76. El-Sheekh MM, Hassan LHS, Morsi HH. Evaluation of antimicrobial activities of blue-green algae-mediated silver and gold nanoparticles. Rend Lincei Sci Fis Nat. 2021;32:747–759.
77. Dağlıoğlu Y, Yılmaz Öztürk B. A novel intracellular synthesis of silver nanoparticles using Desmodesmus sp. (Scenedesmaceae): different methods of pigment change. Rend Lincei Sci Fis Nat. 2019;30:611–621.
78. Priyadharshini RI, Prasannaraj G, Geetha N, Venkatachalam P. Microwave-mediated extracellular synthesis of metallic silver and zinc oxide nanoparticles using macro-algae (Gracilaria edulis) extracts and its anticancer activity against human PC3

cell lines. Appl Biochem Biotechnol. 2014;174:2777–2790.
79. Begum S, Chanu KD, Sharma N, Singh RKL. Elsholtzia communis leaf extract mediated synthesis of silver nanoparticles: enhanced antioxidant, antidiabetic and antiproliferative activity. Dig J Nanomater Biostruct. 2024;19:251–262.
80. Ali MY, Mahmoud ABS, Abdalla M, Hamouda HI, Aloufi AS, Almubaddil NS, et al. Green synthesis of bio-mediated silver nanoparticles from Persea americana peels extract and evaluation of their biological activities: in vitro and in silico insights. J Saudi Chem Soc. 2024;28:101863.
81. Geremew A, Gonzalles J 3rd, Peace E, Woldesenbet S, Reeves S, Brooks N Jr, et al. Green synthesis of novel silver nanoparticles using *Salvia blepharophylla* and *Salvia greggii*: antioxidant and antidiabetic potential and effect on foodborne bacterial pathogens. Int J Mol Sci. 2024;25:645.
82. Sekar V, Al-Ansari MM, Narenkumar J, Al-Humaid L, Arunkumar P, Santhanam A. Synthesis of gold nanoparticles (AuNPs) with improved anti-diabetic, antioxidant and anti-microbial activity from *Physalis minima*. J King Saud Univ Sci. 2022;34:102197.
83. Balu SK, Andra S, Damiri F, Sivaramalingam A, Sudandaradoss MV, Kumarasamy K, et al. Size-dependent antibacterial, antidiabetic, and toxicity of silver nanoparticles synthesized using solvent extraction of *Rosa indica* L. petals. Pharmaceuticals. 2022;15:1052.
84. Sivasakthi V, Selvam K, Prakash P, Shivakumar MS, SenthilNathan S. Characterization of silver nanoparticles using *Ixora brachiata* Roxb. and its biological application. Curr Res Green Sustainable Chem. 2022;5:100257.
85. Seekonda S, Rani R. Eco-friendly synthesis, characterization, catalytic, antibacterial, antidiabetic, and antioxidant activities of *Embelia robusta* seeds extract stabilized AgNPs. J Sci Adv Mater Devices. 2022;7:100480.
86. Das G, Shin HS, Patra JK. Multitherapeutic efficacy of curly kale extract fabricated biogenic silver nanoparticles. Int J Nanomedicine. 2022;17:1125–1137.
87. Majeed S, Danish M, Zakariya NA, Hashim R, Alkahtani MTAS, Hasnain MS. In vitro evaluation of antibacterial, antioxidant, and antidiabetic activities and glucose uptake through 2-NBDG by Hep-2 liver cancer cells treated with green synthesized silver nanoparticles. Oxid Med Cell Longev. 2022;2022:6187913.
88. Kaliammal R, Parvathy G, Maheshwaran G, Velsankar K, Kousalya Devi V, Krishnakumar M, et al. Zephyranthes candida flower extract mediated green synthesis of silver nanoparticles for biological applications. Adv Powder Technol. 2021;32:4408–4419.
89. Das G, Patra JK, Shin HS. Biosynthesis and potential effect of fern mediated biocompatible silver nanoparticles by cytotoxicity, antidiabetic, antioxidant, and antibacterial studies. Mater Sci Eng C. 2020;114:111011.
90. Das G, Shin HS, Patra JK. Key health benefits of Korean Ueong dry root extract combined silver nanoparticles. Int J Nanomedicine. 2022;17:4261–4275.
91. Al-Radadi NS. Biogenic proficient synthesis of (Au-NPs) via aqueous extract of Red Dragon pulp and seed oil: characterization, antioxidant, cytotoxic properties, anti-diabetic anti-inflammatory, anti-Alzheimer, and their anti-proliferative potential against cancer cell lines. Saudi J Biol Sci. 2022;29:2836–2855.
92. Essghaier B, Dridi R, Mottola F, Rocco L, Zid MF, Hannachi H. Biosynthesis and characterization of silver nanoparticles from the extremophile plant *Aeonium haworthii* and their antioxidant, antimicrobial and anti-diabetic capacities. Nanomaterials. 2022;13:1091.
93. Jamil S, Dastagir G, Foudah AI, Alqarni MH, Ertürk HSYHMÖ, Shah MAR, et al. *Carduus edelbergii* Rech. f. mediated fabrication of gold nanoparticles; characterization and evaluation of antimicrobial, antioxidant, and antidiabetic potency of the synthesized AuNPs. Molecules. 2022;27:3350.
94. Naveed M, Batool H, Rehman Su, Javed A, Makhdoom SI, Aziz T, et al. Characterization and evaluation of the antioxidant, antidiabetic, anti-inflammatory, and cytotoxic activities of silver nanoparticles synthesized using *Brachychiton populneus* leaf extract. Processes. 2022;10:2269.
95. Wahab M, Bhatti A, John P. Evaluation of antidiabetic activity of biogenic silver nanoparticles using *Thymus serpyllum* on streptozotocin-induced diabetic BALB/c mice. Polymers. 2022;14:1470.
96. Perumalsamy R, Krishnadhas L. Anti-diabetic activity of silver nanoparticles synthesized from the hydroethanolic extract of *Myristica fragrans* seeds. Appl Biochem Biotechnol. 2022;194:1136–1148.
97. Inam M, Shah A, Khan WN, Sharif S, Saqib NU. Biosynthesis of silver nanoparticles: preparation, optimization, and in vitro anti-diabetic effect. BioNanoScience. 2021;11:1154–1159.
98. Saratale RG, Saratale GD, Ahn S, Shin HS. Grape pomace extracted tannin for green synthesis of silver nanoparticles: assessment of their antidiabetic, antioxidant potential and antimicrobial activity. Polymers. 2021;13:1777.
99. Das G, Patra JK, Debnath T, Ansari A, Shin HS. Investigation of antioxidant, antibacterial, antidiabetic, and cytotoxicity potential of silver nanoparticles synthesized using the outer peel extract of *Ananas comosus* (L.). PLoS ONE. 2019;14:e0219747.
100. Patra JK, Shin HS, Das G. Characterization and evaluation of multiple biological activities of silver nanoparticles fabricated from dragon tongue bean outer peel extract. Int J Nanomedicine. 2021;16:977–987.
101. Gauthami R, Vinitha UG, Anthony SP, Muthuraman MS. *Cissampelous pairera* mediated synthesis of silver nanoparticles and its in vitro antioxidant, antibacterial and antidiabetic activities. Mater Today Proc. 2021;47:853–857.

102. Nazer S, Andleeb S, Ali S, Gulzar N, Raza A, Khan H, et al. Cytotoxicity, anti-diabetic, and hepato-protective potential of *Ajuga bracteosa*-conjugated silver nanoparticles in Balb/c mice. Curr Pharm Biotechnol. 2022;23:318–336.
103. Chirumamilla P, Dharavath SB, Taduri S. Eco-friendly green synthesis of silver nanoparticles from leaf extract of *Solanum khasianum*: optical properties and biological applications. Appl Biochem Biotechnol. 2022;194:1–13.
104. Sher N, Ahmed M, Mushtaq N, Khan RA. Enhancing antioxidant, antidiabetic, and antialzheimer performance of *Hippeastrum hybridum* (L.) using silver nanoparticles. Appl Organomet Chem. 2022;36:e6044.
105. Lan Chi NT, Narayanan M, Chinnathambi A, Govindasamy C, Subramani B, Brindhadevi K, et al. Fabrication, characterization, anti-inflammatory, and anti-diabetic activity of silver nanoparticles synthesized from *Azadirachta indica* kernel aqueous extract. Environ Res. 2022;208:112684.
106. Faisal S, Khan MA, Jan H, Shah SA, Abdullah, Shah S, et al. Edible mushroom (*Flammulina velutipes*) as biosource for silver nanoparticles: from synthesis to diverse biomedical and environmental applications. Nanotechnology. 2020;32:045701.
107. Chavan AB, Goyal S, Patel AM. Formulation of silver nanoparticles using *Gymnema sylvestre* leaf extract and in-vitro anti-diabetic activity. J Pharm Res Int. 2022;34:39–49.
108. Senthilkumar P, Surendran L, Sudhagar B, Ranjith Santhosh Kumar DS. Facile green synthesis of gold nanoparticles from marine algae *Gelidiella acerosa* and evaluation of its biological potential. SN Appl Sci. 2019;1:1–12.
109. Johnson P, Krishnan V, Loganathan C, Govindhan K, Raji V, Sakayanathan P, et al. Rapid biosynthesis of *Bauhinia variegata* flower extract-mediated silver nanoparticles: an effective antioxidant scavenger and α-amylase inhibitor. Artif Cells Nanomed Biotechnol. 2018;46:1488–1494.
110. Pirabbasi E, Zangeneh MM, Zangeneh A, Moradi R, Kalantar M. Chemical characterization and effect of *Ziziphora clinopodioides* green-synthesized silver nanoparticles on cytotoxicity, antioxidant, and antidiabetic activities in streptozotocin-induced hepatotoxicity in Wistar diabetic male rats. Food Sci Nutr. 2024;12:3443–3451.
111. Ma Y, Bao M, Peng Y, Gao J, Bao J. Eco-friendly nanoparticles synthesized from *Salvia sclarea* ethanol extract protect against STZ-induced diabetic nephropathy in rats via antioxidant, anti-inflammatory, and apoptosis mechanisms. J Oleo Sci. 2024;73:1057–1067.
112. Ratib MO, El-Magid ADA, Sliem MH, El-Hamid OMA, Said ASM. Evaluation of antidiabetic and nephroprotective effects of *Origanum majorana* (Marjoram) leaf extract and its nanoparticles on streptozotocin-induced diabetes in rats. Afr J Biol Sci. 2024;6:786–800.
113. Subramaniam S, Roy A, Vivekanandan KE, Ahamed AA, Bharathiraja C, Kumarasamy S, et al. An investigation on antidiabetic competence of *Ferula assafoetida* mediated AgNPs on diabetic (STZ) induced albino rats. Biocatal Agric Biotechnol. 2024;56:103043.
114. Huda NU, Ahmed M, Mushtaq N. Bio-fabrication and characterization of nano-silver using *Kickxia elatine* plant and its anti-diabetic effect on alloxan-induced Sprague Dawley rats—An in vivo approach. Appl Organomet Chem. 2024;38:e6044.
115. Berlin Grace VM, Wilson DD, M, V. S, Siddikuzzaman, Gopal R. A new silver nano-formulation of *Cassia auriculata* flower extract and its anti-diabetic effects. Recent Pat Nanotechnol. 2022;16:160–169.
116. Kalakotla S, Jayarambabu N, Mohan GK, Mydin RBSMN, Gupta VR. A novel pharmacological approach of herbal mediated cerium oxide and silver nanoparticles with improved biomedical activity in comparison with *Lawsonia inermis*. Colloids Surf B Biointerfaces. 2019;174:199–206.
117. Shanker K, Naradala J, Mohan GK, Kumar GS, Pravallika PL. A sub-acute oral toxicity analysis and comparative: in vivo anti-diabetic activity of zinc oxide, cerium oxide, silver nanoparticles, and *Momordica charantia* in streptozotocin-induced diabetic Wistar rats. RSC Adv. 2017;7:37158–37167.
118. Karuppannan P, Saravanan K, Averal HI. Antidiabetic activity of silver nanoparticles biosynthesized using *Ventilago maderaspatana* leaf extract. Drug Dev Cancer Diabetes. 2020;263–273.
119. Ullah S, Shah SWA, Qureshi MT, Hussain Z, Ullah I, Kalsoom UE, et al. Antidiabetic and hypolipidemic potential of green AgNPs against diabetic mice. ACS Appl Bio Mater. 2021;4:3433–3442.
120. Shanker K, Krishna Mohan G, Mayasa V, Pravallika L. Antihyperglycemic and anti-hyperlipidemic effect of biologically synthesized silver nanoparticles and *G. sylvestre* extract on streptozotocin induced diabetic rats-an in vivo approach. Mater Lett. 2017;195:240–244.
121. Jamil K, Khattak SH, Farrukh A, Begum S, Riaz MN, Muhammad A, et al. Biogenic synthesis of silver nanoparticles using *Catharanthus roseus* and its cytotoxicity effect on Vero cell lines. Molecules. 2022;27:6191.
122. Haq MNU, Shah GM, Menaa F, Ali Khan R, Althobaiti NA, Albalawi AE, et al. Green silver nanoparticles synthesized from *Taverniera couneifolia* elicits effective anti-diabetic effect in alloxan-induced diabetic Wistar rats. Nanomaterials. 2022;12:1–13.
123. Ul Haq M, Shah GM, Gul A, Foudah AI, Alqarni MH, Yusufoglu HS, et al. Biogenic synthesis of silver nanoparticles using *Phagnalon niveum* and its in vivo anti-diabetic effect against alloxan-induced diabetic Wistar rats. Nanomaterials. 2022;12:830.
124. Mahmoudi F, Mahmoudi F, Gollo KH, Amini MM. Biosynthesis of novel silver nanoparticles using *Eryngium thyrsoideum* Boiss extract and comparison of their antidiabetic activity with chemical synthesized silver nanoparticles in diabetic rats. Biol Trace Elem Res. 2021;199:1967–1978.
125. Mahmoudi F, Mahmoudi F, Gollo KH, Amini MM. Novel gold nanoparticles: Green synthesis with

Eryngium thyrsoideum Boiss extract, characterization, and in vivo investigations on inflammatory gene expression and biochemical parameters in type 2 diabetic rats. Biol Trace Elem Res. 2021;200:2223–2232.
126. Nazer S, Andleeb S, Ali S, Gulzar N, Raza A, Khan H, et al. Cytotoxicity, anti-diabetic, and hepato-protective potential of *Ajuga bracteosa*-conjugated silver nanoparticles in Balb/c mice. Curr Pharm Biotechnol. 2021;23:318–336.
127. Kalakotla S, G P, Banu A, Shaik S. Development of plant-mediated silver nanoparticles & their pharmacological evaluation. 2022. Preprint (Version 1) available at Research Square.
128. Lakshmi JB. Evaluation of antidiabetic activity of aqueous extract of bark of *Pterocarpus Marsupium* silver nanoparticles against streptozotocin and nicotinamide induced type 2 diabetes in rats. Biomed J Sci Technol Res. 2022;43:34254–34268.
129. Garg A, Pandey P, Sharma P, Shukla A. Synthesis and characterization of silver nanoparticle of ginger rhizome (*Zingiber officinale*) extract: synthesis, characterization. Eur J Biomed Pharm Sci. 2016;3:605–611.
130. Nagaraja S, Ahmed SS, Bharathi DR, Goudanavar KM, Rupesh KM, Fattepur S, et al. Green synthesis and characterization of silver nanoparticles of *Psidium guajava* leaf extract and evaluation for its antidiabetic activity. Molecules. 2022;27:1–12.
131. Ambrose HW. Green synthesis of silver nanorods using aqueous seed extract of *Nigella sativa* and study of its antidiabetic activity. Aust J Basic Appl Sci. 2015;9:295–298.
132. Elekofehinti OO. *Momordica charantia* nanoparticles potentiate insulin release and modulate antioxidant gene expression in pancreas of diabetic rats. Egypt J Med Hum Genet. 2022;23:1–11.
133. Anbazhagan P, Murugan K, Jaganathan A, Sujitha V, Samidoss CM, Jayashanthani S, et al. Mosquitocidal, antimalarial, and antidiabetic potential of *Musa paradisiaca*-synthesized silver nanoparticles: in vivo and in vitro approaches. J Clust Sci. 2017;28:91–107.
134. Campoy AHG, Gutierrez RMP, Manriquez-Alvirde GM, Ramirez AM. Protection of silver nanoparticles using *Eysenhardtia polystachya* in peroxide-induced pancreatic β-cell damage and their antidiabetic properties in zebrafish. Int J Nanomedicine. 2018;13:2601–2612.
135. Sengottaiyan A, Aravinthan A, Sudhakar C, Selvam K, Srinivasan P, Govarthanan M, et al. Synthesis and characterization of *Solanum nigrum*-mediated silver nanoparticles and its protective effect on alloxan-induced diabetic rats. J Nanostruct Chem. 2016;6:41–48.
136. Oladipo IC, Lateef A, Azeez MA, Asafa TB, Yekeen TA, Ogunsona SB, et al. Antidiabetic properties of phytosynthesized gold nanoparticles (AuNPs) from *Datura stramonium* seed. IOP Conf Ser: Mater Sci Eng. 2020;805:1–8.
137. Javanshir R, Honarmand M, Hosseini M, Hemmati M. Anti-dyslipidemic properties of green gold nanoparticle: improvement in oxidative antioxidative balance and associated atherogenicity and insulin resistance. Clin Phytoscience. 2020;6:1–8.
138. Abdel-Halim AHG, Fyiad AAA, Aboulthana WM, El-Sammad NM, Youssef AM, Ali MM. Assessment of the anti-diabetic effect of *Bauhinia variegata* gold nano-extract against streptozotocin-induced diabetes mellitus in rats. J Appl Pharm Sci. 2020;10:77–91.
139. Saipriya, Daisy P. Biochemical analysis of *Cassia fistula* aqueous extract and phytochemically synthesized gold nanoparticles as hypoglycemic treatment for diabetes mellitus. Int J Nanomedicine. 2012;7:1189–1199.
140. Ayyoub S, Al-Trad B, Aljabali AAA, Alshaer W, Al Zoubi M, Omari S, et al. Biosynthesis of gold nanoparticles using leaf extract of *Dittrichia viscosa* and in vivo assessment of its anti-diabetic efficacy. Drug Deliv Transl Res. 2022;12:2993-2999.
141. Karthick V, Kumar VG, Dhas TS, Singaravelu G, Sadiq AM, Govindaraju K. Effect of biologically synthesized gold nanoparticles on alloxan-induced diabetic rats—An in vivo approach. Colloids Surf B Biointerfaces. 2014;122:505–511.
142. Nayak D, Chopra H, Chakrabartty I, Saravanan M, Barabadi H, Mohanta YK. Chapter 15 - Opportunities and challenges for bioengineered metallic nanoparticles as future nanomedicine. In: Barabadi H, Saravanan M, Mostafavi E, Vahidi H, editors. Bioengineered Nanomaterials for Wound Healing and Infection Control. Woodhead Publishing; 2023; 517–540.
143. Stater EP, Sonay AY, Hart C, Grimm J. The ancillary effects of nanoparticles and their implications for nanomedicine. Nat Nanotechnol. 2021;16:1180–1194.
144. Thu HE, Haider M, Khan S, Sohail M, Hussain Z. Nanotoxicity induced by nanomaterials: A review of factors affecting nanotoxicity and possible adaptations. OpenNano. 2023;14:100190.
145. Barabadi H, Jounaki K, Karami K, Mobaraki K, Noqani H, Ashouri F, et al. Laboratory evidence supports thrombolytic performance and blood compatibility of green-synthesized silver and gold nanomaterials. Results Surf Interfaces. 2024;17:100309.
146. Patra N, Kar D, Pal A, Behera A. Antibacterial, anticancer, anti-diabetic and catalytic activity of bio-conjugated metal nanoparticles. Adv Nat Sci: Nanoscience Nanotechnol. 2018;9:1–12.
147. Balan K, Qing W, Wang Y, Liu X, Palvannan T, Wang Y, et al. Antidiabetic activity of silver nanoparticles from green synthesis using *Lonicera japonica* leaf extract. RSC Adv. 2016;6:40162–40168.
148. Agarwal H, Venkat Kumar S, Rajeshkumar S. Antidiabetic effect of silver nanoparticles synthesized using lemongrass (*Cymbopogon citratus*) through conventional heating and microwave irradiation approach. J Microbiol Biotechnol Food Sci. 2018;7:371–376.
149. Saratale GD, Saratale RG, Benelli G, Kumar G, Pugazhendhi A, Kim DS, et al. Anti-diabetic potential of silver nanoparticles synthesized with *Argyreia nervosa* leaf extract: high synergistic antibacterial

activity with standard antibiotics against foodborne bacteria. J Clust Sci. 2017;28:1709–1727.
150. Yakoob AT, Tajuddin NB, Hussain MIM, Mathew S, Govindaraju A, Qadri I. Antioxidant and hypoglycemic activities of *Clausena anisata* (Willd.) Hook F. ex Benth. root-mediated synthesized silver nanoparticles. Pharmacognosy J. 2016;8:579–586.
151. Sarfraz RA, Ashraf R, Bedi S, Sardar I. Bioactivity-guided nanoparticle synthesis from *Zingiber officinale* and *Mentha longifolia*. Bioinspired Biomimetic Nanobiomaterials. 2021;10:70–77.
152. Korkmaz N, Ceylan Y, Taslimi P, Karadağ A, Bülbül AS, Şen F. Biogenic nano silver: Synthesis, characterization, antibacterial, antibiofilms, and enzymatic activity. Adv Powder Technol. 2020;31:2942–2950.
153. Vishnu Kiran M, Murugesan S. Biogenic silver nanoparticles by *Halymenia poryphyroides* and its in vitro anti-diabetic efficacy. J Chem Pharm Res. 2013;5:1001–1008.
154. Vijayakumar S, Divya M, Vaseeharan B, Chen J, Biruntha M, Silva LP, Durán-Lara EF, Shreema K, Ranjan S, Dasgupta N. Biological compound capping of silver nanoparticle with the seed extracts of Blackcumin (*Nigella sativa*): A potential antibacterial, antidiabetic, anti-inflammatory, and antioxidant. J Inorg Organomet Polym Mater. 2021;31:624–635.
155. Vishnu Kiran M, Murugesan S. Biological synthesis of silver nanoparticles from marine alga *Colpomenia sinuosa* and its in vitro anti-diabetic activity. AJBBL. 2014;1:1–7.
156. Sati SC, Kour G, Bartwal AS, Sati MD. Biosynthesis of metal nanoparticles from leaves of *Ficus palmata* and evaluation of their anti-inflammatory and anti-diabetic activities. Biochemistry. 2020;59:3019–3025.
157. Chinnasamy G, Chandrasekharan S, Bhatnagar S. Biosynthesis of silver nanoparticles from *Melia azedarach*: Enhancement of antibacterial, wound healing, antidiabetic, and antioxidant activities. Int J Nanomedicine. 2019;14:9823–9836.
158. Govindappa M, Hemashekhar B, Arthikala MK, Ravishankar Rai V, Ramachandra YL. Characterization, antibacterial, antioxidant, antidiabetic, anti-inflammatory and antityrosinase activity of green synthesized silver nanoparticles using *Calophyllum tomentosum* leaves extract. Results Phys. 2018;9:400–408.
159. Lava MB, Muddapur UM, Basavegowda N, More SS, More VS. Characterization, anticancer, antibacterial, anti-diabetic and anti-inflammatory activities of green synthesized silver nanoparticles using *Justica wynaadensis* leaves extract. Mater Today Proc. 2020;46:5942–5947.
160. Andleeb S, Tariq F, Muneer A, Nazir T, Shahid B, Latif Z, Abbasi SA, Haq I, Majeed Z, Ud S, Khan D. In vitro bactericidal, antidiabetic, cytotoxic, anticoagulant, and hemolytic effect of green-synthesized silver nanoparticles using *Allium sativum* clove extract incubated at various temperatures. Green Process. Synth. 2020;1:538–553.
161. Das G, Shin HS, Patra JK. Comparative assessment of antioxidant, anti-diabetic and cytotoxic effects of three peel/ shell food waste extract-mediated silver nanoparticles. Int J Nanomedicine. 2020;15:9075–9088.
162. Das G, Patra JK, Basavegowda N, Vishnuprasad CN, Shin HS. Comparative study on antidiabetic, cytotoxicity, antioxidant and antibacterial properties of biosynthesized silver nanoparticles using outer peels of two varieties of Ipomoea batatas (L.) Lam. Int J Nanomedicine. 2019;14:4741–4754.
163. Sulthana HB, Ranjani S, Hemalatha S. Comparison of efficacy of nanoparticles synthesized from leaves and flowers of Russelia equisitiformis. Inorg Nano-Metal Chem. 2020;52:75–81.
164. Yarrappagaari S, Gutha R, Narayanaswamy L, Thopireddy L, Benne L, Mohiyuddin SS, Vijayakumar V, Saddala RR. Eco-friendly synthesis of silver nanoparticles from the whole plant of Cleome viscosa and evaluation of their characterization, antibacterial, antioxidant and antidiabetic properties. Saudi J Biol Sci. 2020;27:3601–3614.
165. Saratale GD, Saratale RG, Kim DS, Kim DY, Shin HS. Exploiting fruit waste grape pomace for silver nanoparticles synthesis, assessing their antioxidant, antidiabetic potential and antibacterial activity against human pathogens: A novel approach. Nanomaterials. 2020;10:1–18.
166. Rathinam L, Sevarkodiyone SP, Pandiarajan J. Efficacy of silver and gold nanoparticles obtained from vermiwash: In vitro study on antimicrobial and antidiabetic activities. J Appl Nat Sci. 2021;13:1317–1325.
167. Chung IM, Rekha K, Rajakumar G, Thiruvengadam M. Elicitation of silver nanoparticles enhanced the secondary metabolites and pharmacological activities in cell suspension cultures of bitter gourd. 3 Biotech. 2018;8:1–12.
168. Popli D, Anil V, Subramanyam AB, MN RM, VR RV, Rao SN, Rai RV, Govindappa M. Endophyte fungi, Cladosporium species-mediated synthesis of silver nanoparticles possessing in vitro antioxidant, anti-diabetic and anti-Alzheimer activity. Artif Cells Nanomed Biotechnol. 2018;46:676–683.
169. Malapermal V, Botha I, Krishna SBN, Mbatha JN. Enhancing antidiabetic and antimicrobial performance of Ocimum basilicum, and Ocimum sanctum (L.) using silver nanoparticles. Saudi J Biol Sci. 2017;24:1294–1305.
170. Dharavath SB, Chirumamilla P, Taduri S. Evaluation of antioxidant, anti-inflammatory and antidiabetic activities of green synthesized silver nanoparticles and in vivo plant extracts of Nothapodytes foetida. Vegetos. 2022;1–12.
171. Velsankar K, Preethi R, Ram PSJ, Ramesh M, Sudhahar S. Evaluations of biosynthesized Ag nanoparticles via Allium sativum flower extract in biological applications. Appl Nanosci (Switzerland). 2020;10:3675–3691.
172. Saratale RG, Shin HS, Kumar G, Benelli G, Kim DS, Saratale GD. Exploiting antidiabetic activity of silver nanoparticles synthesized using Punica granatum

leaves and anticancer potential against human liver cancer cells (HepG2). Artif Cells Nanomed Biotechnol. 2018;46:211–222.
173. Patra JK, Das G, Shin HS. Facile green biosynthesis of silver nanoparticles using Pisum sativum L. outer peel aqueous extract and its antidiabetic, cytotoxicity, antioxidant, and antibacterial activity. Int J Nanomedicine. 2019;14:6679–6690.
174. Kiran MS, Latha MS, Gokavi NB, Pujar GH, Rajith Kumar CR, Shwetha UR, Betageri VS, Betageri VS. Facile green synthesis and characterization of Moringa oleifera extract-capped silver nanoparticles (MO-Agnps) and its biological applications. IOP Conf Ser Mater Sci Eng. 2020;925:1–12.
175. Mohammed SS, Lawrance AV, Sampath S, Sunderam V, Madhavan Y. Facile green synthesis of silver nanoparticles from sprouted Zingiberaceae species: Spectral characterisation and its potential biological applications. Mater Technol. 2022;37:533–546.
176. Jayawardane KM, Hettiarachchi H, Gunathilake K. Functional properties of Averrhoa bilimbi and green synthesis and characterization of silver nanoparticles using its fruit extracts. J Med Plants Stud. 2022;10:5–12.
177. Bagyalakshmi J, Haritha H. Green synthesis and characterization of silver nanoparticles using Pterocarpus marsupium and assessment of its in vitro antidiabetic activity. Am J Adv Drug Deliv. 2017;5:1–7.
178. Das B, De A, Podder S, Das S, Ghosh CK, Samanta A. Green biosynthesis of silver nanoparticles using Dregea volubilis flowers: Characterization and evaluation of antioxidant, antidiabetic and antibacterial activity. Inorg Nano-Metal Chem. 2021;51:1066–1079.
179. Zubair M, Azeem M, Mumtaz R, Younas M, Adrees M, Zubair E, Khalid A, Hafeez F, Rizwan M, Ali S. Green synthesis and characterization of silver nanoparticles from Acacia nilotica and their anticancer, antidiabetic and antioxidant efficacy. Environ Pollut. 2022;304:119249.
180. Vinodhini S, Vithiya BSM, Prasad TAA. Green synthesis of silver nanoparticles by employing the Allium fistulosum, Tabernaemontana divaricate and Basella alba leaf extracts for antimicrobial applications. J King Saud Univ Sci. 2022;34:101939.
181. Jini D, Sharmila S. Green synthesis of silver nanoparticles from Allium cepa and its in vitro antidiabetic activity. Mater Today Proc. 2020;22:432–438.
182. Kumar V, Singh S, Srivastava B, Bhadouria R, Singh R. Green synthesis of silver nanoparticles using leaf extract of Holoptelea integrifolia and preliminary investigation of its antioxidant, anti-inflammatory, antidiabetic and antibacterial activities. J Environ Chem Eng. 2019;7:103094.
183. Debnath G, Das P, Saha AK. Green synthesis of silver nanoparticles using mushroom extract of Pleurotus giganteus: characterization, antimicrobial, and α-amylase inhibitory activity. Bio Nano Science. 2019;9:611–619.
184. Sasidharan Jayabal SP, Meenakshi RV. Green synthesis, characterization and evaluation of in-vitro antioxidant & anti-diabetic activity of nanoparticles from a polyherbal formulation-Mehani. J Environ Nanotechnol. 2018;7:51–59.
185. Vankudoth S, Dharavath S, Veera S, Maduru N, Chada R, Chirumamilla P, Gopu C, Taduri S. Green synthesis, characterization, photoluminescence and biological studies of silver nanoparticles from the leaf extract of Muntingia calabura. Biochem Biophys Res Commun. 2022;630:143–150.
186. Azeem MNA, Ahmed OM, Shaban M, Elsayed KNM. In vitro antioxidant, anticancer, anti-inflammatory, anti-diabetic and anti-Alzheimer potentials of innovative macroalgae bio-capped silver nanoparticles. Environ Sci Pollut Res. 2022;59930–59947.
187. Badmus JA, Oyemomi SA, Adedosu OT, Yekeen TA, Azeez MA, Adebayo EA, Lateef A, Badeggi UM, Botha S, Hussein AA, Marnewick JL. Photo-assisted bio-fabrication of silver nanoparticles using Annona muricata leaf extract: exploring the antioxidant, anti-diabetic, antimicrobial, and cytotoxic activities. Heliyon. 2020;6:e05413.
188. Natasha A, Mohib S, Samreen S, Hadia R. Plant-mediated synthesis of silver nanoparticles and their biological applications. Bull Chem Soc Ethiop. 2018;32:399–405.
189. Wilson S, Cholan S, Vishnu U, Sannan R, Jananiya R, Vinodhini S, Manimegalai S, Devi Rajeswari V. In vitro assessment of the efficacy of free-standing silver nanoparticles isolated from Centella asiatica against oxidative stress and its antidiabetic activity. Der Pharmacia Lettre. 2015;7:194–205.
190. Suchithra MR, Bhuvaneswari S, Sampathkumar P, Dineshkumar R, Chithradevi K, Beevi Farhana Noor M, Madhumitha R, Kavisri M. In vitro study of antioxidant, antidiabetic and antiurolithiatic activity of synthesized silver nanoparticles using stem bark extracts of Hybanthus enneaspermus. Biocatal Agric Biotechnol. 2021;38:102219.
191. Avwioroko OJ, Anigboro AA, Atanu FO, Otuechere CA, Alfred MO, Abugo JN, Omorogie MO. Investigation of the binding interaction of α-amylase with Chrysophyllum albidum seed extract and its silver nanoparticles: a multi-spectroscopic approach. Chem Data Collect. 2020;29:100517.
192. Vijaya Sankar AS. In-vitro screening of antidiabetic and antimicrobial activity against green synthesized $AgNO_3$ using seaweeds. J Nanomed Nanotechnol. 2015;s6:1–6.
193. Hassan AMS, Mahmoud ABS, Ramadan MF, Eissa MA. Microwave-assisted green synthesis of silver nanoparticles using Annona squamosa peels extract: characterization, antioxidant, and amylase inhibition activities. Rendicont Lincei. 2022;33:83–91.
194. Rathinam L, Pandiarajan J. Multi-faceted role of silver and gold nanoparticles synthesized from biowaste and its in vitro antibacterial, antifungal and antidiabetic activities. Lett Appl Nano Bio Sci. 2021;11:3076–3092.

195. Sai Nivetha S, Ranjani S, Hemalatha S. Synthesis and application of silver nanoparticles using Cissus quadrangularis. Inorg Nano-Metal Chem. 2022;52:82–89.
196. Govindharaja L, Shivakumara D, Krishnasamy R, Arumugam R. Synthesis and characterisation of silver nanoparticles using Syzygium aromaticum and their in vitro antioxidant and antidiabetic activity. 2016;2:6–11.
197. Shah M, Nawaz S, Jan H, Uddin N, Ali A, Anjum S, Giglioli-Guivarc'h N, Hano C, Abbasi BH. Synthesis of bio-mediated silver nanoparticles from Silybum marianum and their biological and clinical activities. Mater Sci Eng C. 2020;112:110889.
198. Sivakumar T. Synthesis of silver nanoparticles using Cassia auriculata leaves extracts and their potential antidiabetic activity. Int J Bot Stud. 2021;6:35–38.
199. Johnson MAA, Shibila T, Amutha S, Menezes IRA, Da Costa JGM, Sampaio NFL, Coutinho HDM. Synthesis of silver nanoparticles using Odontosoria chinensis (L.) J. Sm. and evaluation of their biological potentials. Pharmaceuticals. 2020;13:1–10.
200. Keskin M. Synthesis, characterization and antidiabetic potential of bee pollen based silver nanoparticles. El-Cezeri J Sci Eng. 2022;9:266–275.
201. Saminathan U, Ramasamy P, Chinathambi A, Paramasivam S, Vadamalai S, Chinnaiyan U, Singh R. Synthesis, characterization of silver nanoparticles from Punica granatum L. and its in vitro antidiabetic activity. Nanotechnol Environ Eng. 2022;7:923–930.
202. Das SK, Behera S, Patra JK, Thatoi H. Green synthesis of silver nanoparticles using Avicennia officinalis and Xylocarpus granatum extracts and in vitro evaluation of antioxidant, antidiabetic and anti-inflammatory activities. J Cluster Sci. 2019;30:1103–1113.
203. Kong Y, Paray BA, Al-Sadoon MK, Albeshr MF. Novel green synthesis, chemical characterization, toxicity, colorectal carcinoma, antioxidant, anti-diabetic, and anticholinergic properties of silver nanoparticles: a chemopharmacological study. Arab J Chem. 2021;14:103193.
204. Thatoi P, Kerry RG, Gouda S, Das G, Pramanik K, Thatoi H, Patra JK. Photo-mediated green synthesis of silver and zinc oxide nanoparticles using aqueous extracts of two mangrove plant species, Heritiera fomes and Sonneratia apetala and investigation of their biomedical applications. J Photochem Photobiol B. 2016;163:311–318.
205. Elias A, Habbu P, Iliger S. Preparation, characterization and screening of silver nanoparticles using phenolic rich fractions of Amaranthus gangeticus L. for its in vitro antioxidant, anti-diabetic and anti-cancer activities. RGUHS J Pharm Sci. 2021;1–10.
206. Elias A, Habbu PV, Iliger S. Preparation, characterization and screening of gold nanoparticles using phenolic rich fractions of Amaranthus gangeticus L. for its in vitro antioxidant, anti-diabetic and anti-cancer activities. J Pharm Res Int. 2021;33:425–439.
207. Soliman NA, Ismail EH, Abd El-Moaty HI, Sabry DY, Khalil MMH. Anti-Helicobacter pylori, anti-diabetic and cytotoxicity activity of biosynthesized gold nanoparticles using Moricandia nitens water extract. Egypt J Chem. 2018;61:691–703.
208. Velidandi A, Pabbathi NPP, Dahariya S, Baadhe RR. Catalytic and eco-toxicity investigations of bio-fabricated monometallic nanoparticles along with their anti-bacterial, anti-inflammatory, anti-diabetic, anti-oxidative and anti-cancer potentials. Colloids Interface Sci Commun. 2020;38:100302.
209. Xing H. Citrus aurantifulia extract as a capping agent to biosynthesis of gold nanoparticles: characterization and evaluation of cytotoxicity, antioxidant, antidiabetic, anticholinergics, and anti-bladder cancer activity. Appl Organomet Chem. 2021;35:1–10.
210. Abd El-Moaty HI, Soliman NA, Hamad RS, Ismail EH, Sabry DY, Khalil MMH. Comparative therapeutic effects of Pituranthos tortuosus aqueous extract and phyto-synthesized gold nanoparticles on Helicobacter pylori, diabetic and cancer proliferation. S Afr J Bot. 2021;139:167–174.
211. Kiran MS, Rajith Kumar CR, Shwetha UR, Onkarappa HS, Betageri VS, Latha MS. Green synthesis and characterization of gold nanoparticles from Moringa oleifera leaves and assessment of antioxidant, antidiabetic and anticancer properties. Chem Data Collect. 2021;33:100714.
212. Badeggi UM, Ismail E, Adeloye AO, Botha S, Badmus JA, Marnewick JL, Cupido CN, Hussein AA. Green synthesis of gold nanoparticles capped with procyanidins from Leucosidea sericea as potential antidiabetic and antioxidant agents. Biomolecules. 2020;10:1–15.
213. Rajaram K, Aiswarya DC, Sureshkumar P. Green synthesis of silver nanoparticle using Tephrosia tinctoria and its antidiabetic activity. Mater Lett. 2015;138:251–254.
214. Gopalakrishnan V, Muniraj S. In vitro anti-oxidant and in vitro anti-diabetic studies of silver, gold and copper nanoparticles synthesized using the flowers of Azadirachta indica. Indian J Chem Technol. 2021;28:580–586.
215. Aboulthana WMK, Refaat E, Khaled SE, Ibrahim NES, Youssef AM. Metabolite profiling and biological activity assessment of Casuarina equisetifolia bark after incorporating gold nanoparticles. Asian Pac J Cancer Prev. 2022;23:3457–3471.
216. Veeramani S, Narayanan AP, Yuvaraj K, Sivaramakrishnan R, Pugazhendhi A, Rishivarathan I, Jose SP, Ilangovan R. Nigella sativa flavonoids surface coated gold NPs (Au-NPs) enhancing antioxidant and anti-diabetic activity. Process Biochem. 2022;114:193–202.
217. Rose AL, Priya FJ, Vidhya S. Sustainable synthesis of gold nanoparticles and its antidiabetic activity of Anacardium occidentale. Orient J Chem. 2021;37:374–379.
218. Dhas TS, Kumar VG, Karthick V, Vasanth K, Singaravelu G, Govindaraju K. Effect of biosynthesized gold nanoparticles by Sargassum swartzii in alloxan induced diabetic rats. Enzyme Microb Technol. 2016;95:100–106.

219. Ansari SA, Bari A, Ullah R, Mathanmohun M, Veeraraghavan VP, Sun Z. Gold nanoparticles synthesized with Smilax glabra rhizome modulates the anti-obesity parameters in high-fat diet and streptozotocin induced obese diabetes rat model. J Photochem Photobiol B. 2019;201:111643.
220. Guo Y, Jiang N, Zhang L, Yin M. Green synthesis of gold nanoparticles from Fritillaria cirrhosa and its anti-diabetic activity on streptozotocin induced rats. Arab J Chem. 2020;13:5096–5106.
221. Ponnanikajamideen MI, Rajeshkumar S, Vanaja M, Annadurai G. In vivo type 2 diabetes and wound-healing effects of antioxidant gold nanoparticles synthesized using the insulin plant Chamaecostus cuspidatus in albino rats. Can J Diabetes. 2019;43:82–89.e86.
222. Zahid R, Rizvi SNB, Qureshi Z, Din MI. Sustainable synthesis of monodispersed gold nanoparticles from Phoenix dactylifera L. and in vivo anti-diabetic activity on alloxan induced mice. Vib Spectrosc. 2022;120:103371.
223. Opris R, Tatomir C, Olteanu D, Moldovan R, Moldovan B, David L, Nagy A, Decea N, Kiss ML, Filip GA. The effect of Sambucus nigra L. extract and phytosynthesized gold nanoparticles on diabetic rats. Colloids Surf B Biointerfaces. 2017;150:192–200.
224. Virk P. Antidiabetic activity of green gold-silver nanocomposite. Pak J Zool. 2018;50:711–718.
225. Elobeid MA, Awad MA, Virk P, Ortashi KM, Merghani NM, Asiri AM, Bashir EAA. Synthesis and characterization of noble metal/metal oxide nanoparticles and their potential antidiabetic effect on biochemical parameters and wound healing. Green Process Synth. 2022;11:106–115.

Table 1. *In vitro* evaluation of the antidiabetic potential of green-synthesized silver and gold nanomaterials by targeting key enzymes involved in diabetes regulation (α-amylase and α-glucosidase).

Biological source/ Scientific name	NPs type	Size (nm)/ Morphology	Method	Dose of NPs	Positive control	Major outcome	Ref
Plant/ *Elsholtzia communis*	Ag	Average: 11.38/ Spherical	α-amylase	20, 40, 50, 60, 70, 80, 100, 120 $\mu g.mL^{-1}$	Acarbose	IC_{50} (AgNPs)= 40.6 ± 1.77 $\mu g.mL^{-1}$; IC_{50}(Acarbose)= 65.7 ± 0.40 $\mu g.mL^{-1}$.	[79]
			α-glucosidase	20, 40, 50, 60, 70, 80, 100, 120 $\mu g.mL^{-1}$	Acarbose	IC_{50} (AgNPs)= 26.87 ± 1.74 $\mu g.mL^{-1}$; IC_{50} (Acarbose)= 51.46 ± 2.38 $\mu g.mL^{-1}$.	
Plant/ *Persea americana*	Ag	Average: 24/ Spherical	α-amylase	20, 40, 60, 80 $\mu g.mL^{-1}$	Acarbose	IC_{50} (AgNPs)= 66.04 $\mu g.mL^{-1}$; IC_{50}(Acarbose)= 86. 5 $\mu g.mL^{-1}$.	[80]
Plant/ *Salvia blepharophylla*	Ag	Average: 52.4/ Spherical	α-amylase	20, 40, 60, 80, 100 $\mu g.mL^{-1}$	Acarbose	IC_{50} (AgNPs)= between 40 to 60 $\mu g.mL^{-1}$; IC_{50} (Acarbose)= between 20 to 40 $\mu g.mL^{-1}$.	[81]
Plant/ *Salvia greggii*	Ag	Average: 62.5/ Spherical	α-amylase	20, 40, 60, 80, 100 $\mu g.mL^{-1}$	Acarbose	IC_{50} (AgNPs) ~ 50 $\mu g.mL^{-1}$; IC_{50} (Acarbose)= between 20 to 40 $\mu g.mL^{-1}$.	[81]
Plant/ *Saraca asoca*	Ag	Average: 36/ Spherical	α-amylase	0.75-2.5 mM	No data	IC_{50}= 0.35 mM	[146]
Plant/ *Lonicera japonica*	Ag	20-60/ Spherical and hexagonal	α-amylase	20-100 $\mu g.mL^{-1}$	Acarbose	IC_{50} (AgNPs)= 54.56 $\mu g.mL^{-1}$; IC_{50} (Acarbose): between 20 to 40 $\mu g.mL^{-1}$.	[147]
			α-glucosidase	20-100 $\mu g.mL^{-1}$	Acarbose	IC_{50} (AgNPs)= 37.86 $\mu g.mL^{-1}$; IC_{50} (Acarbose): between 20 to 40 $\mu g.mL^{-1}$.	
Plant/ *Myristica fragrans*	Ag	50-60/ Polygonal	α-amylase	200-1000 $\mu g.mL^{-1}$	Acarbose	At highest dose, the NPs inhibited 52.48% enzyme activity; At highest dose, acarbose inhibited 59.15% enzyme activity.	[96]
			α-glucosidase	200-1000 $\mu g.mL^{-1}$	Acarbose	At highest dose, the NPs inhibited 55.6% enzyme activity; At highest dose, the NPs inhibited 71.03% enzyme activity.	

Biological source/ Scientific name	NPs type	Size (nm)/ Morphology	Method	Dose of NPs	Positive control	Major outcome	Ref
Plant/ *Cymbopogon citratus*	Ag	Average: 75/ Spherical	α-amylase	20, 40, 60, 80, and 100 µL (Obtaining from 10 mL extract and 90 mL (1 mM) aqueous solution of $AgNO_3$)	Acarbose	At highest dose, the NPs inhibited about 90% enzyme activity; At highest dose, acarbose inhibited about 90% enzyme activity.	[148]
Plant/ *Argyreia nervosa*	Ag	5-35/ Spherical	α-amylase	20-100 $\mu g.mL^{-1}$	Acarbose	IC_{50} (AgNPs)= 55.5 $\mu g.mL^{-1}$; IC_{50}(Acarbose) ~ 40 $\mu g.mL^{-1}$	[149]
			α-glucosidase	20-100 $\mu g.mL^{-1}$	Acarbose	IC_{50}= 51.7 $\mu g.mL^{-1}$; IC_{50} (Acarbose): between 20 to 40 $\mu g.mL^{-1}$.	
Plant/ *Clausena anisata*	Ag	23-44/ Spherical	α-amylase	100-500 $\mu g.mL^{-1}$	Acarbose	At highest dose, the NPs inhibited 85.24% enzyme activity; At highest dose, acarbose inhibited about 88% enzyme activity.	[150]
Plant/ *Zingiber officinale*	Ag	No data/ No data	α-amylase	40, 50, 70, 100, 1000 $\mu g.mL^{-1}$	Acarbose	At highest dose, the NPs inhibited 80.52% enzyme activity; At highest dose; acarbose inhibited 100% enzyme activity.	[151]
Plant/ *Mentha longifolia*	Ag	No data / No data	α-amylase	40, 50, 70, 100, 1000 $\mu g.mL^{-1}$	Acarbose	At highest dose, the NPs inhibited about 60% enzyme activity; At highest dose, acarbose inhibited 100% enzyme activity.	[151]
Plant/ *Corylus avellana*	Ag	9-50/ Spherical	α-glucosidase	No data	Acarbose	IC_{50} (AgNPs)= 10.75 µM; IC_{50}(Acarbose)= 12.98 µM.	[152])
Alga/ *Halymenia poryphyroides*	Ag	34-80/ Spherical	α-amylase	0.2, 0.4, 0.6, 0.8, and 1 $mg.mL^{-1}$	Acarbose	IC_{50} (AgNPs)= 490 ± 0.02 $\mu g.mL^{-1}$; IC_{50}(Acarbose)= 630 ± 0.01 $\mu g.mL^{-1}$.	[153]
			α-glucosidase	0.2, 0.4, 0.6, 0.8, and 1 $mg.mL^{-1}$	Acarbose	IC_{50}= 385 ± 0.02 $\mu g.mL^{-1}$; IC_{50} (Acarbose)= 695 ± 0.01 $\mu g.mL^{-1}$.	
Plant/ *Nigella sativa*	Ag	20-70/ Spherical	α-amylase	20, 40, 60, 80, and 100 $\mu g.mL^{-1}$	Acarbose	At highest dose, the NPs inhibited about 98% enzyme activity; At highest dose, the acarbose inhibited about 100% enzyme activity.	[154]
			α-glucosidase	20, 40, 60, 80, and 100 $\mu g.mL^{-1}$	Acarbose	At highest dose, the NPs inhibited about 98% enzyme activity; At highest dose, the acarbose inhibited about 100% enzyme activity.	
Alga/ *Colpomenia sinuosa*	Ag	54-65/ Cubical with uniform shape	α-amylase	0.2, 0.4, 0.6, 0.8, and 1 $mg.mL^{-1}$	Acarbose	At highest dose, the NPs inhibited 94.30 ± 0.10% enzyme activity; At highest dose, acarbose inhibited 59.69 ± 0.10% enzyme activity.	[155]
			α-glucosidase	0.2, 0.4, 0.6, 0.8, and 1 $mg.mL^{-1}$	Acarbose	At highest dose, the NPs inhibited 90.50 ± 0.10% enzyme activity; At highest dose, acarbose	

Biological source/ Scientific name	NPs type	Size (nm)/ Morphology	Method	Dose of NPs	Positive control	Major outcome	Ref
Plant/ *Ficus palmata*	Ag	Average: 30/ Spherical	α-amylase	10-90 $\mu g.mL^{-1}$	Acarbose	inhibited 59.63 ± 0.01% enzyme activity. IC_{50} (AgNPs)= 27 $\mu g.mL^{-1}$; IC_{50}(Acarbose)= 18.5 $\mu g.mL^{-1}$.	[156]
			α-glucosidase	10-90 $\mu g.mL^{-1}$	Acarbose	IC_{50} (AgNPs)= 32 $\mu g.mL^{-1}$; IC_{50}(Acarbose)= 21 $\mu g.mL^{-1}$.	
Plant/ *Melia azedarach*	Ag	14-20/ Spherical	α-amylase	200 and 400 $\mu g.mL^{-1}$	Acarbose	At highest dose, the NPs inhibited 85.75 ± 1.20% enzyme activity; At highest dose, acarbose inhibited about 90% enzyme activity.	[157]
			α-glucosidase	200 and 400 $\mu g.mL^{-1}$	Acarbose	At highest dose, the NPs inhibited 80.33 ± 1.94% enzyme activity; At highest dose, acarbose inhibited about 95% enzyme activity.	
Plant/ *Pueraria lobate*	Ag	30-60/ Spherical	α-amylase	200-1000 µL (Obtaining from 10 g dried extract/ 100 mL 80% methanol and 1 mL (0.01 M) aqueous solution of $AgNO_3$)	Not data	At highest dose, the NPs inhibited 36.33% enzyme activity.	[97]
Plant/ *Equisetum arvense*	Ag	No data/ Spherical	α-glucosidase	0.5-2.5 $\mu g.mL^{-1}$	Not data	At highest dose, the NPs inhibited 95.77% enzyme activity.	[89]
Plant/ *Hemigraphis repanda*	Ag	No data/ Spherical	α-glucosidase	0-10 $\mu g.mL^{-1}$	No data	IC_{50}= 1.98 $\mu g.mL^{-1}$.	[100]
Plant/ *Brachychiton populneus*	Ag	Average: 12/ Cubical	α-amylase	25-125 $\mu g.mL^{-1}$	Acarbose	IC_{50} (AgNPs)= 67 $\mu g.mL^{-1}$; IC_{50}(Acarbose)= 110 $\mu g.mL^{-1}$.	[94]
Plant/ *Ixora brachiata*	Ag	15.71–84.97/ Spherical	α-amylase	25, 50, 100, 150, and 200 $\mu g.mL^{-1}$	Not data	At highest dose, the NPs inhibited about 60% enzyme activity.	[84]
			α-glucosidase	25, 50, 100, 150, and 200 $\mu g.mL^{-1}$	Not data	At highest dose, the NPs inhibited about 70% enzyme activity.	
Plant/ *Calophyllum tomentosum*	Ag	Average: 24/ Spherical	α-amylase	250 and 500 $\mu g.mL^{-1}$	Not data	At highest dose, the NPs inhibited about 20% enzyme activity.	[158]
			α-glucosidase	10, 20, 50, 100, and 150 $\mu g.mL^{-1}$	No data	At highest dose, the NPs inhibited about 50% enzyme activity.	
Plant/ *Justica wynaadensis*	Ag	30-50/ Irregular	α-amylase	0, 50, 100, 150, and 200 $\mu g.mL^{-1}$	No data	IC_{50}= 493.87 $\mu g.mL^{-1}$.	[159]
Fungus/ *Lentinus tuber-regium*	Ag	5-20/ Prominently spherical	α-amylase	100, 200, 300, 400, and 500 $\mu g.mL^{-1}$	Acarbose	At highest dose, the NPs inhibited 44.24 ± 0.64% enzyme activity; At highest dose, acarbose inhibited 48.14 ± 0.46% enzyme activity.	[160]
Plant/ *Cissampelos pareira*	Ag	60-118/ Mostly spherical	α-amylase	25, 50, 75, and 100 $\mu g.mL^{-1}$	No data	At highest dose, the NPs inhibited 92% enzyme activity.	[101]

Biological source/ Scientific name	NPs type	Size (nm)/ Morphology	Method	Dose of NPs	Positive control	Major outcome	Ref
Plant/ *Persea americana*	Ag	No data/ Small dots-like and nearly round-shaped	α-glucosidase	1, 2.5, and 5 µg.mL^{-1}	No data	IC_{50}= 2.72 µg.mL^{-1}.	[161]
Plant/ *Beta vulgaris*	Ag	No data/ Small dots-like and nearly round-shaped	α-glucosidase	1, 2.5, and 5 µg.mL^{-1}	No data	IC_{50}= 1.94 µg.mL^{-1}.	[161]
Plant/ *Arachis hypogaea*	Ag	No data/ Small dots-like and nearly round-shaped	α-glucosidase	1, 2.5, and 5 µg.mL^{-1}	No data	IC_{50}= 1.68 µg.mL^{-1}.	[161]
Plant/ *Ipomoea batatas* (red skin)	Ag	No data/ Spherical	α-glucosidase	0.25, 0.5, and 1 µg.mL^{-1}	No data	IC_{50}= 0.36 µg.mL^{-1}.	[162]
Plant/ *Ipomoea batatas* (pumpkin sweet)	Ag	No data/ Spherical	α-glucosidase	0.25, 0.5, and 1 µg.mL^{-1}	No data	IC_{50}= 0.77 µg.mL^{-1}.	[162]
Plant/ *Russelia equisitiformis* (leaves)	Ag	No data/ Spherical	α-amylase	12.5, 25, 50, and 100 µg.mL^{-1}	Acarbose	At highest dose, the NPs inhibited about 60% enzyme activity; At highest dose, acarbose inhibited about 68% enzyme activity.	[163]
Plant/ *Russelia equisitiformis* (flower)	Ag	No data/ Spherical	α-amylase	12.5, 25, 50, and 100 µg.mL^{-1}	Acarbose	At highest dose, the NPs inhibited about 50% enzyme activity; At highest dose, acarbose inhibited about 68% enzyme activity.	[163]
Plant/ *Ajuga bracteosa*	Ag	500-5000/ Tube like	α-glucosidase	50 µg.mL^{-1}	Acarbose	At this dose, the NPs inhibited about 85.14% enzyme activity; At this dose, acarbose inhibited about 90.1% enzyme activity.	[102]
Plant/ *Solanum khasianum*	Ag	Average: 15.96/ Spherical	α-amylase	200, 400, 600, 800, and 1000 µg.mL^{-1}	Acarbose	At highest dose, this NPs inhibit 79.56% enzyme activity; At this dose, acarbose inhibited about 86.43% enzyme activity.	[103]
Plant/ *Cleome viscosa*	Ag	Average: 24/ Spherical and triangular	α-amylase	20, 40, 60, 80, and 100 µg.mL^{-1}	Acarbose	IC_{50} (AgNPs biosynthesized by 1mM $AgNO_3$)= 14.06 ± 0.89 µg.mL^{-1}; IC_{50} (AgNPs biosynthesized by 2mM $AgNO_3$)= 42.44 ± 2.68 µg.mL^{-1}; IC_{50} (AgNPs biosynthesized by 3mM $AgNO_3$)= 21.92 ± 1.74 µg.mL^{-1}; IC_{50}(Acarbose)= 14.06 ± 0.89 µg.mL^{-1}.	[164]
			α-glucosidase	20, 40, 60, 80, and 100 µg.mL^{-1}	Acarbose	IC_{50} (AgNPs biosynthesized by 1 mM $AgNO_3$) = 55.91 ± 2.98 µg.mL^{-1}; IC_{50} (AgNPs biosynthesized by 2 mM $AgNO_3$)= 37.73 ± 2.05 µg.mL^{-1}; IC_{50} (AgNPs biosynthesized by 3 mM $AgNO_3$) = 21.76 ± 1.91 µg.mL^{-1}; IC_{50} (Acarbose)= 18.52 ± 1.23 µg.mL^{-1}.	

Biological source/ Scientific name	NPs type	Size (nm)/ Morphology	Method	Dose of NPs	Positive control	Major outcome	Ref
Plant/ *Embelia robusta*	Ag	5-15/ Almost spherical	α-amylase	20, 40, 60, 80, and 100 µg.mL^{-1}	Acarbose	IC_{50}= 32.3 µg.mL^{-1}; IC_{50} (Acarbose): less than 20 µg.mL^{-1}.	[85]
			α-glucosidase	20, 40, 60, 80, and 100 µg.mL^{-1}	Acarbose	IC_{50}= 30.1 µg.mL^{-1}; IC_{50} (Acarbose): less than 20 µg.mL^{-1}.	
Plant/ *Vitis vinifera*	Ag	22-35/ Spherical	α-amylase	20, 40, 60, 80, and 100 µg.mL^{-1}	Acarbose	IC_{50}= 60.2 µg.mL^{-1}; IC_{50} (Acarbose)= 40.2 µg.mL^{-1}.	[165]
			α-glucosidase	20, 40, 60, 80, and 100 µg.mL^{-1}	Acarbose	IC_{50}= 62.5 µg.mL^{-1}; IC_{50} (Acarbose)= 40 µg.mL^{-1}.	
Animal/ Earthworm vermiwash	Ag	24-50/ Mostly spherical	α-amylase	100, 200, 300, 400, and 500 µg.mL^{-1}	Acarbose	IC_{50}= 218 µg.mL^{-1}; IC_{50} (Acarbose): less than 100 µg.mL^{-1}.	[166]
			α-glucosidase	100, 200, 300, 400, and 500 µg.mL^{-1}	Acarbose	IC_{50}= 221 µg.mL^{-1}; IC_{50} (Acarbose)= 200 µg.mL^{-1}.	
Plant/ *Momordica charantia* L.	Ag	2-12/ Spherical	α-amylase	20-100 µg.mL^{-1}	Acarbose	At highest dose, the NPs inhibited 75.50% enzyme activity; At highest dose, acarbose inhibited 80% enzyme activity.	[167]
Fungus/ *Cladosporium* species	Ag	Average: 24/ Spherical	α-amylase	500 µg.mL^{-1}	No data	At this dose, the NPs inhibited 99.49% enzyme activity.	[168]
			α-glucosidase	10, 25, 50, 100, 150 µg.mL^{-1}	Acarbose	At highest dose, the NPs inhibited 9.47% enzyme activity; At highest dose, acarbose inhibited 38.41% enzyme activity.	
Plant/ *Ocimum basilicum*	Ag	Average: 17.0 ± 8.94/ Spherical	α-amylase	0.0002-2 mg.mL^{-1}	Acarbose	At highest dose, the NPs inhibited 59.57 ± 3.72% enzyme activity; At highest dose, acarbose inhibited 48.27 ± 1.79 % enzyme activity.	[169]
			α-glucosidase	0.2-0.3 mg.mL^{-1}	Acarbose	At highest dose, the NPs inhibited 79.74 ± 9.51% enzyme activity; At highest dose, acarbose inhibited 73.75 ± 12.86% enzyme activity.	
Plant/ *Ocimum sanctum*	Ag	Average: 15.0 ± 12.34/ Spherical	α-amylase	0.0002-2 mg.mL^{-1}	Acarbose	At highest dose, the NPs inhibited 59.79 ± 6.91% enzyme activity; At highest dose, acarbose inhibited 48.27 ± 1.79% enzyme activity.	[169]
			α-glucosidase	0.2-0.3 mg.mL^{-1}	Acarbose	At highest dose, the NPs inhibited 89.31 ± 5.32% enzyme activity; At highest dose, acarbose inhibited 73.75 ± 12.86% enzyme activity.	
Combination of two plants/ *"Ocimum sanctum"* and *"Ocimum basilicum"*	Ag	Average: 17.0 ± 8.44/ Spherical	α-amylase	0.0002-2 mg.mL^{-1}	Acarbose	At highest dose, the NPs inhibited 54.94 ± 6.56% enzyme activity; At highest dose, acarbose inhibited 48.27 ± 1.79% enzyme activity.	[169]
			α-glucosidase	0.2-0.3 mg.mL^{-1}	Acarbose	At highest dose, the NPs inhibited 29.03 ± 15.92% enzyme activity; At	

Biological source/ Scientific name	NPs type	Size (nm)/ Morphology	Method	Dose of NPs	Positive control	Major outcome	Ref
						highest dose, acarbose inhibited 73.75 ± 12.86% enzyme activity.	
Plant/ *Hippeastrum hybridum* L.	Ag	Average: 40/ Spherical	α-amylase	25, 50, 75, and 100 µg.mL^{-1}	No data	At highest dose, the NPs inhibited 75.5 ± 0.002% enzyme activity.	[104]
Plant/ *Pterocarpus Marsupium*	Ag	Average: 132.6/ Spherical	α-amylase	0.2-1 mg.mL^{-1}	Acarbose	At highest dose, the NPs inhibited 81.15% enzyme activity; At highest dose, acarbose inhibited 91.83% enzyme activity.	[128]
Plant/ *Thymus serpyllum*	Ag	Average: 42/ Spherical	α-amylase	10, 20, 40, 60, 80, and 100 µg.mL^{-1}	Acarbose	IC_{50} (AgNPs)= 10 µg.mL^{-1}; IC_{50} (Acarbose)= 7.5 µg.mL^{-1}.	[95]
Plant/ *Nothapodytes foetida*	Ag	No data/ No data	α-amylase	200, 400, 600, 800, and 1000 µg.mL^{-1}	Acarbose	At highest dose, the NPs inhibited 80.43 ± 0.74% enzyme activity; At highest dose, acarbose inhibited 86.48 ± 0.64% enzyme activity.	[170]
			α-glucosidase	200, 400, 600, 800, and 1000 µg.mL^{-1}	Acarbose	At highest dose, the NPs inhibited 79.19 ± 0.51% enzyme activity; At highest dose, acarbose inhibited 87.13 ± 0.58% enzyme activity.	
Plant/ *Allium Sativum*	Ag	20-35/ Spherical	α-amylase	100, 200, 300, 400, and 500 µg.mL^{-1}	Acarbose	IC_{50} (AgNPs)= 306 µg.mL^{-1}; IC_{50}(Acarbose)= 376 µg.mL^{-1}.	[171])
Plant/ *Punica granatum*	Ag	35-60/ Spherical	α-amylase	20-100 µg,mL^{-1}	Acarbose	IC_{50}= 65.2 µg.mL^{-1}; IC_{50} (Acarbose)= between 20 to 40 µg.mL^{-1}.	[172]
			α-glucosidase	20-100 µg.mL^{-1}	Acarbose	IC_{50}= 53.8 µg.mL^{-1}; IC_{50} (Acarbose)= between 20 to 40 µg.mL^{-1}.	
Plant/ *Azadirachta indica*	Ag	10-30/ Spherical	α-amylase	50, 75, and 100 µg.mL^{-1}	Acarbose	IC_{50} (AgNPs)= 76.80 µg.mL^{-1}; IC_{50} (Acarbose)= between 20 to 40 µg.mL^{-1}.	[105]
Plant/ *Pisum sativum* L.	Ag	10-25/ Spherical	α-glucosidase	1, 2.5, 5, and 10 µg.mL^{-1}	No data	IC_{50}= 2.10 µg.mL^{-1}.	[173]
Plant/ *Moringa Oliefera*	Ag	Average: 15.5/ Spherical	α-amylase	50, 100, 150, and 200 µg.mL^{-1}	Metformin	At highest dose, the NPs inhibited 68% enzyme activity; At highest dose, metformin inhibited about 90% enzyme activity.	[174]
Plant/ *Zingiber officinale*	Ag	25-30/ Spherical	α-amylase	25, 50, 100, 150, and 200 µg.mL^{-1}	Acarbose	IC_{50}= 166.83 µg.mL^{-1}; IC_{50} (Acarbose)= 88.29 µg.mL^{-1}.	[175]
			α-glucosidase	25, 50, 100, 150, and 200 µg.mL^{-1}	Acarbose	IC_{50} (AgNPs)=166.30 µg.mL^{-1}; IC_{50} (Acarbose)= 86.74 µg.mL^{-1}.	
Plant/ *Curcuma amada*	Ag	25-30/ Spherical	α-amylase	25, 50, 100, 150, and 200 µg.mL^{-1}	Acarbose	IC_{50} (AgNPs)= 139.29 µg.mL^{-1}; IC_{50} (Acarbose)= 88.29 µg.mL^{-1}.	[175]
			α-glucosidase	25, 50, 100, 150, and 200 µg.mL^{-1}	Acarbose	IC_{50} (AgNPs)=136.47 µg.mL^{-1}; IC_{50} (Acarbose)= 86.74 µg.mL^{-1}.	
Fungus/ *Flammulina velutipes*	Ag	Average: 21.4/ Spherical	α-amylase	25, 50, 100, 200, and 400 µg.mL^{-1}	Acarbose	IC_{50}= 312 ± 0.67 µg.mL^{-1}; IC_{50} (Acarbose)= between 50 to 100 µg.mL^{-1}.	[106]
			α-glucosidase	25, 50, 100, 200, and 400 µg.mL^{-1}	Acarbose	IC_{50}= 357 ± 0.82 µg.mL^{-1}; IC_{50} (Acarbose)= between 50 to 100 µg.mL^{-1}	

Biological source/ Scientific name	NPs type	Size (nm)/ Morphology	Method	Dose of NPs	Positive control	Major outcome	Ref
Plant (Aqueous extract)/ *Gymnema sylvestre*	Ag	70-100/ Spherical	α-amylase	10, 30, and 100 µg.mL^{-1}	Acarbose	At highest dose, the NPs inhibited 42% enzyme activity; At highest dose, acarbose inhibited 58% enzyme activity.	[107]
Plant (Alcoholic extract)/ *Gymnema sylvestre*	Ag	70-100/ Spherical	α-amylase	10, 30, and 100 µg.mL^{-1}	Acarbose	At highest dose, the NPs inhibited 46% enzyme activity; At highest dose, acarbose inhibited 58% enzyme activity.	[107]
Plant/ *Averrhoa bilimbi*	Ag	400-450/ Polyhedral	α-amylase	100 µL (Obtaining from 10 g dried extract/ 100 mL 50% ethanol and 100 mL (0.01 M) aqueous solution of $AgNO_3$)	No data	At this dose, the biosynthesized NPs from fruit inhibited 6.48 ± 0.013% enzyme activity; At this dose, the biosynthesized NPs from leaf inhibited 21.41 ± 0.03% enzyme activity; At this dose, the biosynthesized NPs from flower inhibited 13.43 ± 0.03% enzyme activity.	[176]
Plant/ *Pterocarpus marsupium*	Ag	Average: 148.5/ No data	α-amylase	100, 200, 400, 800, and 1000 µg.mL^{-1}	Acarbose	IC_{50} (AgNPs)= 700 µg.mL^{-1}; IC_{50} (Acarbose)= 180 µg.mL^{-1}.	[177]
Plant/ *Vitas vinifera*	Ag	15-20/ Spherical	α-amylase	20, 40, 60, 80, and 100 µg.mL^{-1}	Acarbose	IC_{50} (AgNPs)= 43.94 µg.mL^{-1}; IC_{50} (Acarbose)= 40.2 µg.mL^{-1}.	[98]
			α-glucosidase	20, 40, 60, 80, and 100 µg.mL^{-1}	Acarbose	IC_{50} (AgNPs)= 48.5 µg.mL^{-1}; IC_{50} (Acarbose)= 40 µg.mL^{-1}.	
Plant/ *Dregea volubilis*	Ag	8.59-19.18/ Spherical	α-amylase	2.5, 5, 7.5, 10, 12.5, and 15 µg.mL^{-1}	Acarbose	IC_{50} (AgNPs)= 10.62 ± 0.22 µg.mL^{-1}; IC_{50} (Acarbose)= 51.17 ± 1.99 µg.mL^{-1}.	[178]
			α-glucosidase	1, 2, 4, 6, 8, and 10 µg.mL^{-1}	Acarbose	IC_{50} (AgNPs)= 6.49 ± 0.03 µg.mL^{-1}; IC_{50} (Acarbose)= 479.60 ± 4.49 µg.mL^{-1}.	
Plant/ *Acacia nilotica*	Ag	20-50/ Variable shapes	α-glucosidase	50, 100, and 250 µg.mL^{-1}	Acarbose	At highest dose, the biosynthesized NPs by 0.1 M $AgNO_3$ inhibited 73.93% enzyme activity; At highest dose, the biosynthesized NPs by 3 mM $AgNO_3$ inhibit 51.28%; At highest dose, acarbose inhibit 59.32% enzyme activity.	[179]
Plant/ *Allium fistulosum*	Ag	Average: 40/ Rod-like	α-amylase	5, 10, 15, 20, and 25 µg.mL^{-1}	Posetive control	At highest dose, the NPs inhibited about 75% enzyme activity; At highest dose, positive control about 75% enzyme activity.	[180]
Plant/ *Tabernaemontana divaricate*	Ag	Average: 55/ Rod-like	α-amylase	5, 10, 15, 20, and 25 µg.mL^{-1}	Posetive control	At highest dose, the NPs inhibited about 80% enzyme activity; At highest dose, positive control about 75% enzyme activity.	[180]
Plant/ *Basella alba*	Ag	Average: 57/ Rod-like	α-amylase	5, 10, 15, 20, and 25 µg.mL^{-1}	Posetive control	At highest dose, the NPs inhibited about 78% enzyme activity; At highest dose, positive control about 75% enzyme activity.	[180]

Biological source/ Scientific name	NPs type	Size (nm)/ Morphology	Method	Dose of NPs	Positive control	Major outcome	Ref
Plant/ *Allium cepa*	Ag	49-73/ Spherical	α-amylase	20, 40, 60, 80, and 100 µg.mL^{-1}	Acarbose	At highest dose, the NPs inhibited about about 75% enzyme activity; At highest dose, acarbose about 60% enzyme activity.	[181]
			α-glucosidase	20, 40, 60, 80, and 100 µg.mL^{-1}	Acarbose	At highest dose, the NPs inhibited about about 60% enzyme activity; At highest dose, acarbose about 60% enzyme activity.	
Plant/ *Holoptelea integrifolia*	Ag	32-38/ Spherical	α-amylase	25, 50, 75, and 100 µg.mL^{-1}	Acarbose	At highest dose, the NPs inhibited about 86.66 ± 5.03% enzyme activity; At highest dose, acarbose inhibited about 95.01 ± 5.41% enzyme activity.	([182]
Fungus/ *Pleurotus giganteus*	Ag	2-20/ Spherical	α-amylase	100, 200, 300, 400, 500 µg.mL^{-1}	Acarbose	At highest dose, the NPs inhibited about about 67% enzyme activity; At highest dose, acarbose inhibited about 62% enzyme activity.	[183]
Combination of five plants/ "*Tinospora cordiofolia", "Curcuma longa", "Trigonella foenum gracum", "Emblica officinale",* and *'Salacia oblonga'*	Ag	70-80/ Spherical	α-amylase	50, 100, 150, 200, and 250 µg.mL^{-1}	Ascorbic acid	At highest dose, the NPs inhibited about about 65% enzyme activity; At highest dose, ascorbic acid inhibited about 73.87% enzyme activity.	[184]
Plant/ *Muntingia calabura*	Ag	10.34-22.12/ Spherical	α-amylase	200, 400, 600, 800, 1000 µg.mL^{-1}	Acarbose	At highest dose, the NPs inhibited 78.16% enzyme activity; At highest dose, acarbose inhibited about about 85% enzyme activity.	[185]
Alga/ *Galaxaura elongata*	Ag	30-90/ Almost spherical	α-amylase	12.5, 25, 50, 100, 150, and 200 µg.mL^{-1}	Acarbose	IC_{50} (AgNPs)= 102.55 µg,.mL^{-1}; IC_{50} (Acarbose)= 74.66 µg.mL^{-1}.	[186]
Alga/*Turbinaria ornata*	Ag	20-60/ Almost spherical	α-amylase	12.5, 25, 50, 100, 150, and 200 µg.mL^{-1}	Acarbose	IC_{50} (AgNPs)= 90 µg.mL^{-1}; IC_{50} (Acarbose)= 74.66 µg.mL^{-1}.	[186]
Alga/ *Enteromorpha flexuosa*	Ag	30-90/ Almost spherical	α-amylase	12.5, 25, 50, 100, 150, and 200 µg.mL^{-1}	Acarbose	IC_{50} (AgNPs)= 87.33 µg.mL^{-1}; IC_{50} (Acarbose)= 74.66 µg.mL^{-1}.	[186]
Plant/ *Annona mricata*	Ag	Average: 35/ Spherical	α-amylase	No data	Acarbose	IC_{50} (AgNPs)= 0.90 ± 0.01 µg.mL^{-1}; IC_{50} (Acarbose)= 10.20 ± 0.05 µg.mL^{-1}.	[187]
			α-glucosidase	No data	Acarbose	IC_{50} (AgNPs)= 3.32 ± 0.32 µg.mL^{-1}; IC_{50} (Acarbose)= 610.65 ± 4.27 µg.mL^{-1}.	
Plant/ *Justicia diffusa*	Ag	Average: 50/ Uniform spherical	α-amylase	7.4, 22.4, 66.6, and 200 µg.mL^{-1}	Acarbose	IC_{50} (AgNPs)= between 31.70 to 61.70 µg.mL^{-1}; The amount of enzyme inhibition by acarbose is not mentioned.	[188]

Biological source/ Scientific name	NPs type	Size (nm)/ Morphology	Method	Dose of NPs	Positive control	Major outcome	Ref
Plant/ *Centella asiatica*	Ag	30-50/ Spherical	α-amylase	200, 400, 600, 800, 1000 $\mu g.mL^{-1}$	Acarbose	At highest dose, the NPs inhibited 43.96 ± 0.91% enzyme activity; At highest dose, the NPs inhibited 55.75 ± 0.71% enzyme activity.	[189]
Plant/ *Hybanthus enneaspermus*	Ag	0-10/ Spherical	α-amylase	20, 40, 60, 80, and 100 $\mu g.mL^{-1}$	Acarbose	IC_{50} (AgNPs)= 41.27 ± 0.11 $\mu g.mL^{-1}$; IC_{50} (Acarbose)= 75.07 ± 0.56 $\mu g.mL^{-1}$.	[190]
			α-glucosidase	20, 40, 60, 80, and 100 $\mu g.mL^{-1}$	Acarbose	IC_{50} (AgNPs)= 42.87 ± 0.44 $\mu g.mL^{-1}$; IC_{50} (Acarbose)= 82.00 ± 1.26 $\mu g.mL^{-1}$.	
Plant/ *Ananas comosus* L.	Ag	No data/ Nearly spherical	α-glucosidase	0.008-1 $\mu g.mL^{-1}$	No data	At 0.063 to 1 $\mu g.mL^{-1}$, the NPs inhibited 100% enzyme activity.	[99]
Plant/ *Chrysophyllum albidum*	Ag	No data/ No data	α-amylase	50, 100, 150, 200, 250, and 300 $\mu g.mL^{-1}$	Acarbose	IC_{50} (AgNPs)= 123.7 $\mu g.mL^{-1}$; IC_{50} (Acarbose)= 11.77 $\mu g.mL^{-1}$.	[191]
Plant/ *Gracilaria edulis*	Ag	71-110/ Spherical	α-amylase	100, 200, 300, and 400 $\mu g.mL^{-1}$	No data	At highest dose, the NPs inhibited 98.75% enzyme activity.	[192]
Plant/ *Syringodium isoetifolium*	Ag	71-110/ Spherical	α-amylase	100, 200, 300, and 400 $\mu g.mL^{-1}$	No data	At highest dose, the NPs inhibited 77.25% enzyme activity.	[192]
Plant/ *Arctium lappa*	Ag	Average: 72.656/ Nearly spherical	α-glucosidase	0.12, 0.25, and 0.5 $\mu g.mL^{-1}$	No data	IC_{50}= 0.653 $\mu g.mL^{-1}$.	[90]
Plant/ *Annona squamosa*	Ag	18-35/ Almost spherical	α-amylase	25, 50, 100, and 200 $\mu g.mL^{-1}$	Acarbose	IC_{50} (AgNPs)= 80.7 $\mu g.mL^{-1}$; IC_{50} (Acarbose)= 88.6 $\mu g.mL^{-1}$.	[193]
Animal/ Prawn head waste	Ag	23-28/ Spherical	α-amylase	100, 200, 300, 400, and 500 $\mu g.mL^{-1}$	Acarbose	IC_{50} (AgNPs)= 296 $\mu g.mL^{-1}$; IC_{50} (Acarbose)= between 300 to 400 $\mu g.mL^{-1}$	[194]
			α-glucosidase	100, 200, 300, 400, and 500 $\mu g.mL^{-1}$	Acarbose	IC_{50} (AgNPs)= 705 $\mu g.mL^{-1}$; IC_{50} (Acarbose)= 200 $\mu g.mL^{-1}$.	
Plant/ *Brassica oleracea*	Ag	No data/ Almost spherical	α-glucosidase	1, 2.5, and 5 $\mu g.mL^{-1}$	No data	IC_{50}= 2.29 $\mu g.mL^{-1}$.	[86]
Plant/ *Rosa indica* L.(ethanol extract)	Ag	Average: 18/ Spherical	α-amylase	10, 25, 50, 75, and 100 $\mu g.mL^{-1}$	Acarbose	IC_{50} (AgNPs)~ 50 $\mu g.mL^{-1}$; IC_{50} (Acarbose)= between 25 to 50 $\mu g.mL^{-1}$.	[83]
			α-glucosidase	10, 25, 50, 75, and 100 $\mu g.mL^{-1}$	Acarbose	IC_{50} (AgNPs)~ 50 $\mu g.mL^{-1}$; IC_{50} (Acarbose)~ 50 $\mu g.mL^{-1}$.	
Plant/ *Rosa indica* L.(acetone extract)	Ag	Average: 12/ Spherical	α-amylase	10, 25, 50, 75, and 100 $\mu g.mL^{-1}$	Acarbose	IC_{50}~ 50 $\mu g.mL^{-1}$; IC_{50} (Acarbose)= between 25 to 50 $\mu g.mL^{-1}$.	[83]
			α-glucosidase	10, 25, 50, 75, and 100 $\mu g.mL^{-1}$	Acarbose	IC_{50} (AgNPs)~ 50 $\mu g.mL^{-1}$; IC_{50} (Acarbose)~ 50 $\mu g.mL^{-1}$.	
Plant/ *Rosa indica* L.(water extract)	Ag	Average: 770/ Spherical	α-amylase	10, 25, 50, 75, and 100 $\mu g.mL^{-1}$	Acarbose	IC_{50} (AgNPs)~ 75 $\mu g.mL^{-1}$; IC_{50} (Acarbose)= between 25 to 50 $\mu g.mL^{-1}$.	[83]
			α-glucosidase	10, 25, 50, 75, and 100 $\mu g.mL^{-1}$	Acarbose	IC_{50} (AgNPs)~ 75 $\mu g.mL^{-1}$; IC_{50} (Acarbose)~ 50 $\mu g.mL^{-1}$.	

Biological source/ Scientific name	NPs type	Size (nm)/ Morphology	Method	Dose of NPs	Positive control	Major outcome	Ref
Plant/ *Cissus quadrangularis*	Ag	No data/ Irregular shape	α-amylase	12.5, 25, 50, and 100 µg.mL^{-1}	Acarbose	At highest dose, the NPs inhibited between 65 to 70% enzyme activity; At highest dose, acarbose inhibited between 65 to 70 % enzyme activity.	[195]
Plant/ *Syzygium aromaticum*	Ag	No data/ Cubic	α-amylase	0.2-1 mg.mL^{-1}	Acarbose	IC_{50} (AgNPs)= 0.20 µg.mL^{-1}; IC_{50}(Acarbose)= 0.27 µg.mL^{-1}.	[196]
Plant/ *Silybum marianum* (wild plant)	Ag	Average: 22/ Spherical	α-amylase	No data	No data	At highest dose, the NPs inhibited 25.36 ± 1.12% enzyme activity.	[197]
			α-glucosidase	No data	No data	At highest dose, the NPs inhibited 22.45 ± 0.78% enzyme activity.	
Plant/ *Silybum marianum* (seed)	Ag	Average: 19/ Spherical	α-amylase	No data	No data	At highest dose, the NPs inhibited 26.78 ± 1.43% enzyme activity.	[197]
			α-glucosidase	No data	No data	At highest dose, the NPs inhibited 25.41 ± 1.37% enzyme activity.	
Plant/ *Cassia auriculata*	Ag	No data/ No data	α-amylase	10, 20, 30, 40, 50, 100 µg.mL^{-1}	Acarbose	At highest dose, the NPs inhibited about 80% enzyme activity; At highest dose, acarbose inhibited about 70% enzyme activity.	[198]
			α-glucosidase	10, 20, 30, 40, 50, 100 µg.mL^{-1}	Acarbose	At highest dose, the NPs inhibited about 70% enzyme activity; At highest dose, acarbose inhibited about 60% enzyme activity.	
Plant/ *Odontosoria chinensis* (L.)	Ag	22.3-48.2/ Spherical	α-amylase	100, 250, 500, and 1000 µg.mL^{-1}	Acarbose	At highest dose, the NPs inhibited 62% enzyme activity; At highest dose, acarbose inhibited 78% enzyme activity.	[199]
Animal/ Bee pollen	Ag	40-60/ Mostly spherical	α-amylase	No data	Acarbose	IC_{50} (AgNPs)= 2.56 ± 0.10 µg.mL^{-1}; IC_{50} (Acarbose)= 7.32 ± 0.12 µg.mL^{-1}.	[200]
			α-glucosidase	No data	Acarbose	IC_{50} (AgNPs)= 2.13 ± 0.11 µg.mL^{-1}; IC_{50} (Acarbose)= 7.32 ± 0.12 µg.mL^{-1}.	
Plant/ *Punica granatum* (L.)	Ag	No data/ No data	α-amylase	10, 15, and 20 µg.mL^{-1}	Acarbose	At highest dose, the NPs inhibited 84% enzyme activity; At highest dose, acarbose inhibited 64.07 ± 1.43% enzyme activity.	[201]
			α-glucosidase	10, 15, and 20 µg.mL^{-1}	Acarbose	At highest dose, the NPs inhibited 79% enzyme activity; The amount of enzyme inhibition by acarbose is not mentioned.	
Plant/ *Bauhinia variegata*	Ag	5-15/ Spherical	α-amylase	10, 20, 30, 40, and 50 µg.mL^{-1}	Acarbose	IC_{50} (AgNPs)= 38 µg.mL^{-1}; IC_{50} (Acarbose)= between 20 to 30 µg.mL^{-1}.	[109]
Plant/ *Zephyranthes candida*	Ag	Average: 33/ Face-centred cubic	α-amylase	50, 100, 200, 250, and 500 µg.mL^{-1}	Acarbose	At highest dose, the NPs inhibited 73.3% enzyme activity; At highest dose, acarbose inhibited about 80% enzyme activity.	[88]
Plant/ *Avicennia officinalis*	Ag	Average: 98.77/	α-amylase	0.1, 0.2, and 0.5 mg.mL^{-1}	Acarbose	IC_{50} (AgNPs)= 0.28 ± 0.002 mg.mL^{-1}; IC_{50} (Acarbose)= 0.15 mg.mL^{-1}.	[202]

Biological source/ Scientific name	NPs type	Size (nm)/ Morphology	Method	Dose of NPs	Positive control	Major outcome	Ref
Plant/ *Xylocarpus granatum*	Ag	Polydispersed	α-glucosidase	0.1, 0.2, and 0.5 $mg.mL^{-1}$	Acarbose	IC_{50} (AgNPs)= 0.15 ± 0.012 $mg.mL^{-1}$; IC_{50} (Acarbose)= 0.11 $mg.mL^{-1}$.	[202]
		Average: 181.4/ Polydispersed	α-amylase	0.1, 0.2, and 0.5 $mg.mL^{-1}$	Acarbose	IC_{50} (AgNPs)= 0.19 ± 0.011 $mg.mL^{-1}$; IC_{50} (Acarbose)= 0.15 $mg.mL^{-1}$.	
			α-glucosidase	0.1, 0.2, and 0.5 $mg.mL^{-1}$	Acarbose	IC_{50} (AgNPs)= 0.13 ± 0.005 $mg.mL^{-1}$; IC_{50} (Acarbose)= 0.11 $mg.mL^{-1}$.	
Plant/ *Cannabis sativa* (L.)	Ag	Average: 11.5/ Spherical	α-glucosidase	No data	Acarbose	IC_{50} (AgNPs)= 32.31 $\mu g.mL^{-1}$; IC_{50} (Acarbose)= 133.34 $\mu g.mL^{-1}$.	[203]
Plant/ *Heritiera fomes*	Ag	No data/ No data	α-amylase	No data	No data	IC_{50}= 114.88 $\mu g.mL^{-1}$.	[204]
Plant/ *Sonneratia apetala*	Ag	No data/ No data	α-amylase	No data	No data	IC_{50}= 95.51 $\mu g.mL^{-1}$.	[204]
Plant/ *Amaranthus Gangeticus* (L.)	Ag	10-20/ Sperical	α-amylase	100, 200, 300, 400, and 500 $\mu g.mL^{-1}$	Acarbose	At highest dose, the NPs inhibited about 75% enzyme activity; At highest dose, acarbose inhibited about 90% enzyme activity.	[205]
			α-glucosidase	100, 200, 300, 400, and 500 $\mu g.mL^{-1}$	Acarbose	At highest dose, the NPs inhibited about 75% enzyme activity; At highest dose, acarbose inhibited about 90% enzyme activity.	
Plant/ *Saraca asoca*	Au	Average: 24/ Spherical	α-amylase	0.25-0.75 mM	No data	IC_{50}= 1.5 mM	[146]
Animal/ Earthworm vermiwash	Au	24-50/ Spherical	α-amylase	100, 200, 300, 400, and 500 $\mu g.mL^{-1}$	Acarbose	IC_{50} (AuNPs)= 384 $\mu g.mL^{-1}$; IC_{50} (Acarbose)= less than 100 $\mu g.mL^{-1}$.	[166]
			α-glucosidase	100, 200, 300, 400, and 500 $\mu g.mL^{-1}$	Acarbose	IC_{50} (AuNPs)= 290 $\mu g.mL^{-1}$; IC_{50} (Acarbose)= 200 $\mu g.mL^{-1}$.	
Plant/ *Hylocereus polyrhizus*	Au	Average: 25.31/ Spherical	α-amylase	50, 100, and 200 $\mu g.mL^{-1}$	Acarbose	At highest dose, the NPs inhibited 40.07 ± 0.65% enzyme activity; At highest dose, acarbose inhibited 50.10 ± 0.13% enzyme activity.	[91]
Plant/ *Amaranthus gangeticus* (L.)	Au	10-200/ Almost spherical	α-amylase	100, 200, 300, 400, and 500 $\mu g.mL^{-1}$	Acarbose	IC_{50} (AuNPs)= 234.71 ± 1.32 $\mu g.mL^{-1}$; IC_{50} (Acarbose)= between 100 to 200 $\mu g.mL^{-1}$.	[206]
			α-glucosidase	100, 200, 300, 400, and 500 $\mu g.mL^{-1}$	Acarbose	IC_{50} (AuNPs)= 238.31 ± 1.15 $\mu g.mL^{-1}$; IC_{50} (Acarbose)= between 100 to 200 $\mu g.mL^{-1}$.	
Animal/ Prawn head waste	Au	20-27/ Spherical	α-amylase	100, 200, 300, 400, and 500 $\mu g.mL^{-1}$	Acarbose	IC_{50} (AuNPs)= 356 $\mu g.mL^{-1}$; IC_{50} (Acarbose)= between 300 to 400 $\mu g.mL^{-1}$	[194]
			α-glucosidase	100, 200, 300, 400, and 500 $\mu g.mL^{-1}$	Acarbose	IC_{50} (AuNPs)= 2475 $\mu g.mL^{-1}$; IC_{50} (Acarbose)= 200 $\mu g.mL^{-1}$.	
Plant/ *Moricandia Nitens*	Au	5-20/ Spherical	α-glucosidase	1.95-1000 $\mu g.mL^{-1}$	Acarbose	IC_{50} (AuNPs)= 159.3 $\mu g.mL^{-1}$; IC_{50} (Acarbose)= 30.54 $\mu g.mL^{-1}$.	[207]
Plant/ *Carduus edelbergii*	Au	Average: 15.6/ Spherical	α-amylase	250, 500, 750, and	No data	At highest dose, the NPs inhibited 63.7 ± 5.1% enzyme activity.	[93]

Biological source/ Scientific name	NPs type	Size (nm)/ Morphology	Method	Dose of NPs	Positive control	Major outcome	Ref
				1000 $\mu g.mL^{-1}$			
Plant/ *Annona muricata*	Au	Average: 14.89 ± 3.46/ Spherical	α-glucosidase	10, 20, 30, 40, and 50 $\mu g.mL^{-1}$	No data	IC_{50}= 51.37 ± 3.34 $\mu g.mL^{-1}$.	[208]
Plant/ *Citrus aurantifulia*	Au	17-24/ Spherical	α-glucosidase	No data	Acarbose	IC_{50} (AuNPs)= 130.32 $\mu g.mL^{-1}$; IC_{50} (Acarbose)= 133.34 $\mu g.mL^{-1}$.	[209]
Plant/ *Pituranthos tortuosus*	Au	20-40/ Quasi spherical	α-glucosidase	0-1000 $\mu g.mL^{-1}$	Acarbose	IC_{50} (AuNPs)= 77.41 $\mu g.mL^{-1}$; IC_{50} (Acarbose)= 30.57 $\mu g.mL^{-1}$.	[210]
Alga/ *Gelidiella acerosa*	Au	5.81-117.59/ Spherical	α-amylase	1, 2, 3, 4, and 5 $\mu g.mL^{-1}$	Acarbose	IC_{50} (AuNPs)= 2.1 ± 0.01 $\mu g.mL^{-1}$; IC_{50} (Acarbose)= 1.7 ± 0.02 $\mu g.mL^{-1}$.	[108]
			α-glucosidase	1, 2, 3, 4, and 5 $\mu g.mL^{-1}$	Acarbose	IC_{50} (AuNPs)= 2.8 ± 0.02 $\mu g.mL^{-1}$; IC_{50} (Acarbose)= 2.5 ± 0.01 $\mu g.mL^{-1}$.	
Plant/ *Moringa oleifera*	Au	35-51/ Hexagonal	α-amylase	50, 100, 150, and 200 $\mu g.mL^{-1}$	Metformin	IC_{50} (AuNPs)= 130 $\mu g.mL^{-1}$; IC_{50} (Metfotmin)= between 100 to 120 $\mu g.mL^{-1}$.	[211]
Plant (Total extract)/ *Leucosidea sericea*	Au	Average: 6/ Spherical	α-amylase	No data	Acarbose	IC_{50} (AuNPs)= 3.0 ± 0.3 $\mu g.mL^{-1}$; IC_{50} (Acarbose)= 10.2 ± 0.6 $\mu g.mL^{-1}$.	[212]
			α-glucosidase	No data	Acarbose	IC_{50} (AuNPs)= 14.5 ± 0.8 $\mu g.mL^{-1}$; IC_{50} (Acarbose)= 610 ± 2.6 $\mu g.mL^{-1}$.	
Plant (Procyanidins fractions of dimers)/ *Leucosidea sericea*	Au	Average: 24/ Spherical	α-amylase	No data	Acarbose	IC_{50} (AuNPs)= 1.8 ± 0.3 $\mu g.mL^{-1}$; IC_{50} (Acarbose)= 10.2 ± 0.6 $\mu g.mL^{-1}$.	[212]
			α-glucosidase	No data	Acarbose	IC_{50} (AuNPs)= 7.3 ± 0.3 $\mu g.mL^{-1}$; IC_{50} (Acarbose)= 610 ± 2.6 $\mu g.mL^{-1}$.	
Plant (Procyanidins fractions of trimers)/ *Leucosidea sericea*	Au	Average: 21/ Spherical	α-amylase	No data	Acarbose	IC_{50} (AuNPs)= 10.5 ± 0.1 $\mu g.mL^{-1}$; IC_{50} (Acarbose)= 10.2 ± 0.6 $\mu g.mL^{-1}$.	[212]
			α-glucosidase	No data	Acarbose	IC_{50} (AuNPs)= 4.5 ± 0.6 $\mu g.mL^{-1}$; IC_{50} (Acarbose)= 610 ± 2.6 $\mu g.mL^{-1}$.	
Plant/ *Tephrosia tinctoria*	Ag	Average: 73/ Spherical	α-amylase	25, 50, and 75 $\mu g.mL^{-1}$	Acarbose	At highest dose, the NPs inhibited 94.76 ± 0.86% enzyme activity; At highest dose, acarbose inhibited 97.79 ± 0.63% enzyme activity.	[213]
			α-glucosidase	25, 50, and 75 $\mu g.mL^{-1}$	Acarbose	At highest dose, the NPs inhibited 83.52 ± 0.71% enzyme activity; At highest dose, acarbose inhibited 96.25 ± 1.40% enzye activity.	
Plant/ *Azhadirachta indica*	Au	Average: 38.48/ No data	α-glucosidase	20, 40, 60, 80, and 100 $\mu g.mL^{-1}$	Acarbose	IC_{50} (AuNPs)= 58.66 $\mu g.mL^{-1}$; IC_{50} (Acarbose)= 43.08 $\mu g.mL^{-1}$.	[214]
			α-amylase	20, 40, 60, 80, and 100 $\mu g.mL^{-1}$	Acarbose	IC_{50} (AuNPs)= 45.72 $\mu g.mL^{-1}$; IC_{50} (Acarbose)= 40.879 $\mu g.mL^{-1}$.	
Plant/ *Azhadirachta indica*	Ag	Average: 16.11/ No data	α-glucosidase	20, 40, 60, 80, and 100 $\mu g.mL^{-1}$	Acarbose	IC_{50} (AgNPs)= 48.01 $\mu g.mL^{-1}$; IC_{50} (Acarbose)= 43.08 $\mu g.mL^{-1}$.	[214]

Biological source/ Scientific name	NPs type	Size (nm)/ Morphology	Method	Dose of NPs	Positive control	Major outcome	Ref
Bacterium/ *Salmonella enterica*	Ag	7.18-13.24/ Spherical	α-amylase	20, 40, 60, 80, and 100 µg.mL^{-1}	Acarbose	IC_{50} (AgNPs)= 44.07 µg.mL^{-1}; IC_{50} (Acarbose)= 40.879 µg.mL^{-1}.	[87]
			α-amylase	62.25, 125, 250, 500, and 1000 µg.mL^{-1}	Acarbose	IC_{50} (AgNPs)= 428.60 µg.mL^{-1}; IC_{50} (Acarbose)= 295.42 µg.mL^{-1}.	
			α-glucosidase	62.25, 125, 250, 500, and 1000 µg.mL^{-1}	Voglibose	IC_{50} (AgNPs)= 562.02 µg.mL^{-1}; IC_{50} (Voglibose)= 313.62 µg.mL^{-1}.	
Plant/ *Casuarina equisetifolia*	Au	Average: 15/ Spherical	α-amylase	No data	Acarbose	The NPs inhibited 60.67 ± 0.88% enzyme activity enzyme activity; Acarbose inhibited 65.00 ± 0.58% enzyme activity enzyme activity.	[215]
Plant/ *Nigella sativa*	Au	20-30/ Spherical	α-amylase	100. 200, 300, 400, and 500 µg.mL^{-1}	No data	At highest dose, the NPs inhibited 81% enzyme activity.	[216]
			α-glucosidase	100. 200, 300, 400, and 500 µg.mL^{-1}	No data	At highest dose, the NPs inhibited 82. 3% enzyme activity.	
Plant/ *Anacardium occidentale*	Au	No data/ Spherical	α-glucosidase	20, 40, 60, 80, and 100 µg.mL^{-1}	Acarbose	At highest dose, the NPs inhibited 79 ± 0.26% enzyme activity; At highest dose, acarbose inhibited 95.68 ± 1.38% enzyme activity.	[217]
Plant/ *Physalis minima*	Au	Average: 15/ Spherical	α-amylase	100. 200, 300, 400, and 500 µg.mL^{-1}	Acarbose	At highest dose, the NPs inhibited 93% enzyme activity; The amount of enzyme inhibition by acarbose is not mentioned.	[82]
Plant/ *Aeonium haworthii*	Ag	35-55/ Spherical	α-amylase	10-120 µg.mL^{-1}	Acarbose	IC_{50} (AgNPs)= 62.84 µg.mL^{-1}; IC_{50} (Acarbose)= 100.73 µg.mL^{-1}.	[92]

Table 2. *In vivo* assessment of the antidiabetic effects of green-synthesized silver and gold nanomaterials.

Biological source/ Scientific name	NPs type	Size (nm)/ Morphology	Dose	Animal type/ Number of animal in each group	Diabetic model	Routes of administration	[a]Antidiabetic techniques	Major outcome	Ref
Plant/ *Ziziphora clinopodioides*	Ag	1-100/ Spherical	50, 100, 200, 400 mg.kg^{-1}	Diabetic Wistar rat/ 5	Streptozotocin-induced rat	No data	Blood glucose assay	The blood glucose levels in the groups administered 50, 100, 200, and 400 mg.kg^{-1} AgNPs were significantly reduced after 10 and 20 days (P<0.05).	[110]
Plant/ *Salvia sclarea*	Ag	Average: 40 ± 5 / Quasi-spherical	10 mg.kg^{-1}	Diabetic Wistar rat/ 6	Streptozotocin-induced rat	Intraperitoneal injection	FBG assay, HbA_1C assay, and insulin assay	The FBG levels and Hb_1AC in the groups administered 10 mg.kg^{-1} AgNPs were	[111]

Biological source/ Scientific name	NPs type	Size (nm)/ Morphology	Dose	Animal type/ Number of animal in each group	Diabetic model	Routes of administration	[a]Antidiabetic techniques	Major outcome	Ref
								significantly reduced and insulin level also increased (P<0.001).	
Plant/ *Origanum majorana*	Ag	Average: 30 ± 5 / Mostly spherical	20 $mg.kg^{-1}$	Diabetic Wistar rat/ 5	Streptozotocin-induced rat	Oral	Blood glucose assay	The blood glucose levels in the groups administered 20 $mg.kg^{-1}$ AgNPs were significantly reduced after 28 days (P<0.05).	[112]
Plant/ *Ferula assafoetida*	Ag	35-40/ Spherical	100 $mg.kg^{-1}$	Diabetic Wistar rat/ 4	Streptozotocin-induced rat	Oral	Blood glucose assay	The blood glucose levels in the groups administered 100 $mg.kg^{-1}$ AgNPs were significantly reduced after 28 days (P<0.05).	[113]
Plant/ Kickxia elatine	Ag	Average: 42.47 / Spherical	150, 300, and 450 $mg.kg^{-1}$	Diabetic Sprague Dawley rat/ 5	Alloxan-induced rat	Oral	FBG	The FBG levels in the groups administered 150, 300, and 450 $mg.kg^{-1}$ AgNPs were significantly reduced after 7, 14, and 21 days (P<0.01).	[114]
Plant/ *Cassia auriculata*	Ag	40-100/ Nearly spherical	50 and 200 $mg.kg^{-1}$	Diabetic Wistar rat/ 3	Streptozotocin-induced rat	Intraperitoneal injection	FBG assay	The levels of FBG in groups administered 50 and 200 $mg.kg^{-1}$ AgNPs were significantly reduced after 10 days (P<0.01).	[115]
Plant/ Lawsonia inermis	Ag	Average: 14.9/ Spherical	200 $mg.kg^{-1}$	Diabetic Wistar rat/ 6	Streptozotocin-induced rat	Oral	FBG assay and fasting insulin assay	The blood glucose levels in the group administered 200 $mg.kg^{-1}$ AgNPs were significantly reduced after 14 days and the fasting insulin level also increased (P<0.001).	[116]
Plant/ *Momordica charantia*	Ag	Average: 22.5/ Spherical	100 and 200 $mg.kg^{-1}$	Diabetic Wistar rat/ 6	Streptozotocin-induced rat	Oral	Blood glucose assay, OGTT assay, and fasting insulin assay	The blood glucose levels in the groups administered 100 and 200 $mg.kg^{-1}$ AgNPs after 14 days and OGTT level	[117]

Biological source/ Scientific name	NPs type	Size (nm)/ Morphology	Dose	Animal type/ Number of animal in each group	Diabetic model	Routes of administration	[a]Antidiabetic techniques	Major outcome	Ref
								after 120 min were significantly reduced and the fasting insulin level increased (P<0.001).	
Plant/ *Ventilago maderaspatana*	Ag	10-50/ Spherical	20 $mg.kg^{-1}$	Albino rat/ 3	Streptozotocin-induced rat	Not mentioned	Blood glucose assay, HbA_1C assay, and insulin assay	The blood glucose level and HbA_1C in the group administered 20 $mg.kg^{-1}$ AgNPs decreased after 15 days and the insulin level increased after 15 days.	[118]
Plant/ *Emblica phyllanthus*	Ag	5-47/ Spherical	150 and 300 $mg.kg^{-1}$	Albino mouse/ 6	Alloxan-induced mouse	Oral	Blood glucose assay	The blood glucose levels in the groups administered 150 and 300 $mg.kg^{-1}$ AgNPs were significantly reduced after 3, and 5 h and 4, 7, 10, and 15 days (P<0.05).	[119]
Plant/ *Gymnema sylvestre*	Ag	Average: 21.5/ Spherical	100 and 200 $mg.kg^{-1}$	Wistar rat/ 6	Streptozotocin-induced rat	Oral	Blood glucose assay and fasting insulin assay	The blood glucose levels in the groups administered 100 and 200 $mg.kg^{-1}$ AgNPs were significantly reduced after 14 days and the fasting insulin level also increased (P<0.05).	[120]
Plant/ *Catharanthus roseus*	Ag	Average: 45/ Spherical	500 $mg.kg^{-1}$ with aqueous *Catharanthus roseus* extract	Wister rat/ 10	Streptozotocin-induced rat	Intragastrically	OGTT assay	The OGTT levels in the groups administered 500 $mg.kg^{-1}$ AgNPs with aqueous *Catharanthus roseus* extract were significantly reduced after 60 and 120 min (P<0.05).	[121]
Plant/ *Phagnalon niveum*	Ag	12-28/ Spherical	10 $mg.kg^{-1}$	Wistar rat/ 5	Alloxan-induced rat	Oral	FBG assay and OGTT assay	The FBG levels in the groups administered 10 $mg.kg^{-1}$ AgNPs after 15 and 21	[123]

Biological source/ Scientific name	NPs type	Size (nm)/ Morphology	Dose	Animal type/ Number of animal in each group	Diabetic model	Routes of administration	[a]Antidiabetic techniques	Major outcome	Ref
								days were significantly reduced (P<0.05) and OGTT level after 90 and 120 min decreased.	
Plant/ *Eryngium thyrsoideum Bioss*	Ag	Average: 45/ Spherical	2.5 $mg.kg^{-1}$	Rat/ 5	Alloxan-induced rat	Intraperitoneal injection	FBG assay and HbA_1C assay	The levels of FBG in groups administered 50 and 2.5 $mg.kg^{-1}$ AgNPs were significantly reduced after 7 and 15 days and the level of HbA_1C also decreased (P≤0.05).	[124]
Plant/ *Ajuga bracteosa*	Ag	500-5000/ Tube like	200 and 400 $mg.kg^{-1}$	Balb/c mouse/ 6	Alloxan-induced mouse	Oral	Blood glucose assay and insulin assay	The blood glucose levels in the groups administered 200 and 400 $mg.kg^{-1}$ AgNPs were significantly reduced after 14 days and the insulin level also increased (P<0.05).	[126]
Plant/ *Moringa olifera*	Ag	20-40/ Spherical	0.2 $mg.kg^{-1}$	Wistar rat/ 6	Streptozotocin-induced rat	Oral	Blood glucose assay and insulin assay	The blood glucose levels in the groups administered 0.2 $mg.kg^{-1}$ AgNPs were significantly reduced after 28 days and the insulin level also increased (P<0.001).	[127]
Plant/ *Pterocarpus marsupium*	Ag	Average: 132.6/ Spherical	200 $mg.kg^{-1}$	Wistar rat/ 8	Streptozotocin and nicotinamide-induced rat	Oral	Blood glucose assay	The blood glucose levels in the groups administered 200 $mg.kg^{-1}$ AgNPs were significantly reduced after 14 days (P<0.001).	[128]
Plant/ *Thymus serpyllum*	Ag	Average: 42/ Spherical	5 and 10 $mg.kg^{-1}$	BALB/c mouse/ 10	Streptozotocin-induced mouse	Oral	FBG assay, IPGTT assay, and ITT assay	The FBG levels in the groups administered 5 and 10 $mg.kg^{-1}$ AgNPs decreased after 7, 14, 21, and 28 days; Besides, IPGTT and ITT decreased.	[95]

Biological source/ Scientific name	NPs type	Size (nm)/ Morphology	Dose	Animal type/ Number of animal in each group	Diabetic model	Routes of administration	[a]Antidiabetic techniques	Major outcome	Ref
Plant/ *Zingiber officinale*	Ag	Average: 123.8/ Spherical	200 $mg.kg^{-1}$	Wistar rat/ 8	Streptozotocin-induced rat	Intraperitoneal injection	FBG assay	The FBG in the groups administered 200 $mg.kg^{-1}$ AgNPs decreased after 3, 5, and 7 days.	[129]
Plant/ *Taverniera couneifolia*	Ag	15-31.44/ Spherical	10 $mg.kg^{-1}$	Wistar rat/ 5	Alloxan-induced rat	Oral	FBG assay and OGTT assay	The FBG levels in the groups administered 10 $mg.kg^{-1}$ AgNPs after 14 and 21 days were significantly reduced (P<0.05) and OGTT level after 60, 90, and 120 min decreased.	[122]
Plant/ *Psidium guajava*	Ag	51.12-65.02/ Spherical	200 and 400 $mg.kg^{-1}$	Wistar rat/ 6	Streptozotocin-induced rat	Oral	Blood glucose assay	The blood glucose levels in the groups administered 200 and 400 $mg.kg^{-1}$ AgNPs were significantly reduced after 1, 7, 14, and 21 days (P<0.001).	[130]
Plant/ *Nigella sativa*	Ag	Average: 77.7/ Spherical	Not mentioned	Albino mouse/ 5	Alloxan-induced mouse	Oral	Blood glucose assay	The blood glucose levels in the groups administered AgNPs decreased after 14 and 28 days.	[131]
Plant/ *Momordica charantia*	Ag	Not mentioned / Tubular clusters	50 $mg.kg^{-1}$	Wistar rat/ 8	Streptozotocin-induced rat	Oral	FBG assay	The FBG levels in the groups administered 50 $mg.kg^{-1}$ AgNPs were significantly reduced after 21 days (P<0.05).	[132]
Plant/ *Musa paradisiaca*	Ag	30-60/ Spherical	50 $\mu g.kg^{-1}$	Sprague–Dawley rat/ 5	Streptozotocin and nicotinamide-induced rat	Oral	Blood glucose assay and insulin assay	The blood glucose levels in the groups administered 5 $\mu g.kg^{-1}$ AgNPs were significantly reduced after 8 weeks and the insulin level increased (P<0.05).	[133]
Plant/ *Eysenhardtia polystachya*	Ag	10-12/ Spherical	5 and 10 $\mu g.mL^{-1}$	Zebrafish/ 20	Glucose-induced zebrafish	Dispersing of samples in the vehicle	Blood glucose assay and insulin assay	The blood glucose levels in the groups administered 5	[134]

Biological source/ Scientific name	NPs type	Size (nm)/ Morphology	Dose	Animal type/ Number of animal in each group	Diabetic model	Routes of administration	[a]Antidiabetic techniques	Major outcome	Ref
								and 10 µg.mL^{-1} AgNPs were significantly reduced after 14 the insulin level also increased (P<0.05).	
Plant/ *Solanum nigrum*	Ag	4-25/ Spherical	10 mg.kg^{-1}	Wistar rat/ 5	Alloxan-induced rat	Oral	Blood glucose assay and OGTT assay	The blood glucose levels in the groups administered 10 mg.kg^{-1} AgNPs after 14, and 21 days were significantly reduced (P<0.05) and OGTT level after 60, 90, and 120 min decreased.	[135]
Plant/ *Datura stramonium*	Au	75.1-156.5/ Nearly spherical	500, 750, and 1000 µg.mL^{-1}	Albino rat/ 6	Alloxan-induced rat	Not mentioned	FBG assay	The FBG levels in the groups administered 500, 750, and 1000 µg.mL^{-1} AuNPs were significantly reduced after 21 day.	[136]
Plant/ *Ziziphus jujuba*	Au	7-27/ Spherical	0.5 and 1 mg.kg^{-1}	Sprague-Dawley rat/ 5	Streptozotocin-induced rat	Not mentioned	FBG assay, HOMA-IR, and insulin assay	The FBG and HOMA-IR levels decreased in groups receiving 1 mg.kg^{-1} AuNPs, while insulin levels increased significantly after 21 days (P<0.03) and at a dose of 0.5 mg.kg^{-1}, FBG decreased and insulin increased non-significantly, but HOMA-IR levels were significantly reduced (P<0.05).	[137]
Plant/ *Cassia fistula*	Au	55.2-98.4/ Rectangular and triangular	60 mg.kg^{-1}	Wistar rat/ 5	Streptozotocin-induced rat	Oral	FBG assay and HbA_1C assay	The FBG levels in the group administered 60 mg.kg^{-1} AuNPs were significantly reduced after 15 and 30 days and HbA_1C were significantly reduced after 30 days (P<0.05).	[139]

Biological source/ Scientific name	NPs type	Size (nm)/ Morphology	Dose	Animal type/ Number of animal in each group	Diabetic model	Routes of administration	[a]Antidiabetic techniques	Major outcome	Ref
Plant/ *Dittrichia viscosa*	Au	20-50/ Spherical	2.5 $mg.kg^{-1}$	Sprague-Dawley rat/ 6-8	Streptozotocin-induced rat	Intraperitoneal injection	Blood glucose assay	The blood glucose levels in the group administered 2.5 $mg.kg^{-1}$ AuNPs were significantly reduced after 21 days (P<0.02).	[140]
Plant/ *Gymnema sylvestre*	Au	Average: 50/ Spherical	0.5 $mg.kg^{-1}$	Wistar rat/ 6	Alloxan-induced rat	Oral	FBG assay, HbA_1C assay, and insulin assay	The FBG levels and HbA_1C in the groups administered 0.5 $mg.kg^{-1}$ AuNPs were significantly reduced after 28 days and insulin level also increased (P<0.001).	[141]
Plant/ *Sargassum swartzii*	Au	Average: 37/ Spherical	0.5 $mg.kg^{-1}$	Wistar rat/ 6	Alloxan-induced rat	Oral	FBG assay, HbA_1C assay, and insulin assay	The FBG levels and Hb_1AC in the groups administered 0.5 $mg.kg^{-1}$ AuNPs were significantly reduced after 28 days and insulin level also increased (P<0.001).	[218]
Plant/ *Smilax glabra*	Au	Average: 21/ Spherical	50 $mg.kg^{-1}$	Wistar rat/ 6	Streptozotocin-induced rat	Oral	FBG assay, HbA_1C assay, and insulin assay	The FBG levels and Hb_1AC in the groups administered 0.5 $mg.kg^{-1}$ AuNPs were significantly reduced after 6 weeks and insulin level also increased (P<0.01).	[219]
Plant/ *Fritillaria cirrhosa*	Au	40-45/ Spherical	10 and 20 $mg.kg^{-1}$	Wistar rat/ 6	Streptozotocin-induced rat	Oral	FBG assay, HbA_1C assay, and insulin assay	The blood glucose levels and Hb_1AC in the groups administered 10 and 20 $mg.kg^{-1}$ AuNPs were significantly reduced and insulin level also increased after 28 days (P≤0.01).	[220]
Plant/ *Chamaecostus cuspidatus*	Au	Average: 50/ Mostly spherical	0.75 and 1.5 $mg.kg^{-1}$	Wistar mouse/ 6	Streptozotocin-induced mouse	Oral	FBG assay and insulin assay	The blood glucose levels in the groups administered 0.75 and 1.5	[221]

Biological source/ Scientific name	NPs type	Size (nm)/ Morphology	Dose	Animal type/ Number of animal in each group	Diabetic model	Routes of administration	[a]Antidiabetic techniques	Major outcome	Ref
								$mg.kg^{-1}$ AuNPs decreased after 21 days and insulin level also increased.	
Plant/ *Eryngium thyrsoideum Bioss*	Au	Average: 9/ Spherical	1, 2.5, and 5 $mg.kg^{-1}$	Wistar rat/ 5	Streptozotocin and nicotinamide-induced rat	Intraperitoneal injection	FBG assay	The FBG levels in the groups administered 1, 2.5, and 5 $mg.kg^{-1}$ AuNPs were significantly reduced after 7, 14, and 21 days ($P \leq 0.05$).	[125]
Plant/ *Phoenix dactylifera* L	Au	Average: 42.5/ Spherical	10 $mg.kg^{-1}$	Albino mouse/	Alloxan-induced mouse	Oral	Blood glucose assay	The blood glucose levels in the groups administered 10 $mg.kg^{-1}$ AuNPs decreased after 28 days.	[222]
Plant/ *Sambucus nigra L.*	Au	4-26/ Spherical	0.3 $mg.kg^{-1}$	Wistar rat/ 6	Streptozotocin-induced rat	Oral	Blood glucose assay and insulin assay	The blood glucose levels in the groups administered 0.3 $mg.kg^{-1}$ AuNPs were significantly reduced after 14 days and insulin level also increased ($P<0.01$).	[223]
Plant/ *Trigonella foenum*	Au-Ag	Average: 73.18/ Spherical and irregular	2 $mg.kg^{-1}$	Wistar rats/ 5	Streptozotocin-induced rat	Oral	Blood glucose assay	The blood glucose levels in the groups administered 2 $mg.kg^{-1}$ Au-Ag NPs were significantly reduced after 7 weeks ($P<0.05$).	[224]
Plant/ *Solenostemma argel*	Au-Ag	Average: 106/ Quasi-spherical	Not mentioned	Wistar rats/ 10	Streptozotocin-induced rat	Oral	Blood glucose assay	The blood glucose levels in the groups administered Au-Ag NPs were significantly reduced ($P<0.05$).	[225]

[a]**Antidiabetic techniques:** Fasting blood glucose test (FBG assay); Oral glucose tolerance test (OGTT); Hemoglobin A_1C human assay (HbA_1C); Intraperitoneal glucose tolerance test (IPGTT); Insulin tolerance test (ITT); Homeostatic model assessment for insulin resistance (HOMA-IR)